UNIVERSITÄTSKLINIKUM HAMBURG-EPPENDORF

Institut für Experimentelle Pharmakologie und Toxikologie
Institutsdirektor Prof. Dr. Thomas Eschenhagen

Modelling catecholaminergic polymorphic ventricular tachycardia with patient-specific iPSC-derived engineered heart tissues

Dissertation

zur Erlangung des Doktorgrades PhD
an der Medizinischen Fakultät der Universität Hamburg.

vorgelegt von:

David Letuffe-Brenière
aus Chambéry

Hamburg 2015

Angenommen von der
Medizinischen Fakultät der Universität Hamburg am: _____

Veröffentlicht mit Genehmigung der
Medizinischen Fakultät der Universität Hamburg.

Prüfungsausschuss, der/die Vorsitzende: Prof. Thomas Eschenhagen
_____

Prüfungsausschuss, zweite/r Gutachter/in: Prof. Boris Fehse
_____

Prüfungsausschuss, dritte/r Gutachter/in: Prof. Stephan Willems
_____

Day of the oral examination: 11.02.2016

Index

Introduction

1. Cardiovascular Disease

1.1. Background

Cardiovascular diseases (CVD) have been the leading cause of death in developed countries in the second half of the 20th century. CVD is a term used to designate all diseases which involve the cardiac muscle and the vascular system supplying vital organs (Gaziano et al. 2001). Worldwide, it jumped from accounting for less than 10% of the deaths at the beginning of the 20th century to 30% in 2001 (Gaziano et al. 2001). However, in high-income countries, CVD can be the cause of up to half of the total deaths (Mathers et al. 2005). The world's increasing industrialisation has been continuously increasing CVD deaths, therefore driving the need for further regimen or treatment strategies.

1.2. Cardiovascular diseases: an interaction between genetics and environment.

As a cause of CVD, many evidences indicate a combination of both environmental and genetic factors (Hennekens 1998; Mammucari et al. 2007). While in rare Mendelian diseases a single gene mutation without any environmental factors can be attributed to the patient's condition, in the more common CVD, an integration of environmental and multigenics factors have to be taken into account to identify the potential cause of the CVD. This principal was discussed as the "Rare Variant- Common Disease Hypothesis" (Marian and Belmont 2011), in which it is hypothesized that a large number of genetic contributors with small impact cause common diseases, whereas a small number of genetic contributors with a large impact cause rare Mendelian disorders (**Fig.1**). This hypothesis is backed up by the finding that the human genome displays a relatively high variability between individuals. A total of ~4.1 million DNA Sequence Variance (DSV) were found between two human

genomes (Levy et al. 2007). From those DSVs, ~7000 were considered potentially harmful variants, ~300 were loss-of-function variants and ~100 of those were already implicated in inherited disorders (Abecasis et al. 2010). In addition, each genome contains ~30 de novo variants, not present in the previous generation. However, although most of the CVDs deaths are due to environmental and multigenic factors, the study of rare Mendelian disorders can still give us a better insight into the fundamental heart physiology, improving our knowledge to allow us to further understand multigenic impacts. In this case Mendelian disorders could be considered as a model allowing the improvement of our global understanding of the heart through a single protein change.
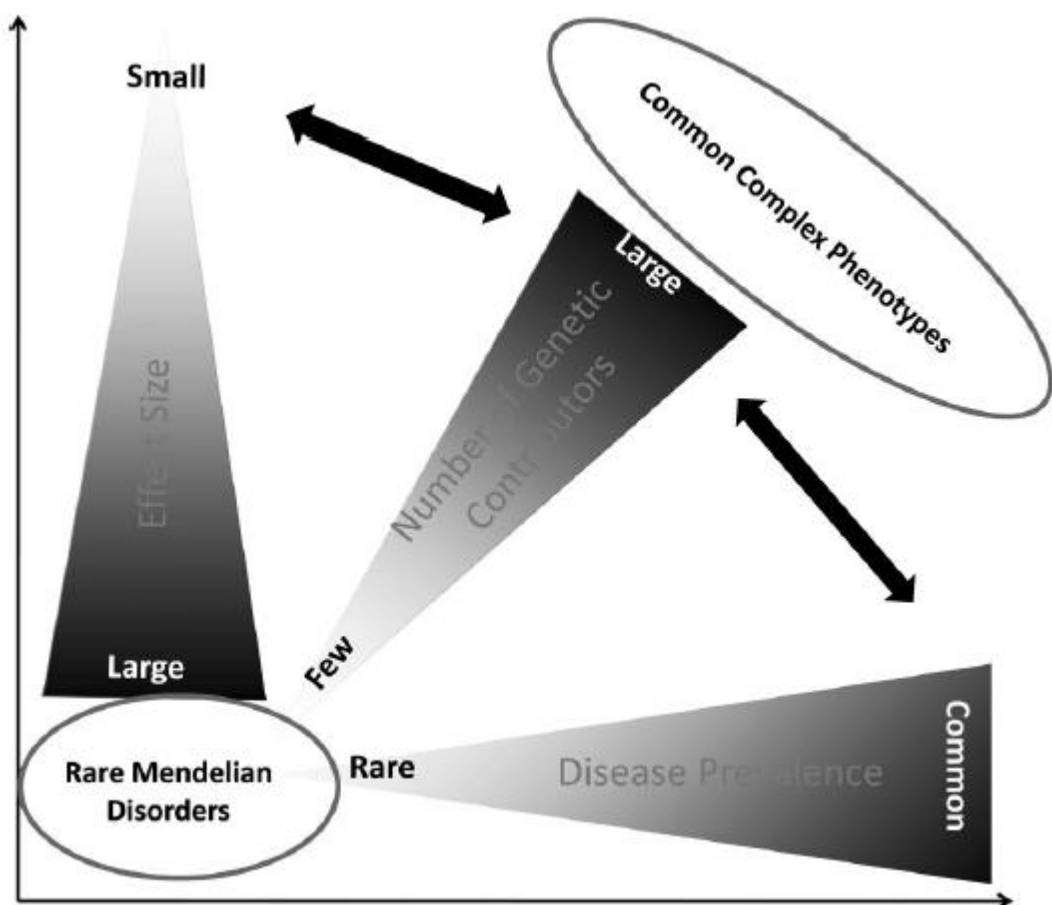
Fig. 1: *The* Rare Variant- Common Disease Hypothesis *states that the effect size of any disease is inversely proportional to its prevalence and the number of genetic contributors. The three parameters are depicted as continuum. On the one side we have rare Mendelian disorders where a single mutation can cause an effect, one the other side of the spectrum very common complex genetic interactions which cause a mild disease phenotype. Reproduced with kind permission from Marian and Belmont 2011.*

However, a cardiac model is required to study Mendelian disorders. During the past decade, the successes of human pluripotent stem cells have raised a huge hope in term of creation of a new *in vitro* model in cardiovascular research.

2. <u>Induced Pluripotent Stem Cells (iPS cells)</u>

2.1. <u>Background</u>

In 2006, Yamanaka's group in Japan could reprogram mice fibroblasts into pluripotent stem cells by transducing only four genes (Takahashi and Yamanaka 2006), and one year later carried out the same approach on human fibroblasts (Takahashi et al. 2007). Those discoveries opened a large new field of research that rapidly started expanding with a publication growth rate of 77% over the period 2008-2012 compared to a 7% growth rate of the entire stem cells field and around 3% growth rate of the overall publications during the same period (**Table 1**). Furthermore, the field-weighted citation impact is also very high, indicating a high quality of those publications (Nakatsuji et al. 2013). However, those figures should still be taken cautiously as fields with low publication volume can have artificially high growing rates, or high quality indicators due to a few papers with a very high impact.

This high publication growth rate could be explained by the enormous research potential of those cells as they open theoretical possibilities that were totally out of reach before the discovery of the iPS cell tool. iPS cells would make possible: the establishment pluripotent stem cells lines out of every individual, *in vivo* production of all cell types of the human body, *in vitro* disease modelling, predictive toxicology and regenerative strategies.

	World Publications		Growth CAGR
	2008	2012	2008-2012
Stem Cells	16172	21193	7.0%
ES cells (all)	2375	2875	4.9%
hES cells	527	642	5.1%
iPS cells (all)	108	1061	77.0%
Total World output all subjects	1,894,727	2,121,740	2.9%

Table 1: CAGR (Compound Annual Growth Rate) for stem cell's field overall, ES cells (all species), hES cells, and iPS cells (all species) between 2008 and 2012. Reproduced with kind permission from Nakatsuji et al. 2013.

This new field could emerge thanks to multiple past discoveries that helped improving the understanding of pluripotency and reprogramming. On the one hand, the discovery of somatic cloning (Gurdon 1962; Wilmut et al. 1997) has proven that the nucleus of differentiated somatic cells contains all the genetic information required to guide the development of a new organism. Furthermore, it also showed that oocytes possessed the ability to reprogram the nucleus of somatic differentiated cells. On the other hand, the establishment of mouse and human embryonic stem cells lines and their *in vitro* culture conditions allowed expansion and experiments with these cell types (Martin 1981; Evans and Kaufman 1981; Thomson 1998). Using those past discoveries and the concept of master regulation, Yamanaka's group hypothesized that only a few factors are necessary to reprogram a differentiated cell to a pluripotent state and identified a set of four genes needed to reprogram fibroblasts to pluripotent cells.

This new discovery is a real breakthrough, especially as it arrived at a time when hES cells were ethically questioned in different countries, more specifically in the United States, making iPS cells potentially more easily obtainable compared to hES cells. Furthermore, the iPS cells were more fitting in the idea of personalised medicine as the iPS cells obtained from a patient would avoid an immunity response if used for treating the patient itself. It also opened the field of disease modelling by making possible the creation of patient specific cell lines which can then be further differentiated to any desired cell lineage. *In vitro* disease

modelling was therefore theoretically possible for all hereditary diseases without disease-specific genetic manipulation.

2.2. Method

Human iPS cells were first obtained by transducing human dermal fibroblasts (HDF) with four genes: Oct3/4, Sox2, c-Myc and Klf4. The cells were then cultured further, and after 30 days, human embryonic stem-like (hES) cell colonies appeared (**Fig. 2D**). These cells were picked and cultured further on a feeder layer (**Fig. 2EF**). The authors observed that the cells exhibited an hES-like morphology with a typical high nucleus:cytoplasm ratio. Furthermore, they did not attach to gelatine coated culture plates, but on the other hand could be cultured on Matrigel® with MEF-conditioned primate ES cell medium. They also showed spontaneous differentiation in nonconditioned medium. All those characteristics are typical for ES cells and therefore the authors named the reprogrammed cells: induced pluripotent stem cells. The cells further depicted expression of classical pluripotency markers such as SSEA-3 and SSEA-4, alkaline phosphatase, Oct4 and NANOG proteins. A teratoma assay in immunodeficient mice showed tumor formation containing all three germ layers (Takahashi et al. 2007). A tumor assay is based on injecting the pluripotent cells in an immunodeficient mouse in order to observe if the cells would grow in a teratoma, and differentiate in tissues issued from the three embryologic germ layers: mesoderm, ectoderm and endoderm. This test is the ultimate proof that the stem cells cultured are pluripotent.

Those findings provide evidence that the expression of only a few genes can permanently and robustly reprogram adult somatic cells, showing that the differentiation process in mammalian cells is more plastic than previously thought.
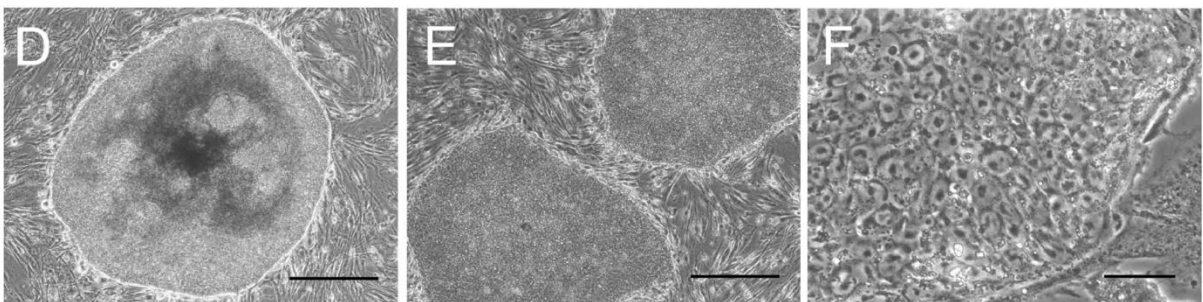
Fig. 2: D. *Representative image of hES cell colony.* ***E.*** *Morphology of an established iPS cell line at passage 6.* ***F.*** *iPS cells colony with higher magnification. Scale: 200 μm (**DE**), 20 μm (**F**). Reproduced with kind permission from Takahashi et al. 2007.*

2.3. <u>iPS cells and ES cells</u>

After the discovery of the iPS cells, a lot of groups previously working with ES cells refocused their research to this new cell type, considering its advantages over ES cells. Despite the similarities shown between iPS and ES cells in terms of morphology, culture method, surface markers and teratoma formation capacity (Takahashi et al. 2007), some groups rapidly started to point out the existence of differences. Noticeably, the iPS cells have less differentiation capacities in some cell lineage in comparison with ES cells. It was found that the capacity of iPS cells to differentiate was dependent on the lineage of the original somatic cell it was derived from giving rise to the concept of "somatic memory" (Hu et al. 2010; Feng et al. 2010). In addition, the treatment of iPS cells with an histone-deacetylase inhibitor and a methylation-resistant cytosine analogue increased their differentiation capabilities, suggesting epigenetic differences between iPS and ES cells (Kim et al. 2010). A failure to demethylate pluripotency genes for example results in only partial reprogramming of iPS cells (Lister et al. 2011). Those epigenetic difference had indeed been found in Yamanaka's original paper, and a consistent difference in gene expression was also observed, especially in young passages of iPS compared to ES cells (Takahashi et al. 2007; Bock et al. 2011). However, such differences could also be due to the fact that embryonic stem cells could be easier to keep in an undifferentiated state as iPS cells due to imperfect reprogramming. Such a difference would lead to less efficient differentiation for iPS cells that could be rescued by an improvement of cell culture technique

It is also unclear whether reprogramming in iPS cells reactivates the epigenetically silenced X chromosome in female cells (Maherali et al. 2007; Tchieu et al. 2010). If indeed the X chromosome was shown to remain silent in iPS cells, it would make it one of the biggest noted differences between iPS and ES cells and would probably limit the use of female iPS cells.

In addition to epigenetic modifications, the DNA itself has also shown differences between ES and iPS cells. The two cell types are prone to acquire different chromosomal abnormalities, for example iPS cells are more susceptible to gain chromosome 1 and 9 additions whereas ES cells would get more chromosome 3 and 20 (Ben-David et al. 2011). iPS cells are also more prone to acquire point mutations in oncogenic pathways or a higher

amount of copy number variants (CNVs) in early iPS cells passages. However the higher CNV number goes down to ES cells levels in the intermediate-passages suggesting that those anomalies are negatively selected by the cell culture procedure which is why iPS cells are not considered as established cell lines before passage 20 (Hussein et al. 2011; Bar-Nur et al. 2011).

Despite growing evidence for genetic and epigenetic differences between ES and iPS cells, the individual-specific and ethically unproblematic use still gives them properties unfulfilled by ES cells, thereby explaining the exponentially growth of this new field.

2.4. Medical potential of iPS cells

One of the major advantages of iPS cells over ES cells in term of medical research is the opportunity to establish patient-specific cell lines, which promises brand new opportunities to gain insight into Mendelian diseases as well as immune-response-free cell therapy. Indeed, as iPS cells from patient's somatic cells can now be routinely made, it is possible to create a library of iPS disease-specific cell lines which can then be studied, stored or shared with other researchers worldwide. Another aspect would be to use patient-specific iPS cells in regenerative medicine to regenerate damaged tissues by implanting the patient's own iPS cells to avoid an immune response (**Fig. 3**).
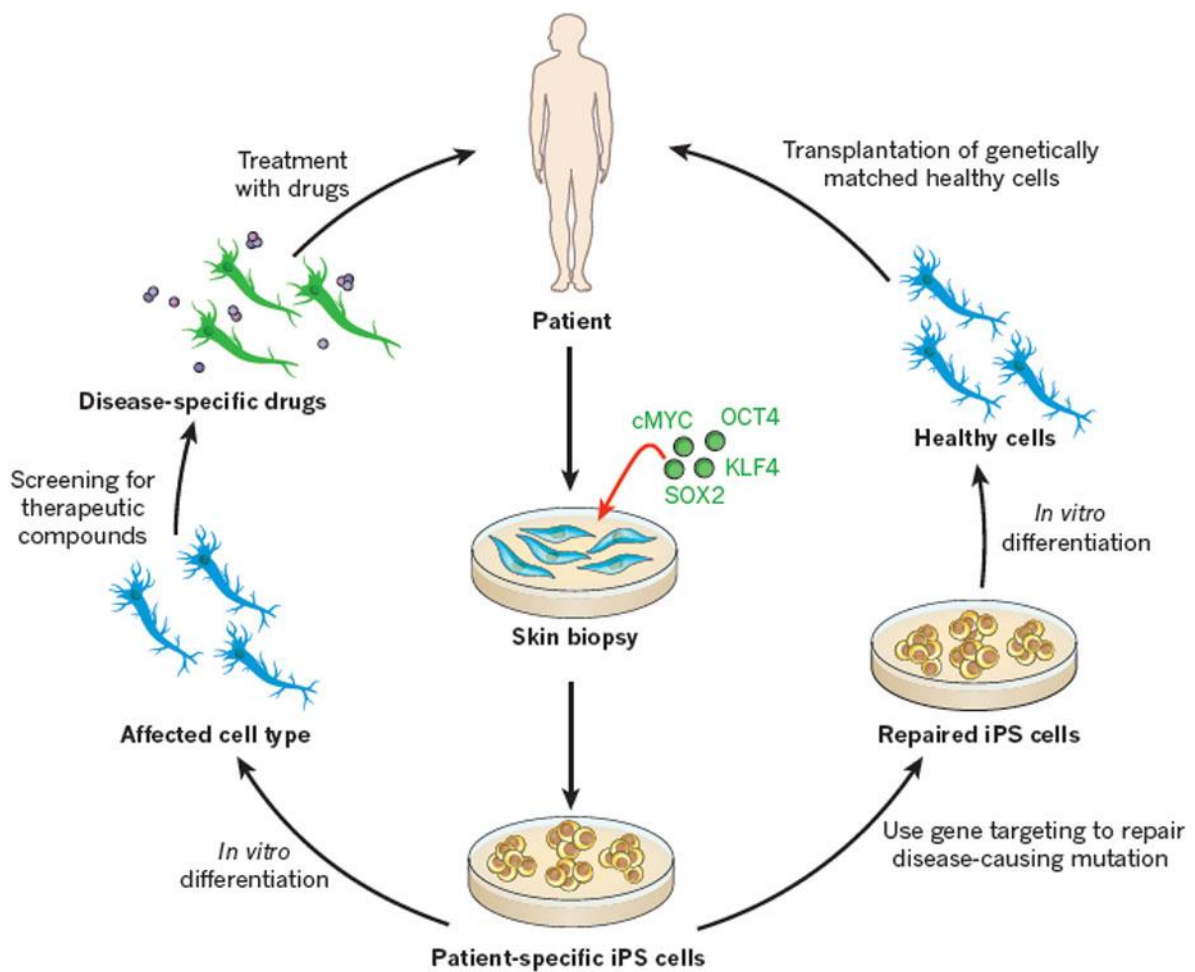
Fig. 3: *Patient-specific iPS cells reprogrammed from a skin biopsy by transduction of the four genes described by Takahashi et al. 2007 (central part of the figure). Those cells can then be differentiated in the desired cell type and used as an in vitro model. This process could either be useful for the discovery of novel compounds or used so that each patient would have a personalised drug screening on its own iPS cells (left part of the figure). Alternatively, the iPS cells could be repaired, in case of a disease-causing mutation, differentiated and transplanted in the patient, thereby avoiding an immune response. If the patient is not affected by a Mendelian disease, the iPS cells could even be used without being repaired (right part of the figure). Reproduced with kind permission from Robinton and Daley 2012.*

2.5. iPS cells as a tool for disease modelling

The first group to successfully achieve disease modelling with iPS cells were Lee et al. in 2009. They made a familial dysautonomia-specific iPS cell line, differentiated the cells into central and peripheral nervous system precursor and could then observe three disease-related phenotypes. This study was a proof of principle to demonstrate that iPS cells could

successfully model disease *in vitro* and could also allow the discovery of new therapeutic compounds (Lee et al. 2009).

In the cardiac field, numerous diseases have been modelled such as Long QT syndrome (LQT), Catecholaminergic Polymorphic Ventricular Tachycardia (CPVT), Dilated Cardiomyopathy (DCM) or Hypertrophic Cardiomyopathy (HCM) (Moretti et al. 2010; Sun et al. 2012; Itzhaki et al. 2012; Lan et al. 2013). In those studies, the authors could find a combination of different histological or electrophysiological abnormalities by studying isolated iPS cell-derived cardiomyocytes. Classical methods used for characterisation include patch clamp recording, micro electrode array and calcium imaging. Some groups could even successfully rescue the phenotype using pharmacological substances. For example, the Long QT 2-specific iPS cells displayed an increasing of the repolarisation time with hERG blockers but phenotype rescue with calcium-channel blockers or ATP-sensitive potassium channel agonists. This rescuing was observed through a decreased duration of the action potential, the elimination of early afterdepolarisations (EADs) and triggered arrhythmias (Moretti et al. 2010). In iPS cells from CPVT patients, the authors could successfully reproduce delayed afterdepolarisations (DADs) and EADs with both β-adrenergic and adenylate cyclase activation. Rescuing of the CPVT phenotype was also observed with flecainide and dantrolene (Birks et al. 2008; Itzhaki et al. 2011; Jung et al. 2012; Sun et al. 2012; Itzhaki et al. 2012).

However iPS cell-derived cardiomyocytes are still immature in comparison to adult myocytes cultured *in vitro* (Yang et al. 2014). This immaturity could deeply modify the physiology of the beating cardiomyocyte as well as its proteomic composition for example. It could lead to masking the disease phenotype or on the contrary creating complex interactions in which the visible phenotype is very different from the one present in mature adult hearts. To conclude, despite their limitations iPS cells can model Mendelian cardiac diseases and have the potential of being a useful platform for fine tuning drug dosage or testing the potential arrhythmogenic effects of a pharmacological agent (Eschenhagen et al. 2015).

2.6. <u>RGB tracking to test cell culture quality</u>

Cell-to-cell variability could be an important issue impacting the quality of the selected clone. Indeed, as iPS cell reprograming leads to the later selection of a unique clone, early inter-cell variability could have a major unknown impact on the quality of the future cell culture. Cell-to-cell variability was first reported in prokaryote cultures were numbers of different parameters of the same culture clone were found to be different from line to line (Novick and Weiner 1957; John L. Spudich & D. E. Koshland 1976). The field of stochastic behaviour in individual cells was then further studied, showing random gene expressions explaining the variability. In our case, we wanted to investigate if the standard cell culture conditions in which were kept iPS cells over a relatively large amount of time affected or not the quality of the culture. Indeed, it could be theorised for example that the longer the cells stay in culture, the more some sub-clones present in the culture could overgrow the rest of the culture. In this case, a late culture could be very different to an earlier one as the initial cells would have been replaced by later generated sub-clones.
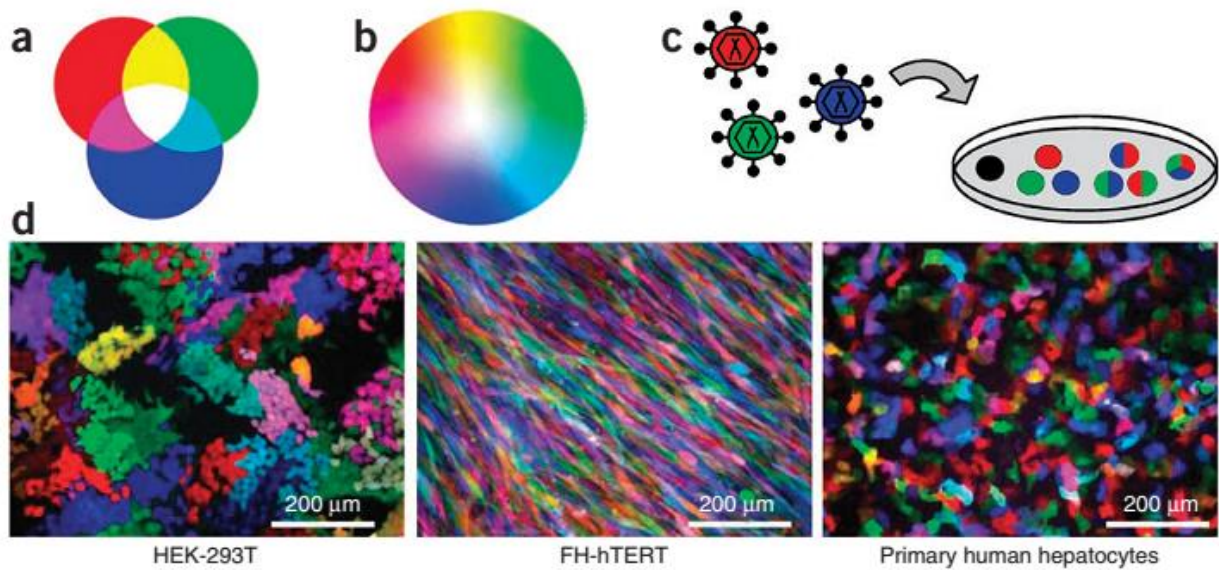
Fig. 4: a. *Colour theory stating that by mixing the three primary colours red, green and blue, the colours white, purple, yellow and turquoise can be obtained.* ***b.*** *If the intensity of each individual primary colour is modulated, the whole spectrum of visible range colours can be obtained.* ***c.*** *The transduction of cells by a random amount of viruses, followed by the stochastic colour expression of each of them due to its unspecific integration site would theoretically lead to the expression of the full colour spectrum, due to a random colour intensity of each primary colour in every cell.* ***d.*** *Confocal pictures of transduced HEK cells, human foetal-liver derived cells and primary human hepatocytes. For the HEK culture, it can be noticed how the daughter cells of a unique colours display a patched repartition in the culture, due to low cell motility. Reproduced with kind permission from Weber et al. 2011.*

In order to verify this hypothesis, we decided to use a simple and elegant tool kindly provided by our collaborator Dr. Riecken known as the RGB staining (Red-Green-Blue). The technique consists in the random expression of the three primary colours red, green and blue in the desired cells, using the stochastic integration and transduction rate of lentivirus vectors. The desired cells are transduced by three lentiviral gene ontology (LeGO) vectors encoding the three primary colours: red, green and blue (Weber et al. 2008; Weber et al. 2011). Due to the random amount of viruses hitting each cells added to the random integration site of the gene, every single cell will display basic colours with different intensities, leading to the display of all of the possible colours (**Fig. 4**). Each colour will then represent all the cells issued from a unique mother cell present at the time of the transduction. Indeed, the long lasting expression of the fluorescent protein makes it a perfect tool for cell tracking over long-term cell culture.

The technique was thus used on our iPS cell culture for two reasons. First to observe if a sub-clone of a specific colour would eventually overgrow the other colours, and second to see if some speed differences could be observed between the different cell lines and the different passage numbers within the same cell line.

3. <u>Catecholaminergic Polymorphic Ventricular Tachycardia (CPVT)</u>

3.1. <u>Background</u>

CPVT was first reported by Coumel et al. (1978) who described an exercise or emotion-induced syncope associated with polymorphic and/or bidirectional ventricular tachycardia (VT) without any structural cardiac abnormalities. Heart rate at rest was also reported lower in some studies (Postma et al. 2005). CPVT is a relatively rare disease with an estimated prevalence of 1:10,000 (Napolitano et al. 2014), and genetic allelic variance is found in 55-65% of the cases, indicating that unknown loci probably contribute to the disease (Ackerman et al. 2011). The main known mutation causing CPVT is in the ryanodine receptor 2 gene, present in 50-55% of patients (Priori 2002) and autosomal dominant. In 2-5% of the cases, CPVT has also been reported with a calsequestrin 2 (CSQ2) mutation, and in a few cases a triadin or a calmodulin 1 mutation (Postma 2002; Nyegaard et al. 2012).

3.2. <u>RyR2 mutations in CPVT</u>

The RyR2 channel is a homotetramer and one of the biggest proteins known with 565 kDa. The firsts ~4300 N-terminal amino acids compose the cytosolic domain, and the lasts ~500 amino acids the six transmembrane domains. The RyR2 mutations in CPVT patients are not evenly distributed in the protein, but concentrated in four different clusters throughout the protein's amino-acid sequence (**Fig. 5**).
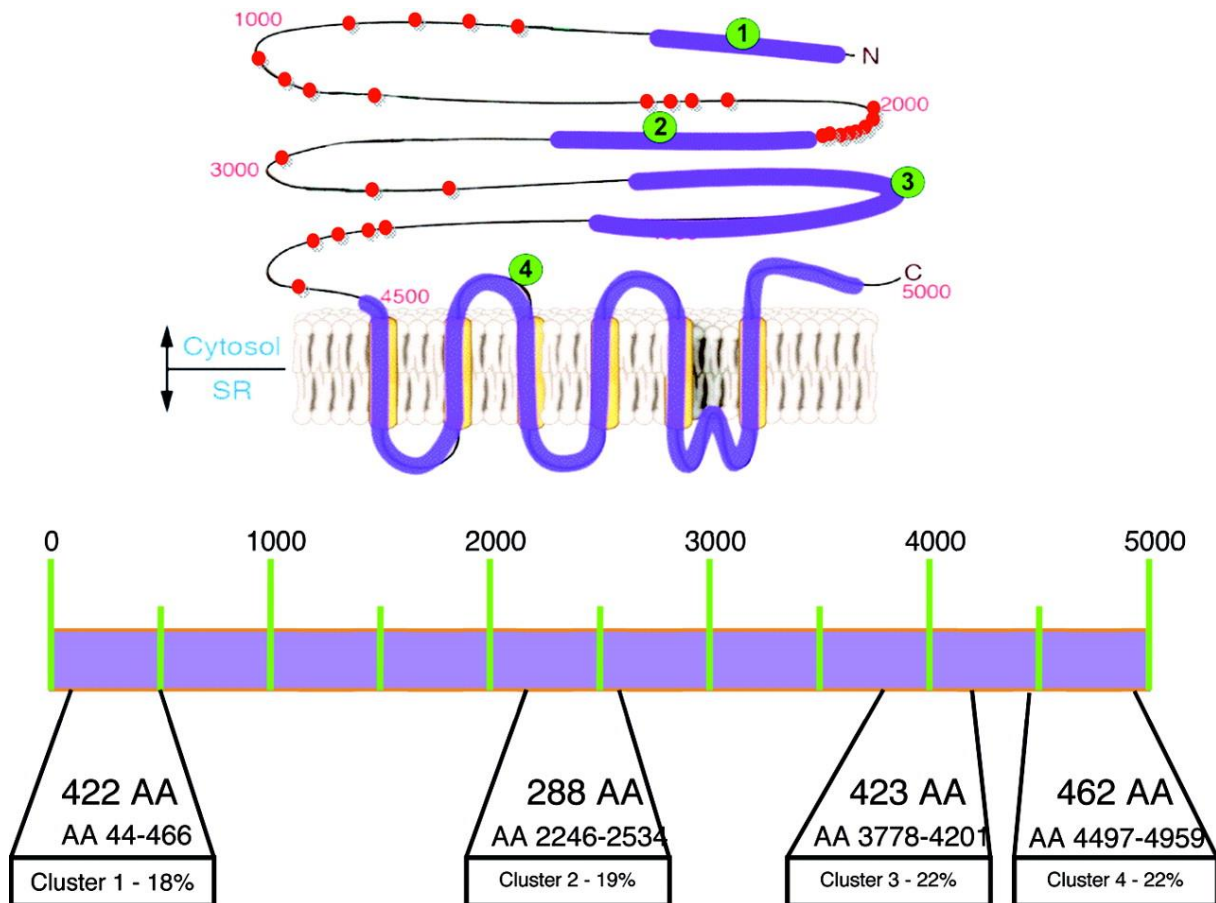
Fig. 5: *(Top) CPVT mutations in the RYR2 protein are mainly point mutations located in four different clusters (blue thick lines). Only 10% of mutations where found outside the canonical clusters (red dots). (Bottom) Location of the mutation clusters in the primary structure of the protein. Reproduced with kind permission from Priori and Chen 2011.*

3.3. Calcium handling in cardiomyocytes of CPVT patients

To understand how CPVT can provoke arrhythmias in the heart, it is important to understand the functioning of the calcium handling in the cardiomyocyte. At rest, the cardiomyocyte is not under β-adrenergic stimulation (**Fig. 6 left**). In this case, the excitation-contraction (EC) coupling is accomplished through a calcium-induced calcium release (CICR) mechanism. During a CICR, the external calcium entering the cell through the L-type calcium channels trigger the release of calcium from the sarcoplasmic reticulum (SR) through the opening of the RyR2. If the cardiomyocyte is under β-adrenergic stimulation, the calcium load is higher (**Fig. 6 right**). Under these conditions, store overload induced calcium-release (SOICR) can occur in CPVT cardiomyocytes, leading to arrhythmia. A SOICR occurs because the RyR2 is

13

also sensitive to the luminal calcium concentration inside the SR, and a higher SR calcium concentration increase its opening probability (Priori and Chen 2011)
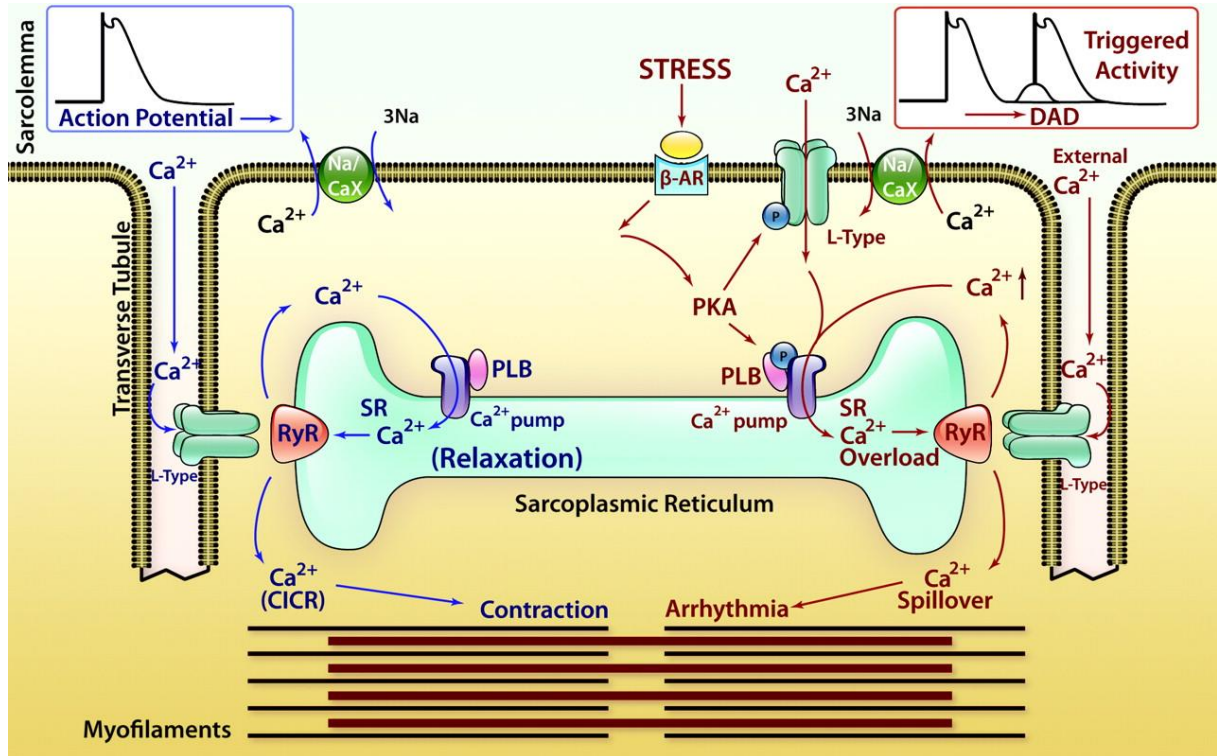
Fig. 6: Standard calcium concentration in the SR (left). The action potential triggers the opening of the L-type calcium channels, mediating a CICR response of the RYR2. Calcium is then liberated from the sarcoplasmic reticulum and provokes a contraction. It is then pumped back in the SR by SERCA or pumped out of the cell by the NCX exchanger. SR calcium overload (right). The β-adrenergic receptors are activated inducing a phosphorylation of calcium handling proteins like phospholamban, L-type calcium channels or RyR2. The phosphorylation of those proteins leads to the activation of SERCA, provoking a SR calcium overload. This overload predisposed to a SOICR due to an increased calcium sensitivity of the mutated RYR2 provoking a SOICR. Reproduced with kind permission from Priori and Chen 2011.

If it the CICR mechanism is responsible for normal contractions, SOICR on the other hand leads to delayed after depolarisations (DADs and triggered arrhythmias). In the case of a RYR-associated CPVT patient, the calcium sensitivity of the ryanodine receptor will be increased (**Fig. 7A**). Although RYR2 releases calcium via the CICR mechanism, and therefore cytosolic calcium, the regulation of the RYR2 is thought to be more regulated through the luminal calcium concentration in the SR (Trafford et al. 2000). The modulation of the RYR2 has little effect on the CICR but has a major effect on SOICR, for example the modulation of

RYR2 by caffeine or tetracaine has a big impact on its sensitivity to SOICR but none on CICR (Eisner et al. 1998).
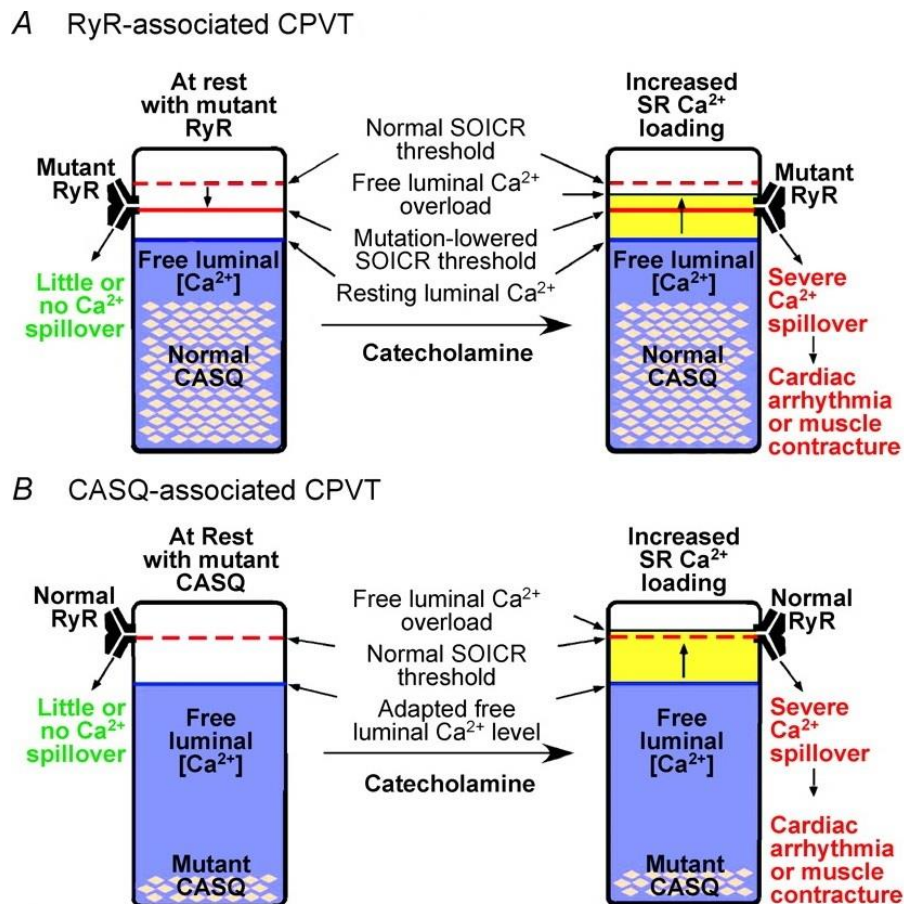
Fig. 7: A. *In CPVT patients, the sensitivity of the RyR2 to luminal calcium is higher leading to a lower SOICR threshold. During β-adrenergic stimulation, SERCA is more active increasing the calcium concentration in the SR. This increased calcium concentration leads to spontaneous calcium release because of the lower SOICR threshold of the mutated RyR2.* **B.** *This hypothesis also hold true for CASQ2 mutation. In this case, the sensitivity of the RyR2 to internal calcium is normal, but the mutated CASQ2 leads to a lower storage capacity of calcium during a β-adrenergic stimulation event, therefore leading to spontaneous SR calcium release. Those two mechanisms explain how SOICR causes arrhythmias of CPVT patients during β-adrenergic stimulation. Adapted with kind permission from MacLennan and Chen 2009.*

These results were confirmed by single channel recording of mutated RYR transduced HEK cells or isolated adult myocytes. Those studies tested a large number of mutations, and found that most of them had a major impact on the luminal calcium sensitivity of the channel, and only little on the cytosolic calcium sensitivity (Jones et al. 2008; Fernández-

Velasco et al. 2009). Furthermore, a higher frequency of SOICR were found in cardiomyocytes of knock-in mice for the RyR2 gene as well as HEK293 cells (Kannankeril et al. 2006; Fernández-Velasco et al. 2009; Uchinoumi et al. 2010). It could also be noticed that the increased sensitivity to SOICR explains better the arrhythmias in CPVT patients compared to an increased sensitivity to excitation-contraction coupling, as the CPVT patients only experience arrhythmias during β-adrenergic stimulation (**Fig. 7**).

3.4. Mechanism of increased luminal calcium's sensitivity.

As it was previously explained, increased luminal calcium sensitivity of the RyR2 seemed to be the major cause to arrhythmias in CPVT patients, due to SOICR events. However the molecular mechanisms leading to this increased sensitivity are still unclear. To date, two main hypotheses are proposed. The first suggests that the N-terminal domain of the protein interacts with the central domain, leading mutations in those two domains to destabilise the protein's closed state (unzipping) and alter its luminal or cytosolic calcium sensitivity (Tateishi et al. 2009). This hypothesis is supported by the fact that important conformational changes occur in the protein during the closing and opening of the channel, making domain-domain interactions likely to have a physiological impact (Lobo and Van Petegem 2009).

The second hypothesis involves the binding of the FK506 binding protein (FKBP12.6) to RyR2. This protein is believed to play an important role in the stabilisation of RyR2. During phosphorylation of RyR2, FKBP12.6 would dissociate, leading to an increased sensitivity to cytosolic calcium in the RyR2. Furthermore, some CPVT mutations were shown to decrease FKBP12.6's sensitivity to the channel, suggesting a role in the CPVT mechanism (Marx et al. 2000; Wehrens et al. 2003). However, despite promising results, more recent studies couldn't further confirm the importance of FKBP12.6 in CPVT arrhythmogenesis as the interaction with FKBP12.6 was not found to be dependent on PKA phosphorylation and some of the results were even in direct contradiction to previous findings concerning the dissociation of FKBP12.6 during RyR2 phosphorylation and its affinity with the receptor (Tiso et al. 2002; Guo et al. 2010). Overall, the hypothesis of domain unzipping seems to be less challenged by contradictory findings than the FKBP12.6 regulation, and therefore more plausible.

To conclude, we have seen in this chapter that CPVT patients suffer deadly cardiac arrhythmias provoked by SOICR due to β-adrenergic stimulation. Those arrhythmias are mainly caused by an increased luminal calcium sensitivity of the RyR2, which is probably caused by mutations leading to a domain unzipping destabilising the protein's conformation.

4. <u>Cardiac differentiation</u>

4.1. <u>Background</u>

The discovery of iPS cells has raised huge hopes in term of disease modelling, as it meant that the creation of disease-specific cell lines could be very easily done just by taking somatic cells from patients with the desired mutation. However, for the technique to be useful in cardiovascular research, a robust and efficient protocol to differentiate pluripotent stem cells to cardiac cells is needed. To achieve cardiac differentiation from pluripotent cells, researchers focused on trying to reproduce *in vitro* the different steps occurring in cardiac development during embryogenesis. To summarise, cardiac development is mainly controlled/conducted by the sequential presence of three families of proteins: bone morphogenic proteins (BMPs), belonging to the transforming growth factor-β family (TGF-β), wingless/INT proteins (WNTs), and fibroblast growth factors (FGFs) (Olson and Schneider 2003). While BMP has been shown to generally promote cardiogenesis in vertebrates, the role of the WNTs pathway action is more complex with a possible activation or inhibition of differentiation to cardiac cells, depending on the spatiotemporal context (Cohen et al. 2008).

4.2. <u>Cardiac differentiation *in vitro*</u>

Three main approaches were developed for cardiac differentiation of human pluripotent stem cells: embryoid body formation (EBs), monolayer culture and inductive co-culture (Mummery et al. 2003; Laflamme et al. 2007; Yang et al. 2008; Burridge et al. 2011). Those approaches rely on mouse development as a classical model for human cardiogenesis. A parallel was found between cardiogenesis and ESC (embryonic stem cells) differentiation, where successive activations and inhibitions of Wnt/β-catenin, BMP, Nodal/Activin and

Notch pathways permits cardiac differentiation in both models (**Fig. 8**). The first method used was differentiation by inductive co-culture. This method is not typically used as it reaches lower cardiomyocyte purity than the two other methods that will be described in the coming paragraph. Stem cells could be differentiated to cardiomyocytes when co-cultured with visceral-endoderm-like cells: END-2 cells. The differentiation effect is mainly due to the secretion of Indian hedgehog growth factor secreted by those cells (Mummery et al. 2003). Despite its extremely low efficiency, this technique can still be used as it is fast, easy and cost effective.
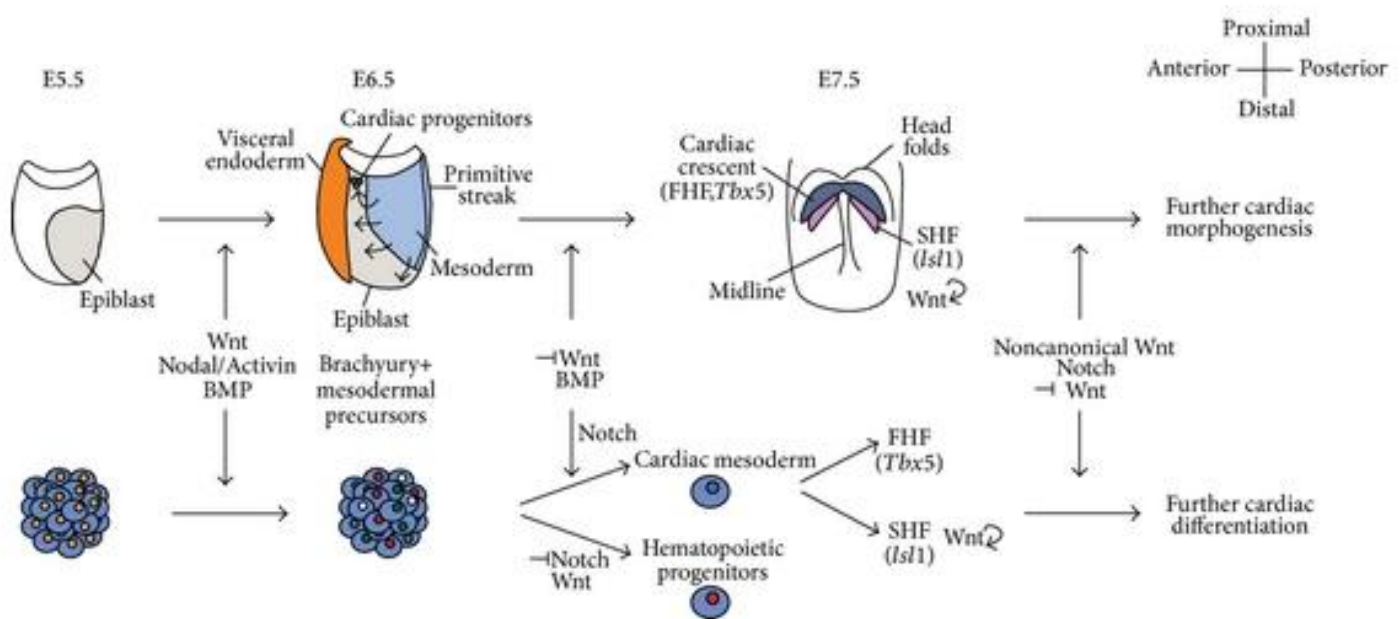
Fig. 8: *This scheme represents the correlation between murine heart development (upper part) and in vitro embryonic stem cell (ESC) cardiac differentiation (lower part). Between embryonic day 5.5 (**E5.5**) and 6.5 (**E6.5**) or in the first stages of differentiation the mesodermal induction is controlled in both systems by the Wnt/β-catenin, Nodal/Activin and BMP signalling pathways which lead to an increased brachyury expression. Between E6.5 and E7.5, formation of the first (FHF) and second heart (SHF) field requires inhibition of the Wnt pathway, and expression of BMPs. In parallel in ESCs, the Notch pathway inhibits Wnt/β-catenin signalling and activates BMP. The Wnt/β-catenin pathway is then activated, increasing proliferation of the secondary heart field (pink). Further cardiac differentiation or cardiogenesis, is then achieved by a further inhibition of the Wnt/β-catenin signalling by Notch and non-canonical Wnt signalling. Those pathways signal the cells to stop proliferating and start differentiating. Reproduced with kind permission from Freire et al. 2014.*

In 2008, Yang et al. found that relatively high efficient cardiomyocyte differentiation could be achieved by sequentially incubating EBs with first a BMP/Activin combination, and second

a Wnt signalling inhibitor: DKK1. Those results show that *in vitro* differentiation precisely replicates *in vivo* cardiogenesis, where Wnt/β-catenin, BMP and Nodal/Activin pathways are also modulated in the same sequence (Yang et al. 2008). A similar approach was performed by Laflamme et. al. but as a monolayer culture, so more practical to use in a cell culture laboratory. In this approach, the mesoderm is also induced by Activin/BMP, but no Wnt pathway inhibitor is used during a later stage. This only partial mimicking of the heart development is however showing the same differentiation efficiencies as described in the previous technique: around 80% cardiomyocyte content (Laflamme et al. 2007; Burridge et al. 2011). This technique was then further optimised by activating Wnt pathway with a small molecule: CHIR 99021 during the mesodermal induction and inhibiting the same pathway during cardiac differentiation with another small molecule like IWR-1 or other analogues (Burridge et al. 2014; Zhang et al. 2015)

4.3. EB formation

Different methods can be used to make EBs from iPS cells with positive and negative sides for each of them. In our case, as large quantities of EBs were required, we had to look for an upscalable and cost-effective method. One of the most commonly used method for EB formation is the "spin EBs" method. It consists of pipetting a defined number of cells in a U or V-shaped 96 well plate and then centrifuge it. The advantage of this approach is that defined EBs can be obtained, with a highly controlled number of cells per EB. However, as EBs have to be pipetted individually, no upscaling is possible with this method (Burridge et al. 2007). The most upscalable methods described for EB formation involves dynamic culture of iPS cells with for example a spinning rotor. In this case, a 24 hours incubation of single cells in a flask with a vertical rotor could successfully and efficiently induce EB formation. This method can easily be used to produce high or low amounts of EBs just by increasing or decreasing the amount of cells and medium in the flask (He et al. 2012).

Cardiomyocyte Lineage | **Transcription Factors** | **Cell-Surface Markers**

ESC/iPSC — Oct4, Nanog, Sox2 — Tra-160, SSEA4, EpCAM

Epithelial-Mesenchymal Transition

Mesoderm Progenitor — Oct4 — NCAM, SSEA1

BMP4, Activin A, FGF2, Wnt3a
Insulin

Precardiac Mesoderm — T, MIXL1

BMP4, Activin A, FGF2, Wnt3a

Cardiac Mesoderm — Mesp1 — KDR, PDGFRα

Wnt ⊢ Dkk1

Heart Field Specific Progenitor — Nkx2.5, GATA4 (Tbx5/Isl1/Tbx20) — SIRPA

Embryonic Cardiomyocyte — Nkx2.5, GATA4 — SIRPA, VCAM-1

Fig. 9: Simplified model of the signalling pathways (left, black) playing a major role in the sequential differentiation of the cardiomyocyte lineage (left, blue circled). Key transcription factors (middle, red) and surface markers (right, green) are also indicated. Reproduced with kind permission from C. L. Mummery et al. 2012.

4.4. Mesodermal induction

During the first days of differentiation, the iPS cells have to be directed to mesodermal lineage in order to be further differentiated to cardiomyocyte. This mesodermal induction can be accomplished by to the activation of either the TGF-β or the WNT pathway. Typically the two pathways can respectively be activated through BMP/Activin or CHIR 99021. In both

cases the concentration of the growth factors will have to be fine-tuned when used for the first time. (Yang et al. 2008; Burridge et al. 2011; Lian et al. 2012).

4.5. Cardiac differentiation

After mesodermal induction, cardiac differentiation has to be induced to increase the efficiency of the protocol. This can be performed by either inhibiting the TGF-β pathway, or more commonly by inhibiting the Wnt pathway both by using small molecules (Kattman et al. 2011; Willems et al. 2011). A large variety of small molecules can be used to inhibit the Wnt pathway such as the IWR and IWP families which are most commonly used. Some teams can also use house made analogues which have as well proven to be very effective. The naturally produced protein inhibiting the Wnt pathway (DKK1) can also be used but in a much higher concentration in order to obtain the same pathway block. In addition, the price of the protein is much higher, making it very expensive to use in order to produce large cardiomyocytes amounts. Differentiation can also be obtained without those inhibitions, however the end purity of cardiomyocyte will be considerably lower. This differentiation is very critical in our case as large amounts of cardiomyocytes are needed, which is not the case for studies using single cell approach where a high cardiomyocyte purity is not necessary. Furthermore, the cost of producing such quantities of cardiomyocyte is substantial, putting an additional challenge on the process.

5. Engineered Heart Tissue

5.1. Background

Research in the cardiac field is highly dependent on reliable models. In 1959, it was noticed that isolated cells from immature chicken heart were a better heart model when forming aggregates rather than in monolayer culture. These aggregates were spontaneously formed from single cells, simply by keeping them rotating in a flask, and were spontaneously beating due to their embryonic-like state (Moscona 1959; McDonald et al. 1972). However, they were not used for further studies since cells aggregates were spontaneously detaching from the surface they first attached to and stopped beating shortly after (Eschenhagen and Zimmermann 2005). Tissue engineering is the integration of cells to an engineered 3D structure in order to produce a tissue construct. Over the past two decades, cardiac tissue engineering experienced an exponential interest and findings. Indeed, three-dimensional cardiac constructs has the unique capability to integrate those intercellular interactions within a three dimensional structure through the study of a functional syncytium of cells. Cardiac constructs therefore are complementary to classical *in vitro* single cell adult cardiomyocyte model for example. Comparisons between the different model systems could reveal some compensatory mechanisms that might be present in the more complex three-dimensional syncytium of cardiac constructs.

Even though it is relatively simple to obtain contracting spheroid bodies from a simple rotating suspension culture (Moscona 1959), it is much more challenging to create a strained tissue contracting between anchor points. Stretching the EHT between fixed poles will indeed be crucial for the alignment of the cardiomyocytes in the tissue and therefore a better maturation state. It has also been shown that providing auxotonic conditions to the EHT either by motorised stretching or providing elastic anchoring poles can further improve its contractility (Zimmermann et al. 2006; Hansen et al. 2010). One of the methods used to obtain EHT is to embed the cardiomyocytes into a hydrogel matrix composed of fibrin, collagen, Matrigel® or a combination of them. The cells will be in this case previously mixed with the matrix before its polymerisation and then casted in a mold of the desired form. It has also been shown that hydrogel will stimulate the cells spreading and forming of intercellular connections (Hirt et al. 2014).

Another approach was to seed cells into a prefabricated porous solid 3D scaffold as it is done in bone tissue engineering. The scaffold can be composed on numerous different materials like alginate, collagen, polyglycolic acid, etc. Those structures can even be incorporated with gold nanofiber as an electrical conductor, making an electrical pacing possible, which might be crucial condition in order to obtain more mature EHTs as *in vivo adult* cardiomyocyte need an external electrical signal from the sinoatrial node to contract. Improvement of cell orientation, tissue structure and function after chronic pacing of 8 days has been proven in collagen sponge structure EHTs (Radisic et al. 2004).

An important parameter in EHTs is also the non-myocyte content of the tissue which is of 70-80% in the human heart and it has been repeatedly shown that their presence improved the EHT's contractility (Radisic et al. 2008). Mouse or hPSC derived EHTs for example require addition of fibroblasts into their highly purified cardiomyocytes mix (Kensah et al. 2013). iPS cell-derived cardiomyocytes at only a 40-60% purity were reported to lead to perfectly contractile EHTs, further confirming the idea of the importance of non-myocyte fraction in the tissue's physiology (Schaaf et al. 2011). It is however not clear if the beneficial effect is paracrine or due to cell-to-cell contacts between myocytes and non-myocytes.

One of the most challenging aspects of *in vitro* cardiac models is the maturity of the cardiomyocytes used. Indeed, adult cardiomyocytes can only survive a few days in culture which make them harder to study, but also poses a physiological problem as those cells could be stressed, and therefore react differently. Foetal or iPS derived cardiomyocytes can be cultured for months in culture, but display an immature phenotype in comparison of adult cardiomyocytes such as spontaneous beating, lower α-myosin heavy chain isoform to β-isoform ratio or an unusual length/width ratio (Tiburcy et al. 2011). However 3D EHTs seems to have more mature properties as its 2D counterpart such as longitudinally orientated and rod shaped cardiomyocytes, increased amount of binucleation or observing Frank-Starling mechanism (Zimmermann et al. 2002; Hansen et al. 2010). A higher maturity of cardiomyocytes in 3D models would indeed be expected as they offer the possibility of auxotonic contractions and multidirectional cell-cell contact, and therefore 3D EHTs have the potential of becoming the next step in a more physiological *in vitro heart* modelling.

5.2. Fibrin-based mini-EHTs

A first attempt to generate EHTs with a direct possibility of force measurement was performed by cardiac myocytes-populated matrices from embryonic chick cardiomyocytes (Eschenhagen et al. 1997). More recently, ring-shaped EHTs from neonatal rat hearts were used to record contractility during a calcium or isoprenaline concentration response curve. However, generation of ring-shaped EHTs requires a relatively high amount of cells, is hard to miniaturise and to automate the contractility measures (Zimmermann et al. 2002). Our group has improved their technique further by the creation of fibrin-based mini-EHTs (FBMEs), where the EHT is reduced to a 150 µl cylinder of 8 mm length containing 600,000 cells. The FBMEs are based on a fibrin Matrigel® matrix mix instead of collagenase I, as it was the case for the ring-shaped EHTs. Our force calculation system is based on a video-optical analysis and custom made figure recognition software (**Fig. 10**). The FBMEs are casted between two silicon posts, providing an auxotonic load for the EHT to contract. The 24-well plate format they are adapted to make them very easy to culture, and therefore allow experiments with increased n numbers. In addition, the video-optical system used for force measurement permits its automation, allowing a higher number of recordings (Hansen et al. 2010).
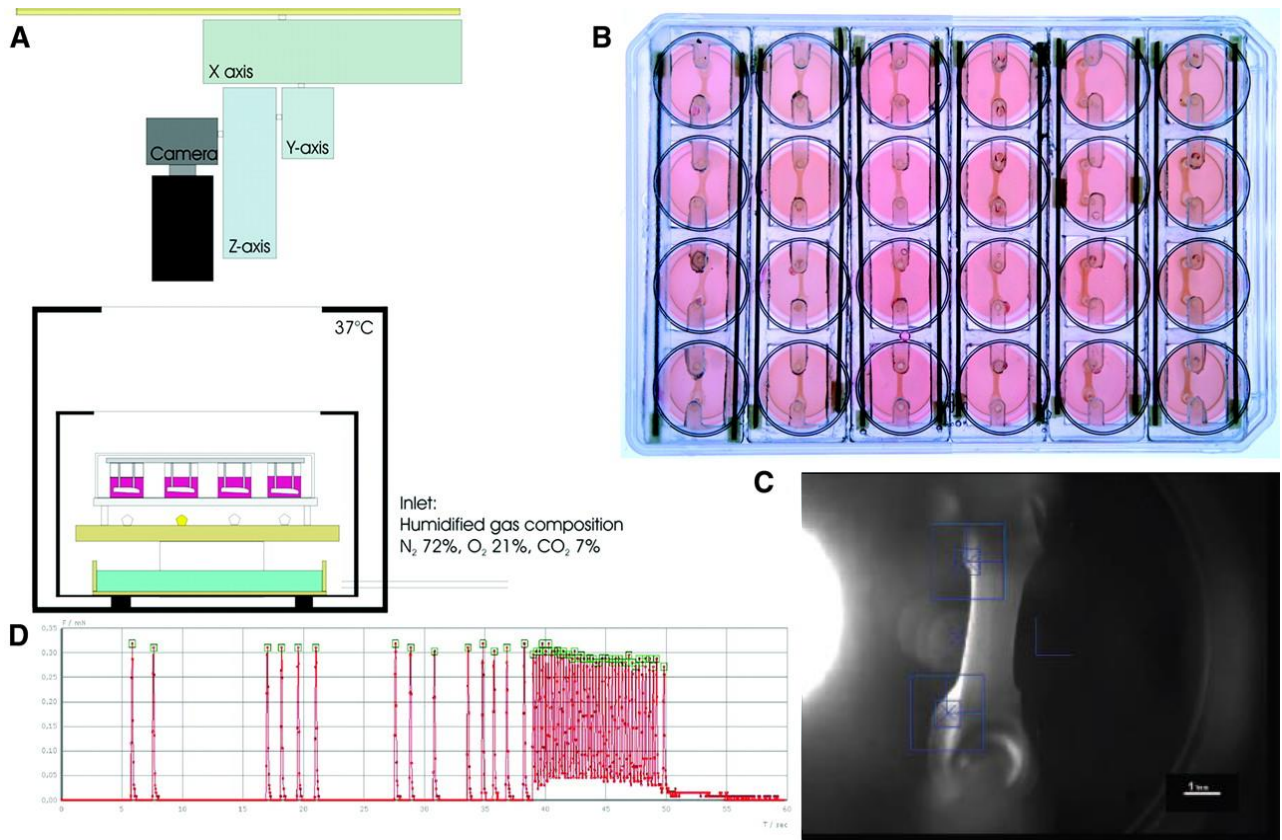
*Fig. 10: **A**. Video-optical recording system with a glass roof incubation chamber. The camera can move in all directions and is coupled to a custom made recording program which can automatize the recording of the entire plate. **B.** Top view of a 24-well plate with silicon racks and EHTs. **C.** View of a rat EHT from the camera with the two blue squares of the figure recognition program. **D.** View of a recording of an EHT's contractions with the force on the y axis and time on the x axis. The green squares represent the peak recognition for further calculation of contractile parameters. Reproduced with kind permission from (Hansen et al. 2010).*

5.3. Adaptation to hES cells and future perspectives

The technique was further successfully adapted by the group to hES cell-derived cardiomyocyte, with a successful reaction to hERG blocker (E4031) isoprenaline and the possibility of measuring a calcium concentration-response curve (Schaaf et al. 2011). However, the model is dependent on a relative efficient cardiomyocyte differentiation for which a robust protocol is still not clearly available, as stated in the paragraph on cardiac differentiation. Despite the challenge of having a robust cardiac differentiation, we believe that the EHT has proved itself to be reliable (Hansen et al. 2010; Conradi et al. 2011; Tiburcy

et al. 2011; Fredersdorf et al. 2012; Hirt et al. 2012; Friedrich et al. 2012; Stöhr et al. 2013; Neuber et al. 2014). Unlike the majority of in vitro studies which study single cells on a monolayer, the EHTs model allows to integrate the response of millions of cells in a three dimensional structure. Furthermore, it also allows to measure contractile force, which is also an unusual possibility for an *in vitro* cardiac model. Therefore, we decided to combine the potential of all those recent findings: iPS cells, fibrin based mini EHTs and improvements in cardiac differentiation in order to create the first model of human based disease-specific engineered heart tissue.

Materials and methods

Materials

6-well cell culture plates (Nunc, 140675)
24-well plates (Nunc, 144530)
15 mL EB estimation falcon (Sarstedt, 62.554.502)
250 mL vacuum filtration "rapid"-filtermax (TPP, 99250)
500 mL vacuum filtration "rapid"-filtermax (TPP, 99500)
Carbon electrode racks (custom made)
CASY® counter (Schärfe System GmbH, Model TT Version 2.1D)
Cell scraper (Sarstedt, 83.1830)

CTMV software (custom made)

Glass pendulum for 500 and 1000mL spinner flasks (Integra, 182 706)
Magnetic stirrer Variomag/ Cimarec Biosystem 4 Direct (Thermo scientific, 50088060)
Magnetic stirrer Variomag/ Cimarec Biosystem Direct (Thermo scientific, 70101)
Silicone racks (custom made)
Spinner flask, 500 mL (Integra, 182 051)
Spinner flask, 1000 mL (Integra, 182 101)
S88X dual output square pulse stimulator (Grass)
T175 cell culture flask (Sarstedt 83.1812.002)
T75 cell culture flask (Sarstedt 83.1813.002)
T80 cell culture flask (Nunc 178905)
Teflon spacer (custom made)
TissueLyser (Qiagen, 85220)
Video-Optical recording glass-roof box (custom made)
V-shaped sedimentation rack (custom made)

Reagents

0.9%-NaCl solution (B.Braun, 3570210)
10xDMEM (Gibco,52100-021)
1-Thioglycerol (Sigma-Aldrich, M6145)
2-Mercaptoethanol (Sigma-Aldrich, P3148)
2-Phospho- L -ascorbic acid trisodium salt (Sigma-Aldrich, 49752)
Agarose (Invitrogen, 15510-027)
Acetic acid (Roth, 6755.2)
Acrylamide/Bis 40% (Bio-rad, 161-0146)
Ammoniumpersulfate (APS) (Bio-rad, 161-0700)
B27® Supplement minus insulin (Gibco, 0050129SA)
B27® Supplement (Gibco, 17504-044)
BIOMYC-1 (PromoCell, PK-CC03-036-1B)
BIOMYC-2 (PromoCell, PK-CC03-037-1B)
Bromphenol Blue (Sigma, B-5525)
$CaCl_2$ (Merck, 2382)

Collagenase II (Worthington, LS004176)
Complete Mini (Roche, 11836153001)
Dithiothreitol (DTT) (Roth, 6908.2)
DMEM (Biochrom, F0415)
DMEM/F-12 (Gibco, 21331)
DNAse II, type V from bovine spleen (Sigma, D8764)
EDTA (Roth, 8043.2)
Fetal Calf Serum (Biochrom superior, S0615)
Fetal Calf Serum (PAA, A15-101)
Geltrex (Gibco, A1413302)
Glycerol (Merck, 1.04092)
HBSS, no calcium, no magnesium, no phenol red (Gibco, 14175-053)
HCl 37% fumant (Merck, 1.00317)
HEPES (Roth, 9105.4)
High-Capacity cDNA Reverse Transcription Kit (Applied Biosystem, 4368813)
Hotstar DNA Polymerase (Qiagen, 203205)
KCl (Merck, 4936)
Knockout Serum Replacement (Gibco, 10828)
Leukocyte Alkaline Phosphatase Kit (Sigma-Aldrich, 06R-1KT)
L-Glutamine (Gibco, 25030)
Lipid Mixture (Sigma-Aldrich, L5146)
Matrigel^{TM} (BD Biosciences, 354234)
Methanol (J. Baker, 8045)
$MgCl_2$ (Fuka, 63063)
Milk powder (Roth, 145.2)
Mitomycin C (Serva, 29805)
NaCl (JT Baker, 7647-14-5)
$NaHCO_3$ (Merck, 207-838-8)
NaH_2PO_4 (Merck, 6346)
NAF (Merck, 6449)
NEAA (Gibco, 11140)
PBS (Gibco, 10010-049)
Penicillin/Streptomycin (Gibco, 15140)
peqGOLD total RNA Kit (S-Line) (Peqlab, 12-6834-02)
Pluronic F-127 (Sigma-Aldrich, P2443)
Polyvinyl alcohol (Sigma-Aldrich, P8136)
Precision Plus Protein All Blue Standard (Bio-rad, 161-0373)
Puromycin dihydrochloride (Sigma-Aldrich, P8833)
RPMI 1640 (Gibco, 21875)
SDS Pellets (Roth, CN30.3)
Sodium selenite (Sigma-Aldrich, 51382)
Temed (Bio-rad, 161-0801)
Titriplex (Merck, 6381-92-6)
Transferrin human (Sigma-Aldrich, T8158)
Tris base (Sigma-Aldrich, T1503)
Trypsin/EDTA (Gibco, 25300)

Proteins and small molecules

Activin-A (R&D systems, 338-AC), stock concentration 50 µg/mL
Aprotinin (Sigma-Aldrich, A1153), stock concentration 33 g/L
Basic FGF (R&D, 233-FB), stock concentration 100 µg/mL
BMP-4 (R&D systems, 314-BP), stock concentration 50 µg/mL
CHIR99021 (Cayman Chemical, 13122), stock concentration 10 mM
DS-I-7 (custom made), stock concentration 100 mM (Lanier et al., 2013; Willems et al., 2011)
Fibrinogen (Sigma-Aldrich, F8630), stock concentration 200 g/L
Human Serum Albumin (Biological Industries, 05-720-1B)
Insulin (Sigma-Aldrich, I9278), stock concentration 10 g/L
IWR-1 (Sigma-Aldrich, I0161), stock concentration 20 g/L
Thrombin (Biopur, BP11-10-1104), stock concentration 100 U/mL
Y-27632 (Biaffin, PKI-Y27632-010), stock concentration 10 mM

Channels interacting drugs

Carvedilol (Sigma-Aldrich, C3993)
JTV-519 (Sigma-Aldrich, SML0549)
Dantrolene (Sigma-Aldrich, D9175)
Flecainide (Sigma-Aldrich, F6777)
Isoprenaline (Sigma-Aldrich, I6504)
SEA-0400 (synthesised by Dr. Ferenc Fülöp and kindly provided by Dr. Norbert Jos)

Stock solutions

EDTA (Roth 8043.2)
0.5 mM in PBS
Filter sterilized 0.2 µm (TPP, 99500), stored at 4°C.

Gelatin (Sigma-Aldrich G1890)
0.1% in water

Polyvinyl alcohol (Sigma-Aldrich, P8136)
4.5 g was dissolved in distilled water by boiling in a beaker.
Hot polyvinyl alcohol solution was poured in 500 mL RPMI 1640 (Gibco, 21875), residues (ca. 0.5 g) in the beaker were ignored.
Filter sterilized 0.2 µm (TPP, 99500), stored at 4°C.

HEPES (Roth, 9105.4)
1 M in PBS, pH adjusted to 7.4 with potassium hydroxide
Filter sterilized 0.2 µm (TPP, 99500), stored at 4°C

Transferrin-Selenium
27 mg of sodium selenite (Sigma-Aldrich, 51382) was dissolved in 400 mL PBS.
55 mg transferrin (Sigma-Aldrich, T8158) was dissolved in 99 mL PBS and 1 mL of previously made sodium selenite solution.

Pluronic® F 127 (Sigma-Aldrich, P2443)
1% (w/v) in PBS.
Filter sterilized 0.2 µm (TPP, 99500), stored at 4°C.

Aprotinin (Sigma-Aldrich, A1153)
33 g/L in aqua ad injectabilia, (Sigma-Aldrich, A1153-100 mg).
Transferred to 250 µL aliquots, stored at -20°C.

FACS Buffer
PBS (Gibco, 10010-049)
2% Fetal Calf Serum (Biochrom superior, S0615)
0.05% Sodium azide (Sigma-Aldrich, 438456)

Fibrinogen (Sigma-Aldrich, F8630)
0.9%-NaCl solution (B.Braun, 3570210) was prewarmed at 37°C
Fibrinogen was dissolved at 200 g/L (e.g. 5 g/25 mL)
Aprotinin stock of 33 g/L was added to reach a final concentration of 100 µg/mL (e.g. 72.1 µL/25 mL of fibrinogen solution).
Transferred to 200 µL aliquots, stored at -20 °C for short term and -80°C for long term.

Thrombin (Biopur, BP11-10-1104)

100 U/mL in 60% PBS.

Mixed thoroughly; transferred to 450 µL aliquots (stock) or 3 µL aliquots for EHT-generation, stored at -20°C.

10xDMEM (Gibco, 52100-021)

Dissolved at 134 g/L (e.g. 670 mg in 5 mL aqua ad injectabilia).

Filter sterilized 0.2 µm (TPP, 99500), stored at 4°C.

DMEM powder container was stored at 4°C and properly closed.

Agarose (Invitrogen, 15510-027)

2% in PBS, autoclaved, stored immediately at 60°C

2X Freezing Medium for pluripotent stem cells

DMSO, 20%

FTDA, 80%

Cell culture media

hES Medium
DMEM/F-12 (Gibco, 21331)
NEAA 1% (Gibco, 11140)
L-Glutamine 1% (Gibco, 25030)
Penicillin/Streptomycin, 0.5% (Gibco, 15140)
2-Mercaptoethanol, 100 µM (Sigma-Aldrich, P3148),
Knockout Serum Replacement 20% (Gibco, 10828)
Basic FGF 5 ng/mL (R&D, 233-FB)
Filter sterilized 0.2 µm (TPP, 99500), stored at 4°C

Mouse Embryonic Fibroblasts Medium
450 mL DMEM (Gibco, 41965-039)
Fetal calf serum, 10% (PAA, A15-101)
Penicillin/Streptomycin, 1% (Gibco, 15140)
L-Glutamine, 1% (Gibco, 25030)
Filter sterilized 0.2 µm (TPP, 99500), stored at 4°C

MEF-Conditioned Medium (CM)
Primary mouse embryonic fibroblasts were cultured from CF-1 mice until passage 3.
MEFs were mitotically inactivated with Mitomycin C (10 µg/mL for 2.5 – 3 h; Serva, 29805)
Inactivated MEFs were then carefully washed with PBS and dissociated with trypsin/EDTA (Gibco, 25300)
T175 cell culture flask (Sarstedt 83.1812.002) were coated with 0.1% gelatin for at least 1 hour at 37°C before plating MEFs
The cell number of inactivated MEF were counted and plated ca. 60000/cm² into each T175 flask ($10x10^6$/T175 cell culture flask) in MEF medium
Cells were evenly distributed across the flask and incubated overnight to attach

MEF-medium was then aspirated and rinsed with PBS
hES medium was added to the cell culture flask
After 24 hours conditioned medium was collected in a sterile receiving unit
Using a 25 mL pipette, 70 mL of hES medium was added to the cell culture flask
Medium was collected after 24 hours
The MEF cell culture flasks were used during 7 – 10 days to produce Conditioned Medium with a daily medium collection
If not used directly, Conditioned Medium was stored at -80°C
MEF were microscopically monitored during the last days of conditioning and the procedure was stopped if MEFs started to detach

Before its use on human pluripotent stem cells:
Conditioned Medium was thawed or used freshly.
Basic FGF (10 ng/mL; R&D, 233-FB) was added to achieve a final concentration of 15 ng/mL
Filter sterilized 0.2 µm (TPP, 99500), stored at 4°C for 1-2 weeks

Collagenase II solution
HBSS, no calcium, no magnesium, no phenol red (Gibco, 14175-053)
Collagenase II (200 units/mL (Worthington, LS004176)
HEPES, 10 mM (Roth, 9105.4)
Filter sterilized 0.2 µm (TPP, 99500), stored at 4°C

DMEM+DNAse

2x DMEM
10xDMEM, 20% (e.g. 2 mL)
Fetal Calf Serum (heat inactivated) 20% (e.g. 2 mL)
Penicillin/ Streptomycin, 2%, (Gibco, 15140), (e.g. 0.2 mL)
Aqua ad injectabilia (e.g. 5.4 mL)
Filter sterilized 0.2 µm (TPP, 99500), stored at 4°C

iPS-EHT medium
DMEM (Gibco, 41965-039)
Penicillin/ Streptomycin, 1%, (Gibco, 15140)
Horse Serum 10%, heat inactivated, (Biochrom, S 0615)
Insulin, 0.1% (=10 µg/mL), (Sigma, I9278)
Aprotinin 0.1% (=33 µg/mL), (Sigma, A1153)
Filter sterilized 0.2 µm (TPP, 99500), stored at 4°C

Tyrode solution (0.2mM Ca)
$CaCl_2$, 29.8 mg/L
$MgCl_2$, 213.6 mg/L
NaCl, 7 g/L
KCL, 400 mg/L
$NaHCO_3$, 1.9 g/L
NaH_2PO_4, 58 mg/L
Glucose, 1 g/L
Titriplex, 18.6 mg/L
Hepes, 25 mM
Soluted in water

Procedures

All procedures described below are described with CM as an example, but the procedures can be performed with any medium used to culture iPS cells.

Geltrex® coating

Geltrex® (Gibco, A1413302) was thawed on wet ice.
It was diluted 1:200 in ice cold DMEM.
1 mL per well (6-well format) or 7 mL per T80 cell culture flask, Nunc (178905) was then added.
Plate was incubated at 37°C for 30-60 minutes.

Freezing of undifferentiated iPS cells

PBS, 0.5 mM EDTA and CM were prewarmed.
Freezing medium was prepared.
iPS cells were washed with PBS.
They were incubated with EDTA 0.5 mM for 10 min at 37 °C.
EDTA solution was removed, flushed and iPS cells were resuspended in CM.
500 µL 2x freezing medium was mixed with 500 µL of the resuspended cells
Y-27632 (10 µM) was added.
The cells were transferred to a freezing tube.
The tube was frozen at -80 °C overnight in a 2-propanol filled freezing container.
Tubes were transferred to liquid nitrogen for long term storage.

Heat inactivation of serum

Fetal Calf Serum (Biochrom superior) was thawed at room temperature.
It was then incubated in a water bath at 57°C for 60 minutes.
50 mL aliquots were then made and stored at -20°C.

Thawing of undifferentiated pluripotent stem cells

Cell culture flasks/dishes were coated with Geltrex®.

CM was prewarmed.

Freezing tube was removed from liquid nitrogen and thawed at 37°C.

Cells were transferred to a 15 mL falcon.

10 mL of CM was added dropwise for the first 2 mL.

Cells were centrifuged at 200 g for 5 min.

Supernatant was removed and re-suspend in desired volume of CM.

Expansion of undifferentiated pluripotent cells

CM medium was aliquoted for a daily medium change.

CM aliquots were prewarmed for daily use.

Cells were fed with 2.5 mL of prewarmed CM per well per day.

One day feeding per week was skipped by feeding with 4 mL CM on the previous day.

Incubator conditions: 37°C, 90% humidity, 5% CO_2

Passaging

Cell culture flasks/dishes were coated with Geltrex®.

15 mL of CM per 6-well dish was aliquoted to reseed the iPS cells.

PBS, 0.5 mM EDTA and CM was prewarmed.

Confluent iPS cells were washed twice with 2 mL prewarmed PBS per well (6-well plate) .

1 mL 0.5 mM EDTA solution was added per well.

Cells were incubated for 5 min at 37°C.

EDTA was removed.

Each well was vigorously flushed with 1.5 mL CM to detach cell clusters.

Detached cell clusters were pooled and gently mixed with remaining medium.

Diluted Geltrex® coating from new 6-well dish was removed and 2.5 mL of cell solution per well was immediately added.

A passage splitting ratio from 1:3 to 1:6 was performed.

Mycoplasma screening

250 µL cell culture medium were transferred to a sterile Eppendorf tube after overnight incubation

750 µL sterile water was added and the tube was mixed.

The diluted sample was incubated for 10 minutes in a thermo block at 100°C.

The tube was centrifuged by a quick spin to gather all droplets.

The supernatant (containing DNA) was used to prepare PCR

Preparation of PCR mastermix (Quiagen, 203205)

Component	Per reaction
H_2O	26.75 µL
10 x buffer	5.0 µL
Q-Solution	10.0 µL
$MgCl_2$ (25mM)	4.0 µL
Primerpool (10 pM)	1.0 µL
DNTP's	1.0 µL
Polymerase	0.25 µL
Sum	48.0 µL

Primer sequences

Myco-dw: 5'-TGC ACC ATC TGT CAC TCT GTT AAC CTC-3'
(Eurofin MWG Operon, H13629 14-3171-2/2)

Myco-up: 5'-ACT CCT ACG GGA GGC AGC AGT A-3'
(Eurofin MWG Operon, H13624 14-3171-1/2)

PCR

2 µL of the sample's supernatant was taken and added to 48 µL mastermix.
The PCR cycler program was started immediately after:

Cycler	time (t)	°C	Cycles
Initiation	15 min.	95	1
Denaturation	30 sec.	94	
Annealing	30 sec.	56	40
Extension	1 min.	72	
Final Extension	10 min.	72	1

After finishing the PCR, the samples were loaded on a 1% agarose gel and ran for 25 minutes.
Positive and negative control samples were used as a reference.

Treatment of mycoplasma infections

For the treatment of mycoplasma infections, BIOMYC Antibiotic Solutions (PromoCell) were used.

BIOMYC-1 and 2 are two antibiotics, which eliminate mycoplasmas very efficiently when used sequentially.

The contaminated cell culture first treated with BIOMYC-1 for four days and then for three days with BIOMYC-2 according to manufacturer's instructions.

2 to 3 treatment cycles were repeated to avoid antibiotic resistance.

Cleaning protocol for spinner flasks

Spinner flasks were cleaned manually with a flask brush and distilled water.

They were then left to dry before being autoclaved.

Freezing of cell pellet

Desired amount of cells were transferred to 1.5 mL tubes.

Tubes were centrifuged at 250 g for 5 min.

Supernatant was removed and tubes were snap frozen in liquid nitrogen.

Tubes were stored at -80 °C.

RNA Lysis (peqGOLD Total RNA Kit)

Single cells were transferred to a 1.5 mL tube and centrifuged after dissociation (cf. Dissociation of differentiated cells).

Cells were resuspended in 400 µL of RNA Lysis Buffer T.

RNA samples were then stored at -80 °C.

PCR

Hotstar DNA Polymerase (Qiagen, 203205) kit was used.
All reagents were stored at -20 °C, thawed the day of the PCR and kept on ice.
The master mix was calculated as following for each reaction mix:

10*PCR Buffer	**50µL**
dNTP mix	1 µL
Primer pool	0.5 µM
HotStarTaq DNA Polymerase	0.5 µL
Distilled water	Variable
Template DNA	1 µg
Total Volume	50 µL

Total volume of the reaction was adjusted with distilled water to equal 50 µL.
10% of extra volume was calculated to compensate pipetting volume loss.
Mastermix was then transferred to the desired amount of tubes and desired DNA was added afterwards.
Tubes were placed in the thermal cycler, and the following program was performed:

Initial heat activation	**15 min**	**95°C**
Denaturation	1 min	94°C
Annealing	1 min	5°C below T_m of primers
Extension	1 min	72°C
Number of cycles	35	
Final extension	10 min	72°C

Tubes were then further stored at 4°C.

Primer sequences

RYR2 (PAS5 ; PAS7)

Forward Primer:

5'-GCGAGCTCGCGGGGCTCGGGAGCCGGCCCCGGCGAGGAGGCGCGGAACCATGGCCGATGG
GGGCGAGGGCGAAGACGAGATCCAGTTCCTGCGAACTGATGATGAAGTGGTTCTGCAGTG
CACCGCAACCATCCACAAAGAACA-3'

Reverse Primer:

5' –TTCTCATCAGTTCGCAGGACTGGATCTCGTCTTCGCCCTCGCCCCCATCGGCCATGGTTC
CGCGCCTCCTCGCCGGGGCCGGCTCCCGAGCCCCGCGGAGCTCGGCGGCGGCGGCGGCCC
CTGGCGCTGCCTTCTGCTTCTGCTGCCAAC-3'

Reverse Transcriptase

High-Capacity cDNA Reverse Transcription Kit (Applied Biosystem, 4568813) was used.
The following mastermix was done:

	Mastermix with Reverse Transcriptas	Mastermix without Reverse Transcriptase
10X RT Buffer	2 μL	2 μL
25X dNTP Mix (100 mM)	0.8 μL	0.8 μL
10X RT Random Primers	2 μL	2 μL
Reverse Transcriptase	1 μL	1 μL
RNA	200 ng	200 ng
Water	Complete to 20 μL	Complete to 20 μL
Total per Reaction	20 μL	20 μL

Tubes were placed in the thermal cycler, and the following program was performed:

	Step 1	Step 2	Step 3
Temperature (°C)	25	37	85
Time (min)	10	120	5

Tubes were then further stored at 4 °C.

Sequencing:
Samples were sent to Eurofin MWG Operon for sequencing

FACS, measuring cardiomyocyte purity

After dissociation, cells were counted and 300,000 were collected into a FACS tube.
The cells were centrifuged at 300 g for 5 min.
The cells were fixed with 100% methanol solution at -20 °C solution, and left at 4 °C for 30 min.
Cells were washed twice with PBS with two centrifugation steps at 300 g for 5 min.
Cells were incubated into FACS-Buffer with 0.5% saponin for 10 min at room temperature.
Cells were then centrifuged, resuspended in a mouse anti-α-MHC primary antibody diluted into the previous buffer (2 μg/mL), and incubated for 45 min at 4 °C.
Cells were washed twice with previous buffer.
Cells were incubated with anti-mouse Alexa 488 (2 μg/mL) secondary antibody for 45 min at 4 °C protected from light.
Cells were washed twice with the previous buffer.
Cells were resuspended in 250 μL PBS.

Generation of human EHT

Prearrangements

Sterile teflon spacer
Sterile silicone racks
Fibrinogen stock
Thrombin aliquots
24-well plates
Liquid sterile agarose (kept in the heated cabinet at 60°C)
2xDMEM
Collagenase II solution
EHT-FCS medium

Preparation of teflon spacers

Teflon spacers were cleaned with water.
Teflon spacers were boiled twice in distilled water.
Teflon spacers were then autoclaved.
Note: No detergents were used to clean the teflon spacers.

Preparation of silicone racks

Silicone racks were cleaned with water.
Silicone racks were boiled twice in distilled water.
Silicone racks were then autoclaved.
It was made sure that the silicone racks wouldn't be kept in a position that could have distorted flexible posts.
Note: No detergents were used to clean silicone racks.

Preparation of mastermix

Total mastermix volume was estimated from the cell count with $0.5x10^6$/EHT.
Mastermix was pipetted up-and-down thoroughly until fibrinogen was dissolved.
Supernatant was discarded, and cell pellet was resuspended in the mastermix.
Cells were kept on ice until use.

Note:
Matrigel^{TM} was added in ice cold medium.
The mastermix was directly added to the cardiomyocytes to avoid shear stress.
Air bubble formation was avoided during pipetting.
If more than 8 EHTs were made, 10% extra mastermix volume was added to the cells to compensate for pipetting loss

Mastermix calculation per EHT

NKM	79 μL
Fibrinogen stock	2.5 μL
Matrigel™	10 μL
2xDMEM	5.5 μL
Y-27632	10μM
Dissociated cells	0.5×10^6

Note: Cardiomyocytes are sensitive to centrifugation at high speed, they were never centrifuged faster than 100 g.

Generation of casting molds

1.6 mL of liquid agarose was pipetted (2%, PBS, 60 °C) into only 8 wells of a 24-well plate as agarose solidifies quickly.
Teflon spacers were placed onto these wells directly after pipetting.
The procedure was repeated until the amount of casting molds equalled the amount of desired EHTs.
Agarose was let to solidify at room temperature for 10-15 minutes.
Teflon spacers were removed, silicone racks were positioned on the 24-well plate and it was made sure that each pair of silicone posts reached into an agarose casting mold.

Note: Nunc, cat# 144530 was used, and as 24-well plates do not have standardised dimensions, plates from other suppliers might not fit. Furthermore, longer agarose solidification times result in fine cracks in the surface, which makes the casting molds leaky and decreases the efficiency of EHT generation.

Pipetting EHTs

97 μL mastermix was briefly mixed with one 3 μL thrombin aliquot.
The mixture was then quickly transferred into an agarose casting mold with the silicone racks placed on top.
This step was repeated for each EHT separately.
The 24-well plate was left for 90-120 minutes in the incubator (37 °C, 7% CO_2, 40% O_2, 90% humidity).
Fibrin gels were topped in the casting molds with 200-300 μL DMEM per well, enough to cover the surface.
Plates were incubated for additional 5 minutes.
A 24-well plate with prewarmed iPS-EHT medium at 1.5 mL per well was prepared, and silicone racks with fibrin gels were carefully transferred from the casting mold plate to the cell culture plate.

Note: A new filter pipette tip was used for pipetting each EHT to avoid thrombin contamination.

The mastermix was carefully resuspended after 4-8 EHTs.

Air bubble formation was avoided during pipetting.

The addition of medium on top of the EHT before transfer will ease the removal from the casting molds and improve the efficiency of the EHT generation.

EHT medium change

The EHTs were maintained under cell culture conditions for 2 weeks (37 °C, CO_2 7%, 40% O_2, 90% humidity).

Medium change was performed on Mondays, Wednesdays and Fridays.

For the feeding, a second 24-well plate with iPS-EHT medium was prepared, and the silicone rack containing EHTs was then carefully transferred.

Two 24-well plates were kept during the entire EHT's life span and they were transferred back and forth between the two.

Microscopic monitoring of EHTs during development

Single cell contraction	Day 2-5
Coherent contraction of small areas of cells	Day 5-10
Coherent contraction of the entire EHT	Day 10-15

EHT measuring

A 24-well plate with 1.5 mL tyrode solution in each well was preincubated for at least 1 hour at 37°C, 90% humidity, 5% CO_2 and 40% O_2.

Gases of the Video-Optical recording glass-roof box ("White box") were switched on 15 min before the starting of the recording in order to get the desired gas composition.

EHTs racks were carefully transferred under sterile conditions to the preincubated tyrode plates. The position of the rack on the 24-well plate was carefully monitored as it could affect the figure-recognition of the CTMV software.

The EHTs were then quickly transferred to the white box before any consequent loss of temperature.

EHTs were left to incubate for at least 10 min before the recording in order compensate for the loss of gases and temperature during the opening of the white box.

After the recording, EHTs were replaced in their initial 24-well plate with feeding medium.

Recording tyrode plate was discarded.

EHT Pacing

A 24-well plate with 2 mL tyrode solution in each well was preincubated for at least 1 hour at 37 °C, 90% humidity, 5% CO_2 and 40% O_2.

Gases of the Video-Optical recording glass-roof box ("White box") were switched on 15 min before the starting of the recording in order to get the desired gas composition.

Carbon electrode rack was placed under sterile conditions in every row of the tyrode 24-well plate.

EHTs racks were carefully transferred under sterile conditions on top of the carbon electrode racks.

The EHTs were then quickly transferred to the white box and all the electrical connections were completed.

EHTs were paced at 2.0 V with bidirectional pulses of 4 ms duration.

The adequate pacing frequency had to be found so that all EHTs would not beat spontaneously but only according to the pacing signal. In some case this was not possible and some EHTs had to be excluded.

Once the experiment was finished, the EHTs were transferred back to their feeding plates and the electrodes were washed for 3 times 12 hours with distilled water, renewing the distilled water for every bath.

Calcium CRC (Concentration Response Curve)

A 24-well plate with 2 mL tyrode solution in each well was preincubated for at least 1 hour at 37 °C, 90% humidity, 5% CO_2 and 40% O_2. The tyrode solution only contained 0.1 mM calcium.

The same procedure was then performed as in the pacing paragraph (cf. **EHT Pacing**).

The EHTs were incubated in the low calcium tyrode solution until they stabilised their beating force and frequency.

They were then recorded, additional calcium was added to each individual well to reach the desired concentration of the next step of the CRC.

EHTs were incubated at least 10 min in the white box before starting every recording.

After the recording, the EHTs were washed 2 times 15 minutes in a standard calcium tyrode concentration of 1.8 mM, renewing the tyrode medium once between the two washes.

EHTs were replaced in their initial 24-well plate with feeding medium.

Recording and washing tyrode plate were discarded.

Post-rest potentiation

The same procedure was first performed as in the pacing paragraph (cf. **EHT Pacing**).

The pacing was then stopped for 1, 2, 4, 8 and 16 seconds intervals before being switched back on again.

EHTs were replaced in their initial 24-well plate with feeding medium.

Recording tyrode plates were discarded and electrodes were washed as described previously (cf. **EHT Pacing**).

Drug stimulation

Similarly to the calcium CRC experiment (cf. **Calcium CRC**) the drug was pipetted in every individual well starting from the lowest and going to the highest concentration. The EHTs however were recorded without pacing as described as in the EHT measuring paragraph (cf. **EHT measuring**)

Overnight calcium

The same procedure was first performed as in the EHT measuring paragraph (cf. **EHT measuring**) except that the tyrode plate was of either 1.8, 3.0 or 5.0 mM calcium concentration.
The EHTs were left to record overnight with one recording every 30 min.
After the recording, the EHTs were washed 2 times 15 minutes in a standard calcium tyrode concentration of 1.8 mM, renewing the tyrode medium once between the two washes.
EHTs were replaced in their initial 24-well plate with feeding medium.
Recording and washing tyrode plate were discarded.

Isolated Ventricular Trabecula Carnae, experiment performed by PD Dr. T. Christ

Explanted hearts were placed immediately (<1 min) after removal from the patient into a cardioplegic solution. The endocardial layer of the right ventricular free wall was rapidly dissected in ice-cold, preoxygenated (95% O_2-5% CO_2) modified Krebs' solution containing (mM) Na^+ 125, K^+ 5, Ca^{2+} 2.25, Mg^{2+} 0.5, Cl^- 98.5, SO_4^{2-} 0.5, HCO_3^- 29, HPO_4^{2-} 1, and EDTA 0.04 at the surgical theater. Trabeculae (width usually <1 and not >1.3 mm) were dissected, set up at optimum length, and paced to contract isometrically at 60 bpm at 37 °C in a bath containing the above solution supplemented with (mM) Na^+ 15, fumarate 5, pyruvate 5, l-glutamate 5, and glucose 10 as described.

Right or left ventricular trabeculae were dissected, mounted on to tissue electrode blocks and electrically paced at 1 Hz to contract; contractile force and its first derivative were recorded simultaneously.

Pictures of iPS cells, performed by Dr. Weber

The iPS cells were placed in an incubation chamber at 37°C.
An Olympus IX81 microscope equipped with appropriate filter sets for mCherry (U-MWIG2, Olympus), Venus (U-MNIBA2, Olympus) and Cerulean (F36-710, Semrock) was used.
Pictures were taken with an Olympus ColorViewII charge-coupled device camera.

Pictures of EHTs, performed by N. Mangels

The EHT was placed in an incubation chamber at 37°C on a petri dish with a few drops of medium on top.
Microscope used was a Nikon T inverted, confocal unit with a A1 camera with a galvano scanner and a resonant scanner unit.
Excitation was performed with 405, 488 and 561nm respectively for mTag BFP, Venus and mCherry.
The filter cube settings were set at 450nm +-50, 525nm +-50 and 595nm+-50 nm.

FACS of RGB cells

After dissociation, cells were resuspended in PBS and collected into a FACS tube.
Cells were then directly analysed by FACS.

Results

Part 1: Cell culture and differentiation

As a prerequisite to study patient-specific EHTs, we had to establish a method to culture and differentiate multiple iPS cell lines into cardiomyocytes. In this first part of my thesis I thus concentrate on results gained in close collaboration with Dr. Schaaf and Dr. Breckwoldt (Schaaf 2011; Breckwoldt 2015), how to optimize cell culture in defined culture medium and describe how we established a unique differentiation protocol to simplify the differentiation process of multiple cell lines to a maximum. The productivity, purity, simplicity and costs of the protocol will be determinant parameters as EHT models require a considerable amount of cardiomyocytes. Although a relative large number of protocols are available for cardiac differentiation, most of them are not adapted for an upscaling of cardiomyocyte production and therefore not applicable to EHT generation.

A fibroblast-derived cell line from a healthy individual was used to optimise the differentiation protocol. This line and different patient-specific cell lines were run in parallel to ensure cell line independence of the protocol. The control cell line was kindly provided by Moretti et al. and the patient-specific ones were reprogrammed in our laboratory by Dr. Laufer and Dr. Shibamyia

All findings described in this section were tested on different cell lines and showed similar results, however some of the figures only show representative result from a single cell line for simplification.

1. **Undifferentiated cell culture**

The first challenge in iPS cell culture is to keep the cells undifferentiated, as iPS cells are prone to spontaneously differentiate, potentially hindering later directed differentiation to cardiomyocytes. In this part, I present some of the key factors and methods we identified as crucial to maintain iPS in an undifferentiated state: how FGF concentrations have a crucial impact on the iPS cells expression of pluripotent markers, how the cells can be successfully changed to a different cell culture medium and how the passaging number can have an impact on the culture.

1.1. Conditioned medium and basic FGF concentration

Basic FGF (bFGF) concentration in stem cell culture medium is crucial in order to keep the cells undifferentiated (Levenstein et al. 2006). The mechanism is believed to be mediated by a stimulatory effect of bFGF on the expression of the pluripotency factor *Nanog* (Frank et al. 2012). To find the optimal bFGF concentration depending on the culture media we were using, we performed an experiment where we cultured different iPS cell lines for 4 days in two different culture media with varying bFGF concentrations. The cells were then dissociated, and a qPCR was performed to measure *Nanog* mRNA concentration, a pluripotency marker (**Fig. 1**).
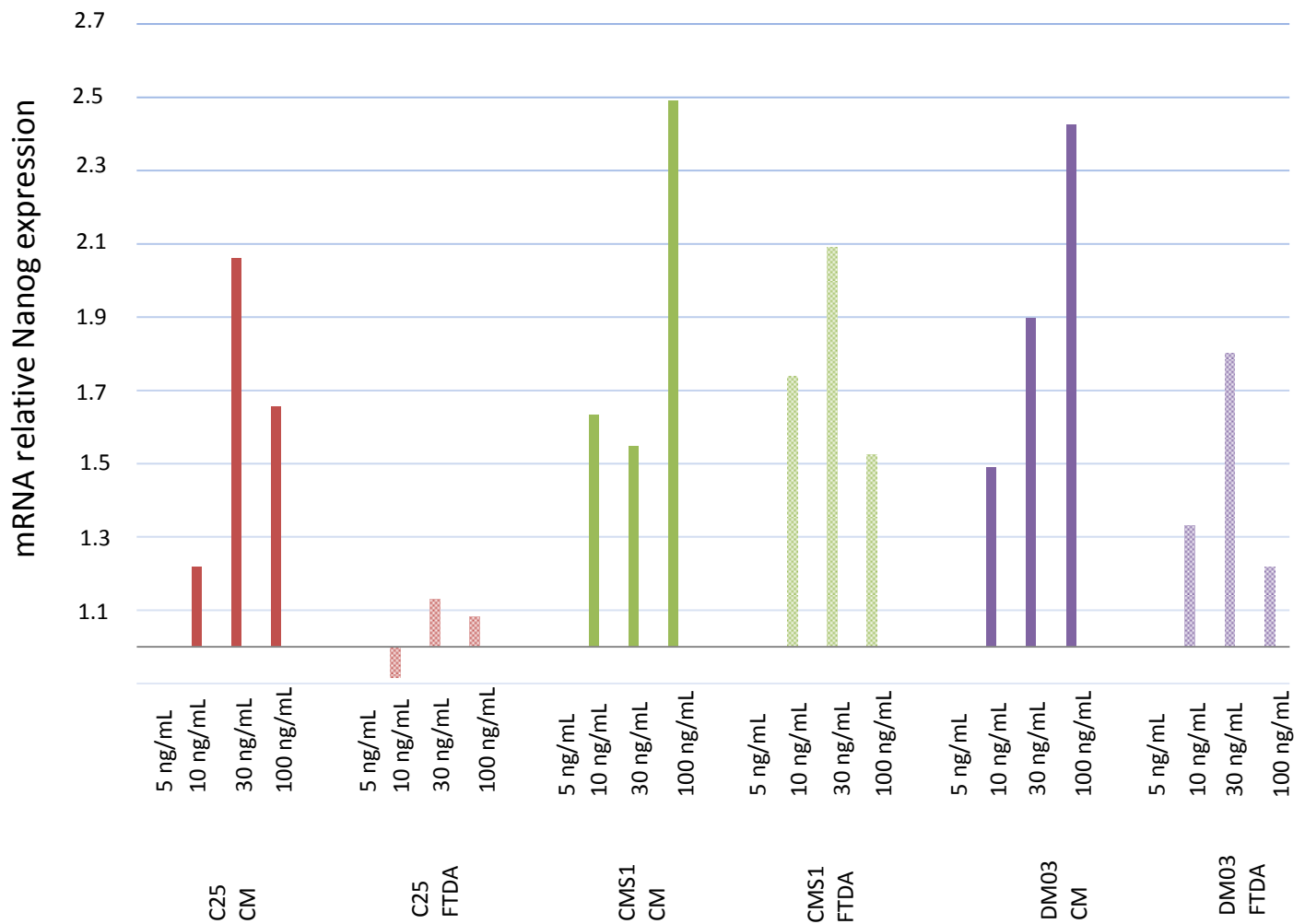
Fig. 1*: Relative Nanog mRNA concentration with qPCR analysis after 4 days of culture in different bFGF concentrations. C25, CMS1, DM03 represent different iPS cell lines while CM (Conditioned Medium) and FTDA represent two different culture media. All results were standardised to the relative Nanog expression of the cells cultured in 5 ng/mL bFGF compared to a housekeeping gene. The results globally show increased expression of Nanog with increased concentrations of bFGF up to 30 ng/mL, independently of the cell line or the cell culture medium. No clear Nanog increase can be observed for the last concentration compared to 30 ng/mL. Experiment performed by Dr. Breckwoldt.*

The previously used cell culture condition of 5 ng/mL almost systematically showed the lowest *Nanog* mRNA concentration, independently of cell line and culture medium. An increase to 10 and 30 ng/ml bFGF increased Nanog mRNA levels of 1.2 and 2.1-fold respectively for C25 in CM medium. Similar data were obtained for CMS01 CM, CMS01 FTDA, DM03 CM and DM03 FTDA. The relative mRNA concentration of *Nanog* increased in all cell lines and all conditions for bFGF > 5 ng/mL in the culture medium, except for C25 FTDA 10

ng/mL bFGF where the relative mRNA concentration of *Nanog* decreased to 0.9 fold of the initial 5 ng/mL bFGF condition. In Conditioned Medium, C25 showed the highest increase in *Nanog* transcript concentration at 30 ng/ml, CMS1 and DM03 at 100 ng/ml. In all cell lines cultured in the defined FTDA medium, the expression level of *Nanog* peaked at 30 ng/ml FGF concentration (**Fig. 1**).

Given that the cells with the highest level of Nanog expression should be the most pluripotent, optimal cell culture conditions should be using 30 ng/mL as standard bFGF concentration according to the experiment. Furthermore, parameters like morphology, cell proliferation and differentiation potential (data not shown) confirmed that 30 ng/ml was a suitable concentration and it was decided to use 30 ng/ml bFGF containing FTDA medium to maintain and expand the iPS cell culture.

1.2. Culture in Essential 8 medium

Variability is a crucial point of iPS cell culture and is at least partially induced by the variability of the medium itself, particular animal-derived supplements such as serum. CM medium was routinely used to culture iPS cells in our facilities due to its cost effective aspect as it can be home-made. To be produced, some chemically defined medium supplemented with serum replacement was incubated overnight on a murine inactivated fibroblast culture. This medium was therefore not fully defined as undefined fibroblast excretions would be present after an overnight incubation. To reduce medium variability, a defined medium Essential 8 (E8), was tested (Chen et al. 2011). This medium is only composed of eight defined compounds, which could avoid batch dependent culture medium.
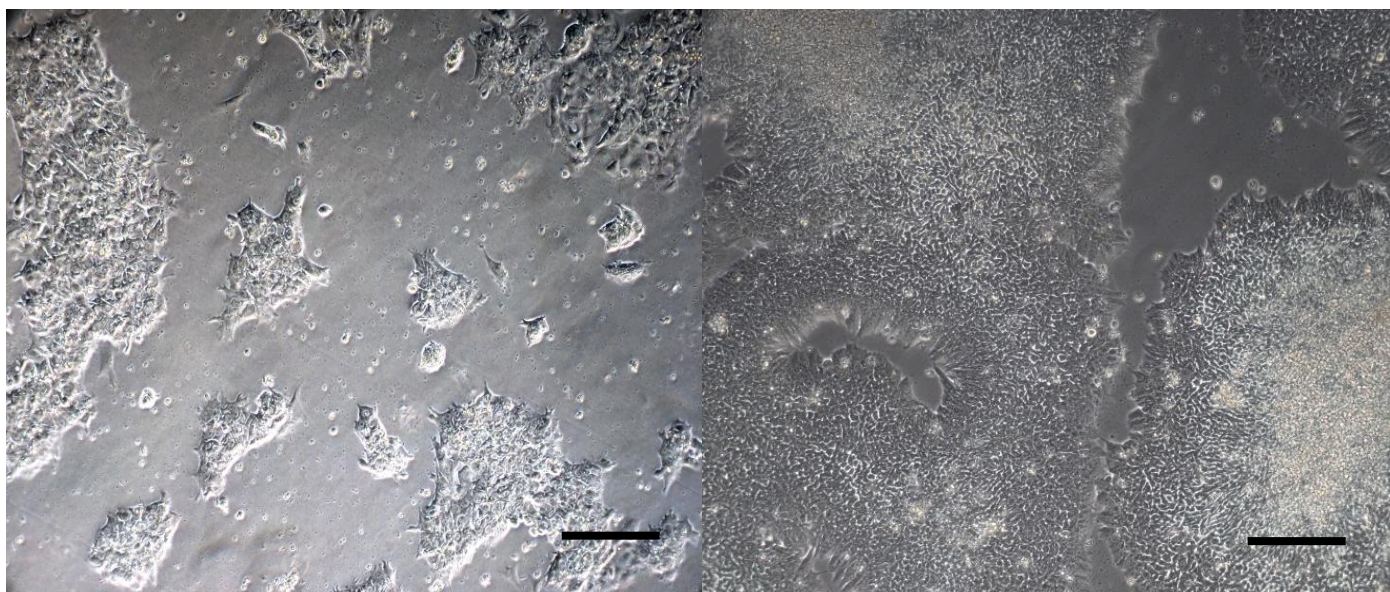
Fig. 2: iPS cell line C25 cultured in CM (left) and in E8 medium after one passage (right). Scale bar, 250 µm.

After one passage in E8, the cells kept their undifferentiated status which could be determined by a typical "cobblestone" morphology (**Fig. 2**). This morphology displays small cells densely packed together, roughly forming a circle after 2 to 3 days of colony expansion. The cells at first seemed to have well endorsed the medium switch to E8, but after four passages, differentiated cell morphology appeared in some of the colonies (**Fig. 3b**). After passage 6, the cells hardly divided anymore and the culture had to be discarded. The three-dimensional stack of cells in the lower right corner clearly indicated a total loss of undifferentiated status (**Fig. 3d**).
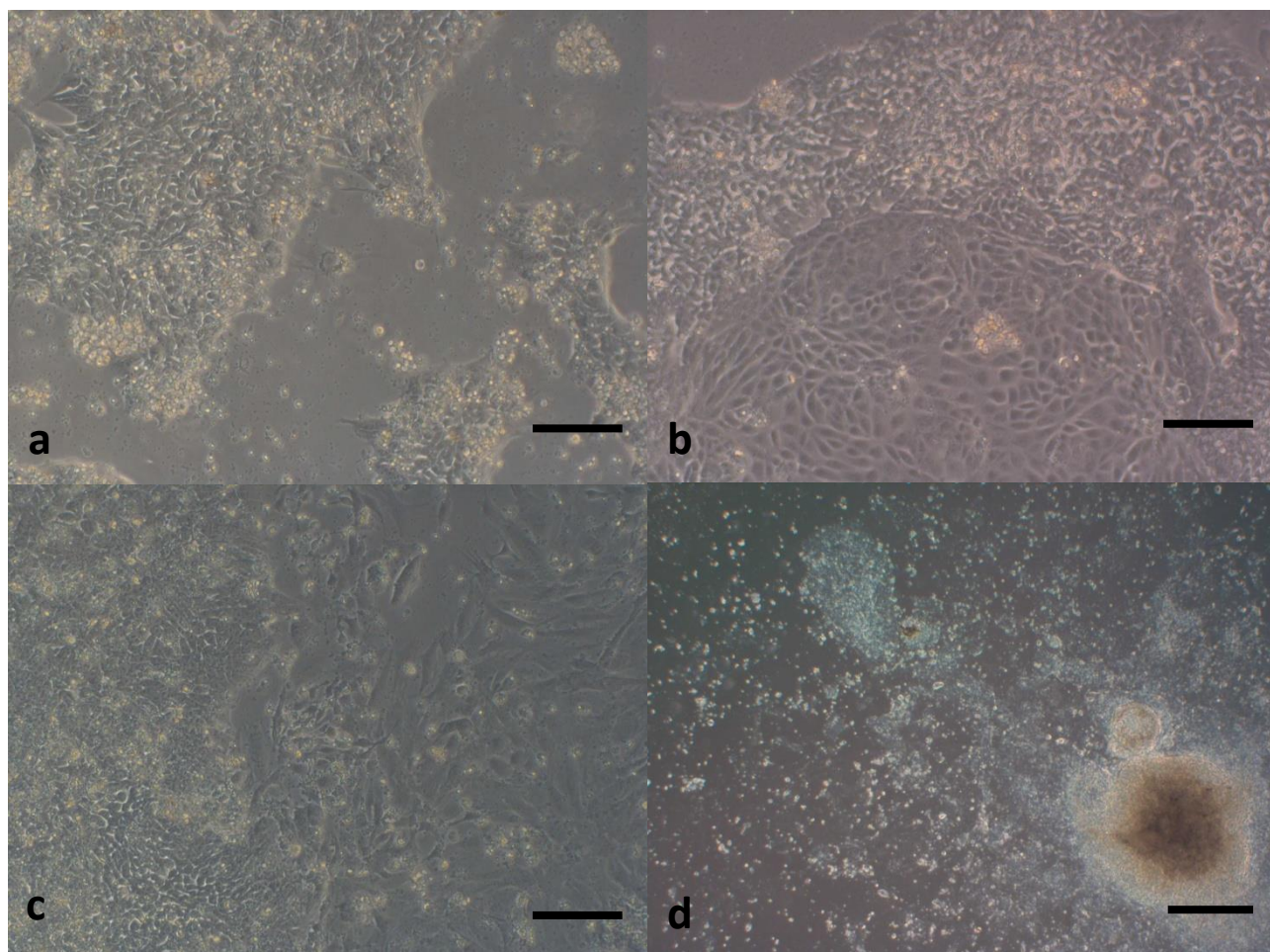
*Fig. 3: iPS cell line C25 cultured in E8 medium. **a.** after 3 passages **b.** after 4 passages **c.** after 5 passages **d.** after 6 passages. Scale bar, **a. b. c.** 250 µm, **d.** 1 mm*

At this point, our attempts to culture the cells in E8 medium did not succeed. However, after a culture guideline was published by Life Technologies™ we could culture the cells in E8 medium by providing a 25% successive stepwise medium change by mixing CM and E8 together (i.e 75% CM 25% E8, 50% CM 50% E8, etc.) (**Fig. 4**). Under these conditions, the typical "cobblestone" morphology of the cells could be observed and indicated the pluripotent state of the cells (**Fig. 4b**). The culture could be cultured up to any desired passage number. However, another defined medium named FTDA was preferred to E8 at the end of the project (Frank et al. 2012).
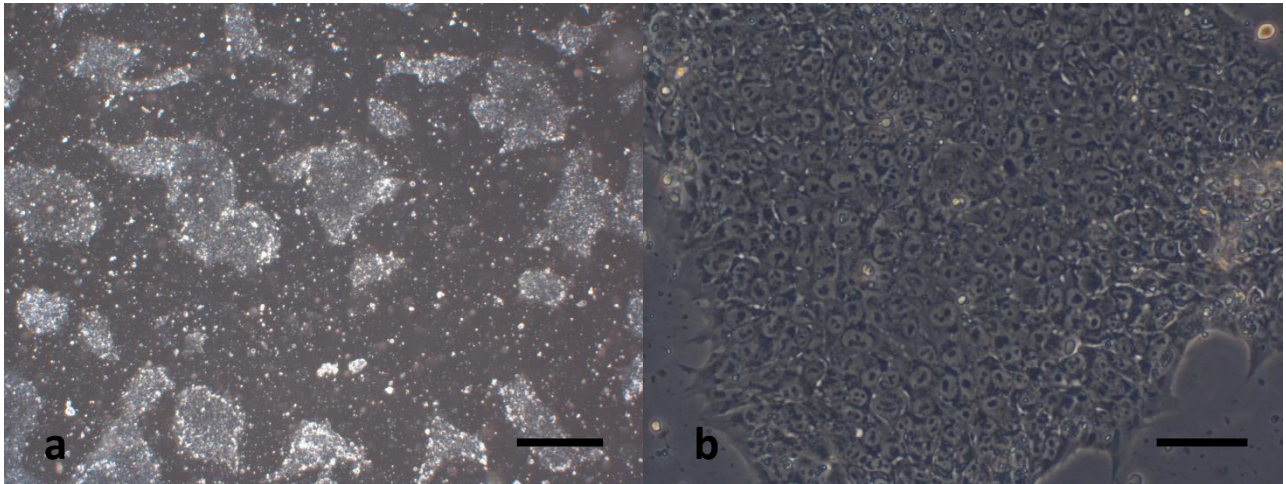
Fig. 4: *iPS cell line C25 routinely cultured in E8 medium.* **a.** *2 days after passage, scale bar 1mm* **b.** *2 days after passage, scale bar 250 µm.*

1.3. Cell culture and high passage number

iPS cells are immortal and can therefore be cultured for theoretically an unlimited amount of time. However, their chances of acquiring mutations and chromosomal abnormalities increase over culture time. If those acquired differences would lead to an advantage in term of proliferation, seeding or survival, it could multiply in the culture and finally be present in every cell, which is why the cells should not be kept for too many passages in culture. This phenomenon will be studied more deeply in the third part of this thesis and will be referred as "sub-clonal dynamics". The karyotype of a younger and an older passage of a cell line was compared using a fluorescence in situ hybridization technique (FISH), and the presence of an extra-chromosome 19d could be observed in the older passage (**Fig. 5**).
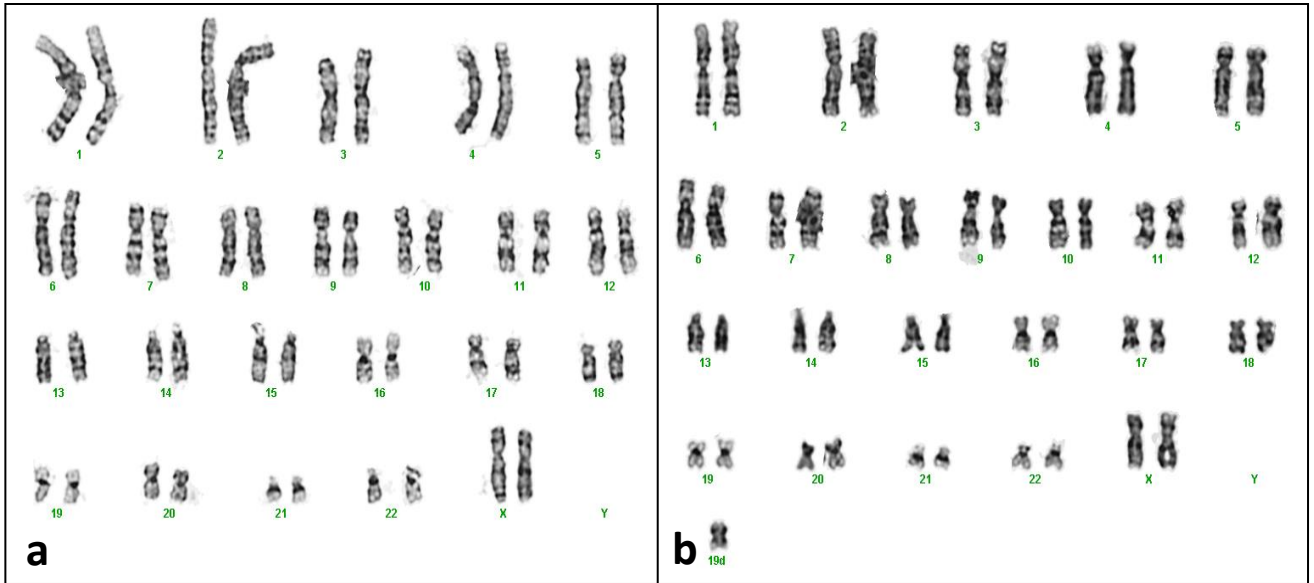
Fig. 5: Karyotype analysis a iPS cell line C25 passage 40, karyotype: 46,XX. b. iPS cell line C25 passage 149, karyotype: 47,XX,+19d, with an aberrant extra-chromosome.

However, an aberrant karyotype could also be found at the beginning of the culture due to an initial abnormal karyotype in the original clone selected after the reprogramming. Therefore, the karyotype of every cell line was verified at the beginning of every cell culture, to make sure that no clone with a chromosomal aberration had been selected (Figures not shown).

2. EB formation

In order to mimic the early embryo conditions, the cells were manipulated so they would generate an embryo-like 3D structure named embryoid body (EB). This conformation was shown to be important for the mimicking of the first steps of embryonic development. In addition, cells were kept at 5% O_2, comparable to the hypoxic conditions during very early embryogenesis before implantation. This stage is the first step of the differentiation process and the formation of EBs was technically challenging. In human cell lines, only a few methods were available: spontaneous EB formation, forced aggregation or spinner flask induced EB

formation. All three methods listed hereafter were tested before deciding which was the most optimal for a relatively large production quantity of different cell lines.

2.1. Spontaneous EB formation

This method is the most basic one which consists of scratching the surface of the cell culture dish with a 5 ml physiological pipette to fragment the hiPSC colonies into small pieces, after a digestion with collagenase I. Pieces then spontaneously formed EBs after an overnight incubation period (**Fig. 6a**). The EBs obtained by this method were of variable size, and the presence of non EB-like structures could be observed (**Fig. 6bc**).
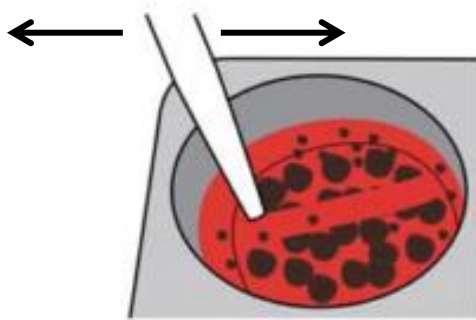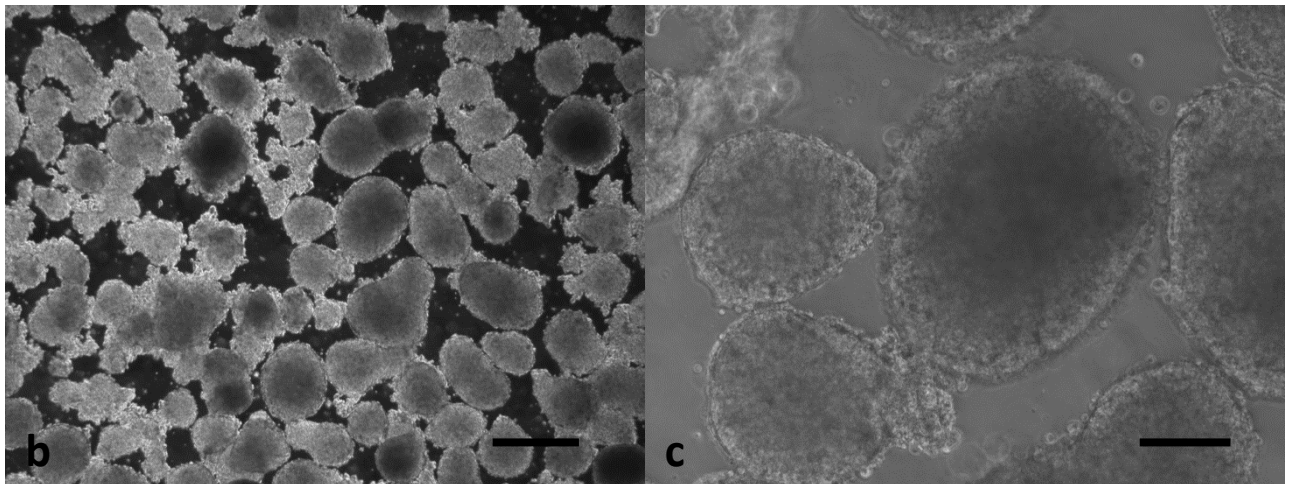
*Fig. 6: Spontaneous EB formation **a.** Scratching of a cell culture surface; modified from (Schaaf et al. 2011). **b. c.** EBs formed spontaneously after scratching the cell colonies with a serological pipette **b.** scale bar: 1 mm. **c.** scale bar: 250 µm*

This method was relatively quick and cost efficient, but the quality and the reproducibility of the technique was relatively low. The upscaling in term of cell quantity was also a problem as the scratching of the cells needed to be conducted slowly to avoid cell damage. Furthermore, as stated previously, the variability obtained in term of EB size and form was much higher than with the two other techniques, and the EB formation was simply not working for some of the cell lines in culture.

2.2. Forced Aggregation

To improve the robustness of the method, EB formation by forced aggregation was tested. The original method was using a V-shaped 96-well plate in which singles cells were added to every individual well (Burridge et al. 2007). The plate was centrifuged and incubated to form an EB in every well. Unfortunately, for our purpose a large amount of cells was required, and an individual or even multi-channel well pipetting EB formation would have been too time consuming. Therefore, the principle was maintained but the method was optimised: a pyramidal micro-cavities surface was engineered using silicone gel and rear reflector (**Fig. 7a**). The cavities were then filled with a single cell suspension solution, leading to formed EBs after centrifugation and 24 hours incubation time (**Fig. 7b**).

Casting of silicone
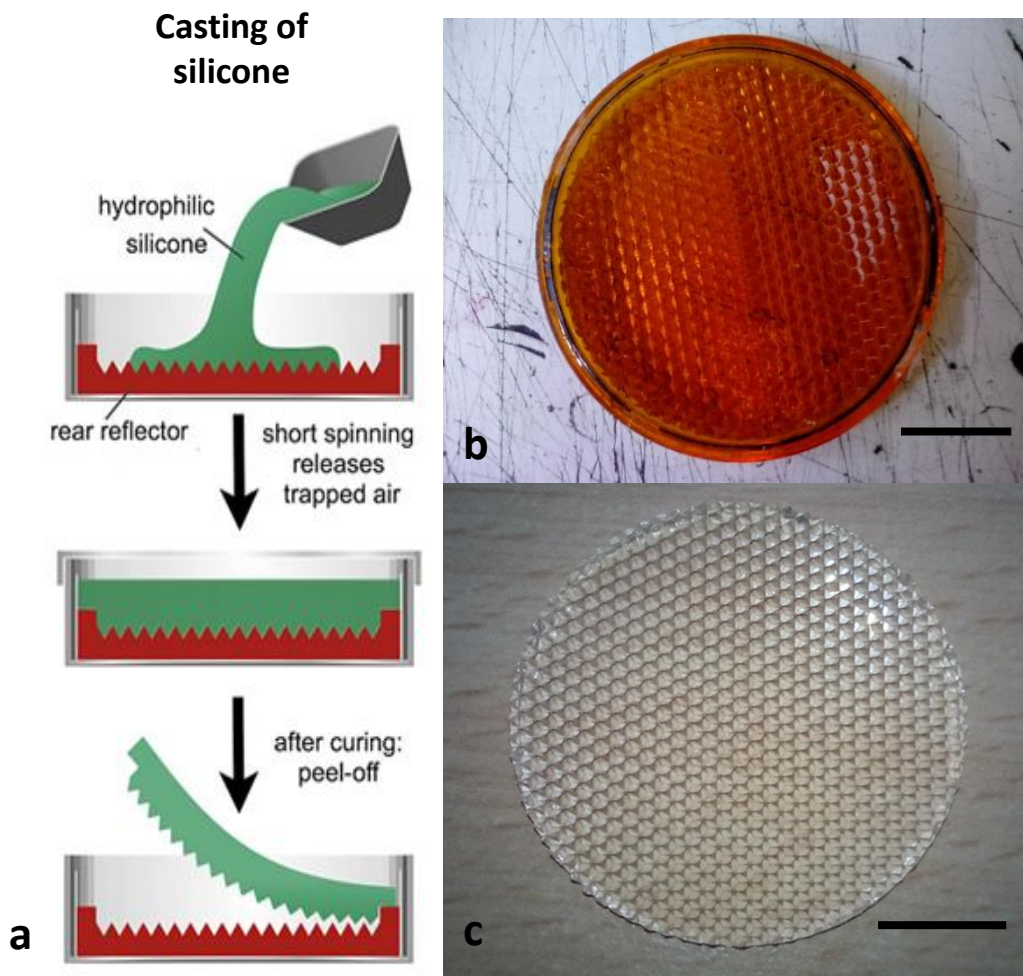
*Fig. 7: Casting silicone gel to perform forced aggregation EB formation. **a.** Hydrophilic silicone was casted on a rear reflector. After cooling, the polymerised gel was peeled-off and cut to the desired format; Adapted from* (Dahlmann et al. 2013). ***b.** Rear reflector used as a mold to cast the silicone microwells, scale bar 1 cm. **c.** Silicone microwells after cutting to 6-well format ; scale 1 cm.*

Once polymerised, the silicone was peeled off the light reflector surface, cut to match the size of a 6-well plate well, then cleaned and autoclaved (**Fig. 7**). The silicone was coated with Pluronic® to facilitate washing off of the EBs from the micro cavities. The method required in addition two centrifugation steps: one before adding the cells to get air bubbles out of the micro cavities, the second after the addition of the cells to induce EB formation. The EBs were washed off with medium and collected (**Fig. 8a**). The obtained EBs were directly compared to the ones from spontaneous EB formation protocol (**Fig. 6a ; Fig. 8c**), and the variability of EB sizes and formation of non EB-like structures was considerably reduced compared to spontaneous EB formation.
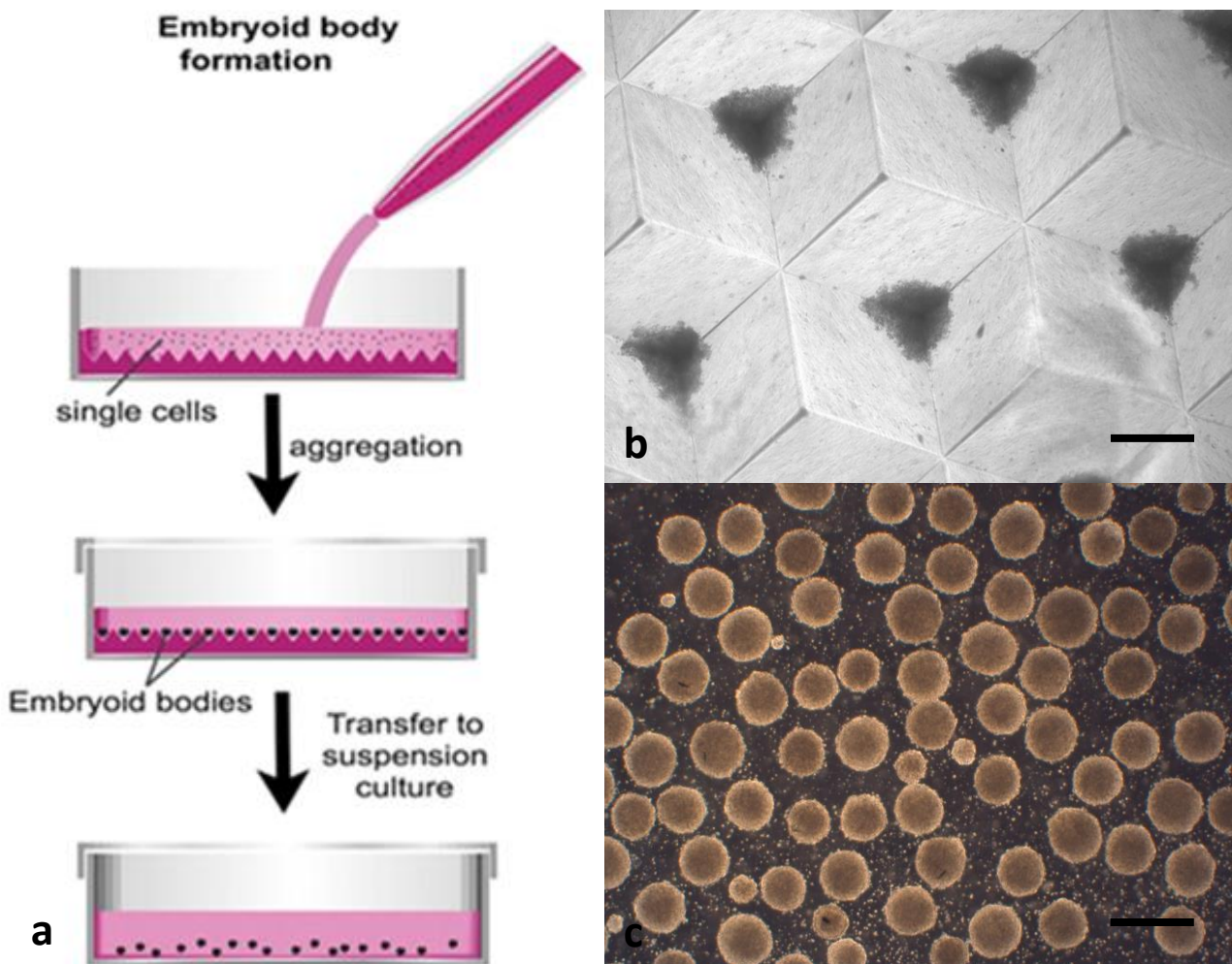
Fig. 8: *Forced aggregation EB formation **a.** A single cell solution was pipetted on top of the silicone micro cavities. After centrifugation and overnight incubation, EBs were formed in the micro cavities and could be washed off; Modified from* (Dahlmann et al. 2013). ***b.*** *The silicone micro cavities with aggregating single cells. The picture was taken after centrifugation and one night incubation, scale bar: 1 mm. **c.** EBs obtained by forced aggregation method, scale bar: 1 mm.*

However, despite the improvement of this method compared to the initial use of 96-well plates, it still remained labour-intensive as numerous steps had to be performed and the silicones must be placed and washed off individually in every 6-well plate. The method required a linear increase of workload with increased EB production and carried a higher risk of fungi contamination due to the manual manipulation of the silicone microwells. It was therefore still not suitable for a large scale cardiomyocytes production.

2.3. Spinner flasks

The final method consisted in using rotating suspension culture (**Fig. 9a**) of single cells for 24 h. Under these conditions, cells spontaneously formed EBs.
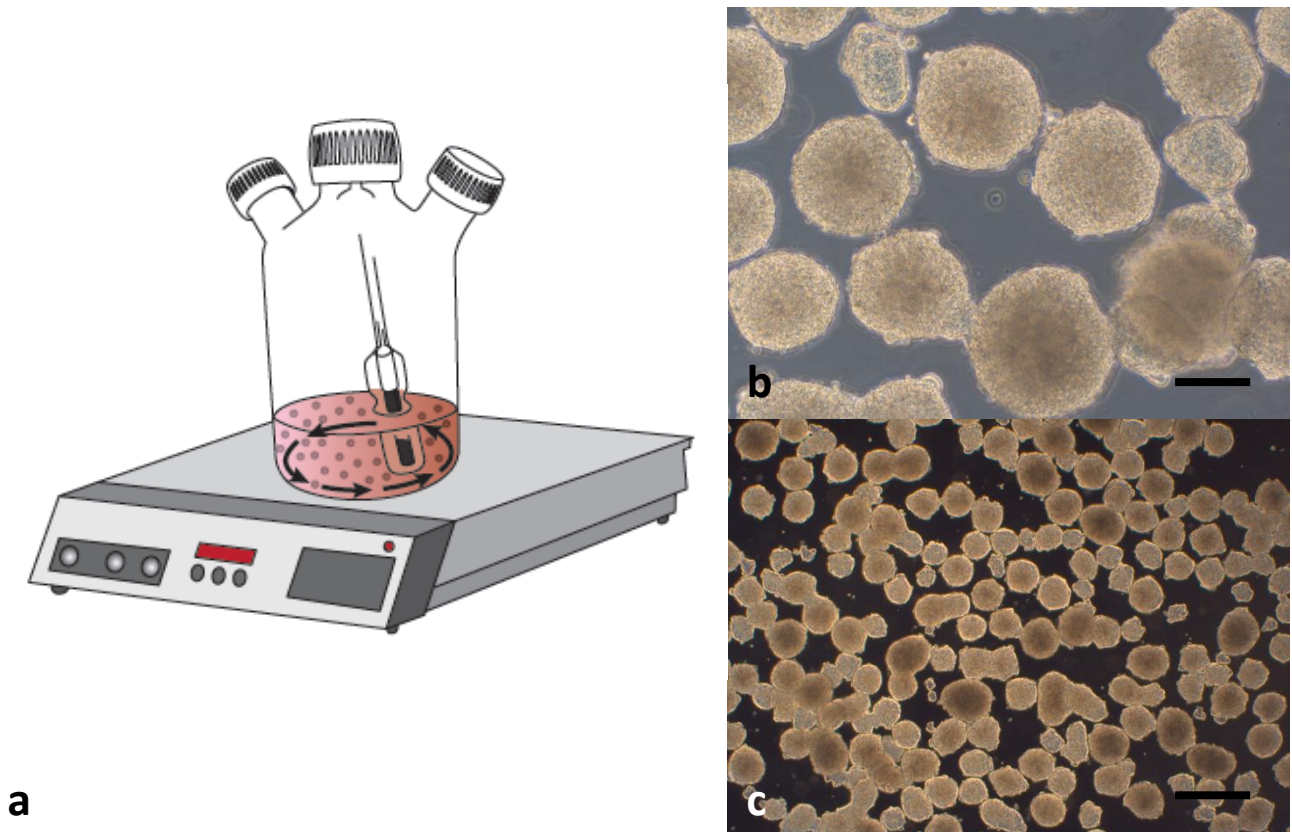
Fig. 9: a. EB formation in a spinner flask with a rotating glass spinner. The EBs start forming after a few hours. b. Embryoid bodies, scale 250 µM. c. Embryoid bodies, scale 1 mm.

The size variability of the spinner flask aggregation method can be directly compared in those pictures. EBs from spinner flask aggregation displayed a smoother and rounder shape than those obtained by spontaneous EB formation, giving an indication of lower variability (**Fig. 6c ; Fig. 9c**). However, they displayed more size variability than the ones obtained with the forced aggregation method variability (**Fig. 8c ; Fig. 9c**). On the other hand, spinner flask EB formation allowed a substantial upscaling of the production as each flask can contain a large amount of cells. Furthermore, the flask only had to be shortly washed with water and autoclaved for reutilisation, which was significantly less time consuming than the forced aggregation protocol.

Since engineering of EHTs required a very high number of cardiomyocytes, the spinner flask EB formation method was the only technique which could provide an upscalable method for cardiomyocytes production. It was therefore preferred for the differentiation protocol.

3. **Mesodermal induction**

After EB formation, the cells were still undifferentiated and had to potential to differentiate in ectoderm, mesoderm or endoderm lineage. The next step was therefore to promote mesodermal lineage differentiation so that the cells could be later brought towards cardiac differentiation. Mesodermal induction could be induced either by activating the TGF-β or Wnt signalling pathway. A large number of parameters had to be optimised for this step called "Stage 1" and only the main aspects will be depicted in this chapter. The difficulties of cultivating cells in suspension will first be shown and then different mesodermal induction methods will be compared.

3.1. Suspension culture

After EB formation, the cells have to be kept in suspension for mesodermal induction as attached cells would lose their three-dimensional structure. Keeping EBs in suspension is actually relatively challenging as they tend to sedimentate rapidly and spontaneously attach to any surface. Furthermore, if the EBs were cultivated further in spinner flasks, they would disaggregate, probably due to the shear force of the rotating glass spinner. The easiest solution was therefore to use a surface which would stop EB adherence.

At first the commercially available Corning® Ultra-low attachment flask were used, but their high price made them unusable for a production upscaling strategy, as a large amount would have been needed. It was therefore decided to coat standard cell culture flasks with Pluronic® instead, a non-ionic surfactant preventing cell attachment to the coated surface (Tharmalingam et al. 2008). It was used at a working concentration of 1% and provided the same effect as the Ultra-low attachment surface of the expensive Corning® flasks. It

therefore providing a very cost-effective routinely used coating material for standard cell culture flasks.

3.2. Insulin effect

Numerous cardiac differentiation protocol of iPS cells found that insulin was playing a major role. However, a positive or negative effect on differentiation could depend on narrow time windows. We therefore decided to test specifically in our differentiation protocol, which time window was benefiting from the presence or absence of insulin. It was found that stage 1 was the most sensitive stage in which insulin was inhibiting future cardiac differentiation, probably by interfering with mesodermal induction (**Fig. 10**).
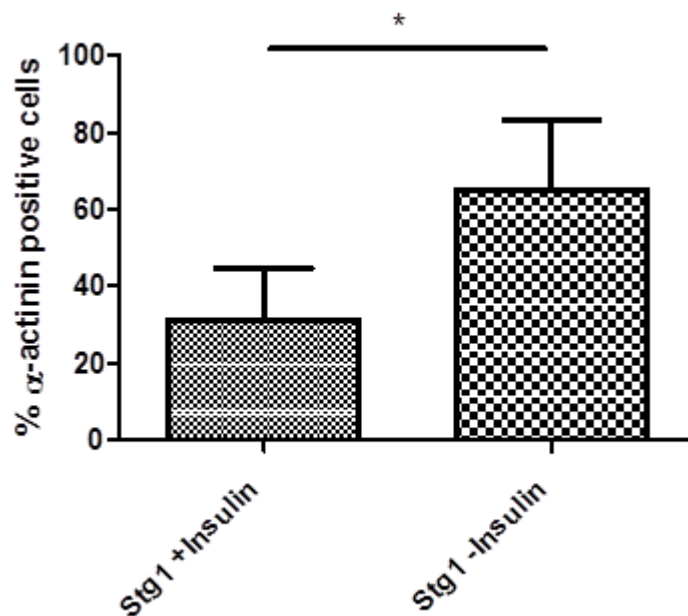
Fig. 10*: Comparison of differentiation runs with or without insulin in stage 1. Data was obtained by α-actinin antibody labelling and FACS analysis. Differentiation was first performed with insulin, during 3 runs, then without during 4. A student t-test was applied to analyse the data. * p<0.05, student t-test, FACS analysis performed by Dr. Breckwoldt.*

The results showed a clear statistically significant increase in cardiomyocyte purity with 31.3% (SD: 13.3) α-actinin positive cells for stage 1 with insulin and 65.0% (SD: 18.5) without ($p<0.05$, student t-test). We therefore decided to keep stage 1 without insulin for the next differentiation runs.

3.3. Replacement of B27® supplement

One of the other challenges in the cell culture field is to replace serum or undefined animal-derived products such as albumin by defined components in order to reduce batch to batch variability. However, it is highly challenging to find the selection of molecules and growth factors which will have an equivalent effect as the thousands which are naturally present in serum. At first, the differentiation was started with B27® based medium, but this supplement contains bovine serum albumin, which is known to bind undefined molecules and other proteins. Such "contaminations" could have drastic effects on cardiac differentiation and be batch-dependent, which is why a chemically defined medium FDM (Fully Defined Medium) was tested to replace B27® (Zhang et al. 2015).
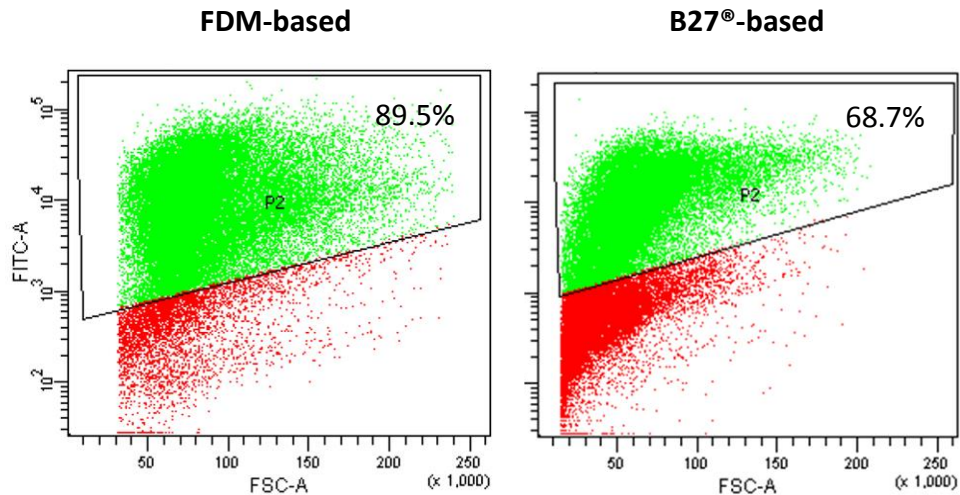
FDM-based   **B27®-based**

Fig. 11: FACS comparison between FDM-based and B27-based differentiation medium. On the Y axis the fluorescence from α-actinin staining and on the X axis the cell size, both in arbitrary units. The red dots represent the α-actinin negative cells and the green positives. The percentage in the top right corner of each diagram expresses the percent of cardiomyocytes within the total population. Two different runs were performed using B27-based or FDM Stage 1 medium, with the use of defined medium leading to a higher cardiomyocyte purity at the end of the differentiation run.

The former medium was then adapted to an FDM basis, and the cardiac differentiation efficiency was then tested by FACS analysis (**Fig. 11**). The data showed higher differentiation efficiency in FDM-based medium compared to B27®-based medium with 89.5% and 68.7%, respectively. Recombinant human albumin was also added in the FDM-based medium as it was found to have a beneficial effect on mesodermal induction and successfully replaced the undefined serum albumin present in the B27® supplement previously used.

3.4. Activation of either BMP/Activin or Wnt pathway

Two main strategies exist for mesodermal induction. One consists in coactivating both the TGF-β and Activin signalling-pathway, while the other only activates the Wnt signalling pathway. To decide between the two methods, the two conditions were tested in parallel on different cell lines. α-actinin staining and FACS analysis was then performed to determine the final cardiomyocyte purity (**Fig. 12**).
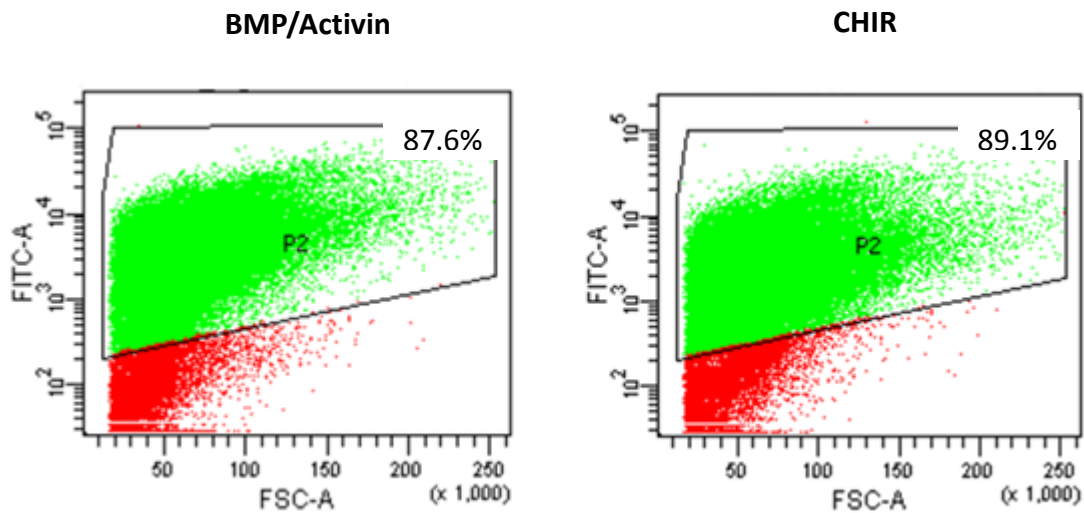
Fig. 12: *FACS comparison between BMP/Activin and CHIR mesodermal induction. On the Y axis the fluorescence from α-actinin staining and on the X axis arbitrary cell size units. The red dots represent the α-actinin negative cells while the green ones are positive. The percentage in the top right corner of each diagram expresses the percent of cardiomyocytes within the total population. The left plot displays differentiation efficiency for the BMP/Activin induction while the right one for Wnt activation with CHIR, a GSK-3β inhibitor. FACS analysis performed by Dr. Breckwoldt.*

This differentiation comparison did not show a convincing difference between the two mesodermal induction methods, leading in both cases to almost 90% cardiomyocytes differentiation. We therefore concluded that both can be used equivalently.

4. Cardiac Differentiation

After mesodermal induction, the cells still have to differentiate towards the cardiac lineage, which is typically done by an inhibition of the Wnt pathway (Lian et al. 2012; Minami et al. 2012). This inhibition was performed either with the embryologically expressed DKK1 protein or a small molecule analogue DSI-7. It was also tested if replating the cells in a monolayer at this step was more favourable than having them in suspension. The last part is a detailed protocol of the latest in-house optimised differentiation procedure. This stage is the last step of differentiation as the cells will start to spontaneously beat, after which the culture will be dissociated to cast EHTs.

4.1. Wnt inhibition

The Wnt inhibition is the most important step to orientate the cells towards the cardiac lineage. It should only be performed after a successful mesodermal induction, otherwise the cells won't differentiate into cardiomyocytes. The initial protocol used the protein DKK-1 for Wnt pathway inhibition, however it is extremely expensive and requires high concentrations because of its low potency. The alternative was to replace DKK-1 proteins by small-molecules analogues which are much cheaper.
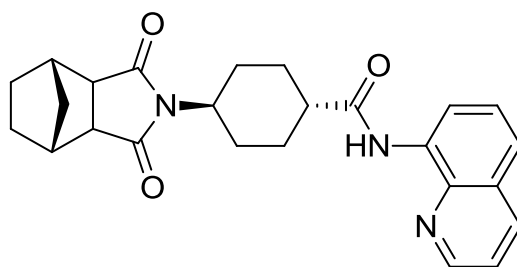
Fig. 13: *DSI-7, an IWR-1 analog: 4-(cis-endo-1,3-dioxooctahydro-2H-4,7-methanoisoindol-2-yl)-N-(quinolin-8-yl)-trans-cyclohexylcarboxamide* (Willems et al. 2011)*. DSI-7 used at a concentration of 100 nM during stage 2 was found to have an equivalent effect as IWR-1 at 4 µM.*

A direct comparison was performed between differentiation with DKK-1 and IWR-1, a small molecule inhibiting the Wnt pathway, and it was found that IWR-1 had a much higher efficacy than DKK-1, leading the observation of a higher number of beating areas after cardiac differentiation. IWR-1 was then replaced by DSI-7 (**Fig. 13**) as it was found to have the same effect on differentiation efficiency and was kindly provided for free by a collaborator: Dr. Schade.

4.2. Suspension and adherent culture

Next we investigated if, after mesodermal induction in the EB format, the cells should be further kept in suspension (3D) or adherent to a surface (2D) (**Fig. 14**).
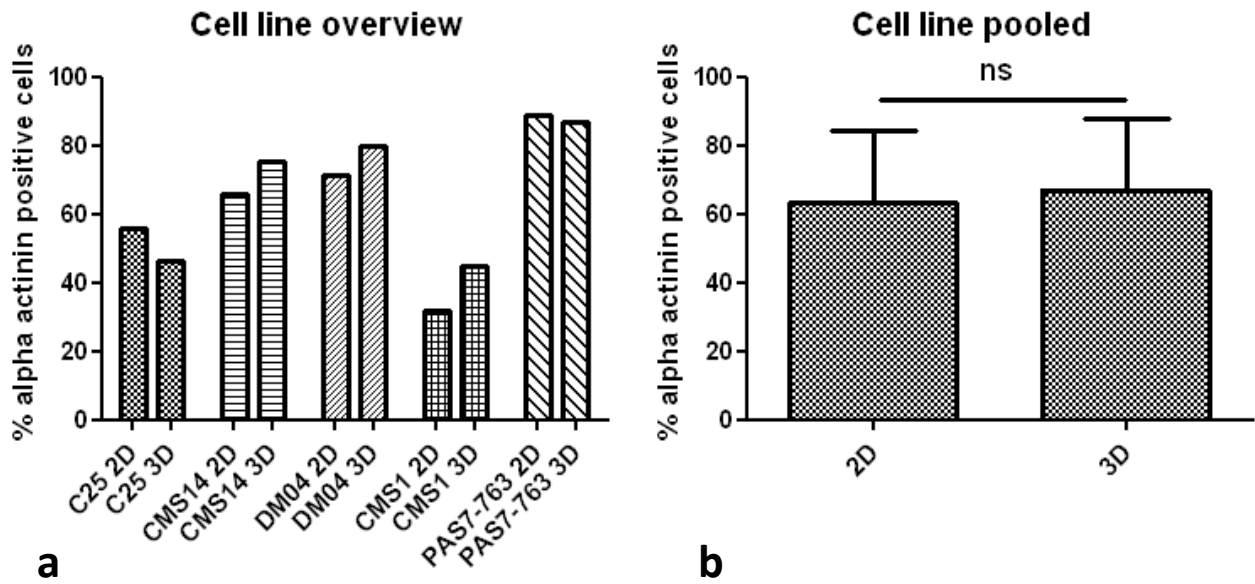
Fig. 14: *Five different cell lines during three different differentiation runs were compared for cardiac differentiation purity between 2D and 3D in stage 2. **a.** Percentage of α-actinin positive cells for each cell line for both conditions. **b.** Cell lines data pooled to directly compare 2D to 3D, n=8 in each condition. ns: non-significant, p>0.05 statistical analysis performed by a student t-test.*

The comparison between different cell lines showed that variations of differentiation efficiency were more important between the cell lines than between 2D and 3D (**Fig. 14a**). No differentiation difference could be observed between the two conditions after a student t-test analysis (p<0.05) (**Fig. 14b**). However, cell yield was slightly higher in 2D than 3D (data not shown) and the daily exchange of the medium was slightly less time-consuming, which indicated a small advantage of the 2D format.

In the microscope, differentiated cardiomyocytes showed typical rhythmic and coordinated contractions in monolayers after plating EBs on a Geltrex® coated surface (**Video 1**). Observing the beating quantity gives in general an accurate estimation of the cardiomyocyte purity of the differentiation run.

5. Optimised protocol

This section provides the final version of the standard operating procedure (SOP) used in the laboratory to differentiate cardiomyocytes. The optimisation includes the previous points described in this chapter, but also others which were not presented. The work was performed in cooperation with Dr. Schaaf and Dr. Breckwoldt (Schaaf 2011; Breckwoldt 2015). Optimisation was performed on different cell lines in parallel which were or not disease-specific. This multi cell line approach, allows building a robust differentiation protocol which is less subject to cell line variability.

Media composition

Stage 0 medium

FTDA medium
Polyvinyl alcohol (Sigma-Aldrich, P8136) 4 g/L
Y-27632 10 µM (Biaffin, PKI-Y27632-010)
Filter sterilized 0.2 µm (TPP, 99500), stored at 4 °C

Stage I FDM medium

RPMI 1640 (Gibco, 21875)
Transferrin selenium 1%
2-Phospho-L-ascorbic acid trisodium salt, 250 µM
Lipid Mixture (Sigma-Aldrich, L5146), 1:1000
Polyvinylalcohol (Sigma-Aldrich, P8136), 4 g/L
Penicillin/Streptomycin, 1%, (Gibco, 15140)
Y-27632, 1 µM, (Biaffin, PKI-Y27632-010)
BMP-4 (R&D systems, 314-BP),10 ng/mL
Activin-A (R&D, 338-AC), 3 ng/mL
Basic FGF 5 ng/mL (R&D systems, 233-FB)
Human Serum Albumin (Biological Industries, 05-720-1B)
Filter sterilized 0.2 µm (TPP, 99500), stored at 4 °C for up to 2 weeks

Note: The differentiation of cardiomyocytes was substantially hampered if insulin was present during mesoderm induction (**Fig. 10**). Absence of basic FGF led to detrimental differentiation outcome.

Stage 2 FDM medium

RPMI 1640 (Gibco, 21875)
Transferrin selenium 1%
2-Phospho-L-ascorbic acid trisodium salt, 250 µM
Lipid Mixture (Sigma-Aldrich, L5146) 1:1000, Penicillin/Streptomycin 0.5% (Gibco, 15140)
Y-27632, 1 µM, (Biaffin, PKI-Y27632-010)
DS-I-7, 100 nM (custom made)
Human Serum Albumin (Biological Industries, 05-720-1B)
Filter sterilized 0.2 µm (TPP, 99500), stored at 4 °C for up to 2 weeks

Stage 2 medium plus insulin

RPMI 1640 (Gibco, 21875)
1-Thioglycerol, 500 µM (Sigma-Aldrich, M6145)
HEPES, 10 mM (Roth, 9105.4)
Penicillin/Streptomycin 0.5% (Gibco, 15140)
Y-27632, 1 µM, (Biaffin, PKI-Y27632-010)
B27®, 2%, (Gibco, 17504-044)DS-I-7, 100 nM (custom made)
Filter sterilized 0.2 µm (TPP, 99500), stored at 4 °C for up to 2 weeks

Stage 3 medium

RPMI 1640 (Gibco, 21875)1-Thioglycerol, 500 µM (Sigma-Aldrich, M6145)
HEPES, 10 mM (Roth, 910.4)
Penicillin/Streptomycin, .5%, (Gibco, 15140)
Y-27632, 1 µM, (Biaffin,PKI-Y27632-010)
B27®, 2%, (Gibco, 1754-044)
Filter sterilized 0.2 µm (TPP, 99500), stored at 4 °C for up to 2 weeks

Differentiation procedure

Stage 0: Embryoid body formation

Prearrangements

Sterile spinner flasks were prepared.
Stage 0 medium was prepared.
PBS, Stage 0 medium and 0.5 mM EDTA solution were prewarmed.
CASY® cell counter was prepared.

Preparation of human induced pluripotent stem cells

FTDA was removed.
Cells were briefly washed twice with PBS.
Prewarmed 0.5 mM EDTA solution (1 mL/well, 7 mL/T80 cell culture flask) was added, cells were incubated for 10 minutes at 37 °C and cell detachment was monitored microscopically to fine-tune the incubation time. Fine-tuning was critical due to variability between the different cell lines.
EDTA solution was removed.
Prewarmed PBS: 1 mL/well, 7 mL/T80 cell culture flask was added.
Flask or plate was tapped to detach the cells which were then transferred to a tube containing 10 mL stage 0 medium.
Cell culture flask or well was rinsed with 5 mL PBS and transferred to a tube.
Cells were triturated by pipetting up and down 4 times with a 10 mL pipette, centrifuged for 5 min at 250 g and resuspended in 10 mL of stage 0 medium.
Cells were counted by CASY® cell counter and resuspended in calculated amount of stage 0 medium (3.10^5 cells/mL).
Cell suspension was added to spinner flask with additional stage 0 medium (3.10^5 cells/mL).
Incubation overnight; rotation: 40 rounds per minute.
Incubator conditions: 37 °C, 90% humidity, 5% CO_2, 5% O_2.

Stage 1: Mesodermal induction

Prearrangements

Cell culture flasks were coated with Pluronic® F 127 solution with an overnight minimum time of incubation.
Stage 1 medium was prepared and prewarmed before processing the EBs.
BMP4 (10 ng/mL), Activin A (3 ng/mL) and bFGF (5 ng/mL) were always freshly added on the day of stage 1 transition.

Pluronic® F 127 coating of cell culture flasks

1% Pluronic® F 127 solution was added to the cell culture with 5 mL per T25 flask, 7 mL per T75 and 13 mL per T175.
Flasks were incubated at 37 °C overnight and washed with PBS with 10 mL per T25 flask, 20 mL per T75 and 30 mL per T175.
PBS was removed.
The cell culture flasks were then ready to use.

Note: Surfaces were not left to get dried. Longer time coating was not observed to be detrimental.

Mesodermal induction with BMP4, Activin A and bFGF

Suspension of EBs was transferred from spinner flask to T175 cell culture flask.
T175 cell culture flask was placed on a V-shaped sedimentation rack.
EBs were left to sediment in the lower corner of the flask for 5 min.
90% of stage 0 medium was removed.
One part of the EBs was transferred into a 15 mL collection tube, were resuspended in 10 mL RPMI medium and left for sedimentation for 5 min.
EB volume was then estimated (See paragraph "Estimation of EB volume").
Supernatant was removed and EBs were resuspended in stage 1 medium supplemented with 10 ng/mL BMP4, 3 ng/mL Activin A and 5 ng/mL bFGF.
EBs were transferred to Pluronic® F 127-coated T175 cell culture flasks with a total of 35 mL Stage 1 medium and 35 µL EB in each.
EBs were incubated for 3 days and medium was changed daily.
Incubator conditions: 37 °C, 90% humidity, 5% CO_2, 21% O_2

Estimation of EB volume

EBs were transferred to a red cap 15 mL tube (Sarstedt, 62.554.502).
EB volume was estimated by the transparent graduations provided under the plain 2 mL graduation (**Fig. 15**).
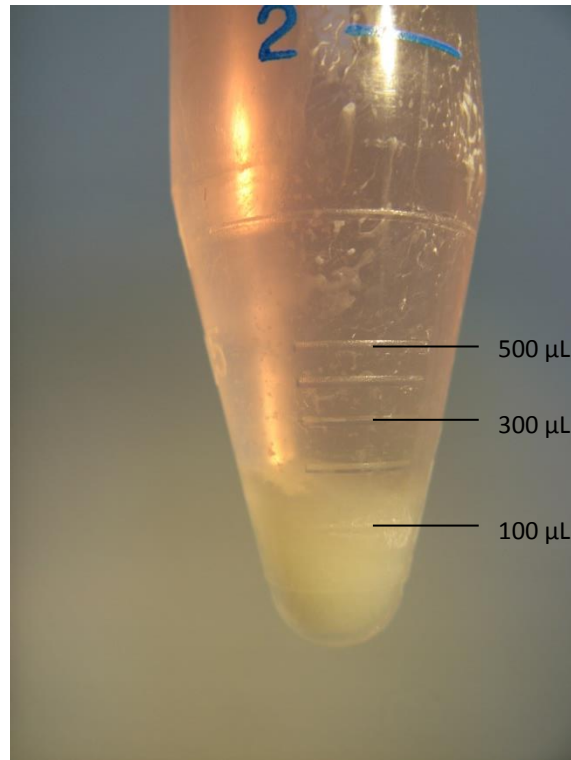
Fig. 15: EB volume was estimated by the transparent graduation of the tube. A few graduations were annotated on this picture. In this example, an EB volume of 150 μL was estimated.

Medium change:

T175 cell culture flask was placed on a V-shaped sedimentation rack.
EBs were left to sediment in the lower corner of the flask for 5 minutes.
90% of media was removed.
50 mL medium/T175 flask was added.
Flask was transferred back to the incubator.

Stage 2: Cardiac differentiation

Prearrangements

FDM Stage 2 medium was prepared and prewarmed. Cell culture flasks or wells were coated with Geltrex® before processing the EBs.

Geltrex® coating

Geltrex® (Gibco, A1413302) was thawed on wet ice.
It was diluted 1:200 in ice cold DMEM.
1 mL per well (6-well format) or 7 mL per T75 cell culture flask, Nunc (178905) was then added.
Plate was incubated at 37 °C for 30-60 minutes.

Preparation of EBs

Flasks from stage 1 were placed on v-shaped sedimentation rack.
EBs were left to sediment for max. 5 min.
90% of the medium was removed.
EBs were washed with warm RPMI containing 10 mM HEPES.
One part of the EBs was transferred into a 15 mL tube and left for sedimentation for 5 min, EB volume was then estimated (See paragraph "Estimation of EB volume").
Supernatant was removed and EBs were carefully resuspended in FDM Stage 2 medium.

EBs were then transferred to prepared cell culture flask or well with:

- 15 µL of EBs per well of a 6-well plate
- 100 µl of EBs per T75 flask in 15 ml medium

Cells were incubated for 3 days with daily medium change
Medium was then changed to stage2+Insulin, with B27® supplement for 4 days with daily medium change.
Cells were then switched to stage 3 medium without DS-I-7, medium was changed every other day.
Incubator conditions: 37 °C, 90% rH, 5% CO_2, 21% O_2
First beating was usually observed 10-12 days after stage 0.

Dissociation of differentiated cells

PBS (Gibco, 10010-049) and collagenase II solution were prewarmed.
Medium was removed.
Cells were carefully washed with PBS.
8 mL collagenase II solution was added per T75 cell culture flask or 1 mL per well of a 6-well plate.
Cells were incubated for 3-4 hours.
Cell dissociation was monitored microscopically.
Incubator conditions: 37 °C, 90% humidity, 5% CO_2, 20% O_2.
Detached cells were transferred to a 50 mL tube.
T75 cell culture flask was flushed with prewarmed DEMEM+DNAse.
Cells were transferred to a 50 mL falcon tube.
Cells were centrifuged for 15 minutes at 100 g.
Supernatant was discarded and cells were resuspended in 10 mL DMEM.
Cells were counted with CASY® counter (Model TT Version 2.1D).
Cells were centrifuged for 15 minutes at 100 g.

After the first beating was observed, the cells were dissociated and casted into EHTs. The EHT casting was performed as described in detail in a previous publication of the group (Hansen et al. 2010). The publication actually describes EHT casting with neonatal rat cardiomyocytes, but the same principle was used for iPS cell-derived cardiomyocytes. As an example, the beating of an EHT from the C25 and the PAS5-641 cell line after 25 days of maturation after casting can be observed here (**Video 2 ; 3**). In these two videos, a beating EHT stretched between two flexible silicone posts can be observed. It can be noticed how the whole EHT was beating coherently, which was a specificity acquired over one week of maturation. Indeed during the days following the casting, each cardiomyocyte was still separated from the others by fibrin matrix, therefore beating in an isolated manner. Both of the poles were moving strictly horizontally, which made it possible for our house-made figure optimisation program to measure its contraction force.

6. Variability in iPSC differentiation

After having used this optimised differentiation protocol for almost a year, very different differentiation efficiencies were observed (**Fig. 16**). The phenomenon may at least in part be related to time-related shifts in sub-clonal populations (cf. **Part 3**), causing the starting material of undifferentiated cell material to be different from months to months of the same iPS cell culture.
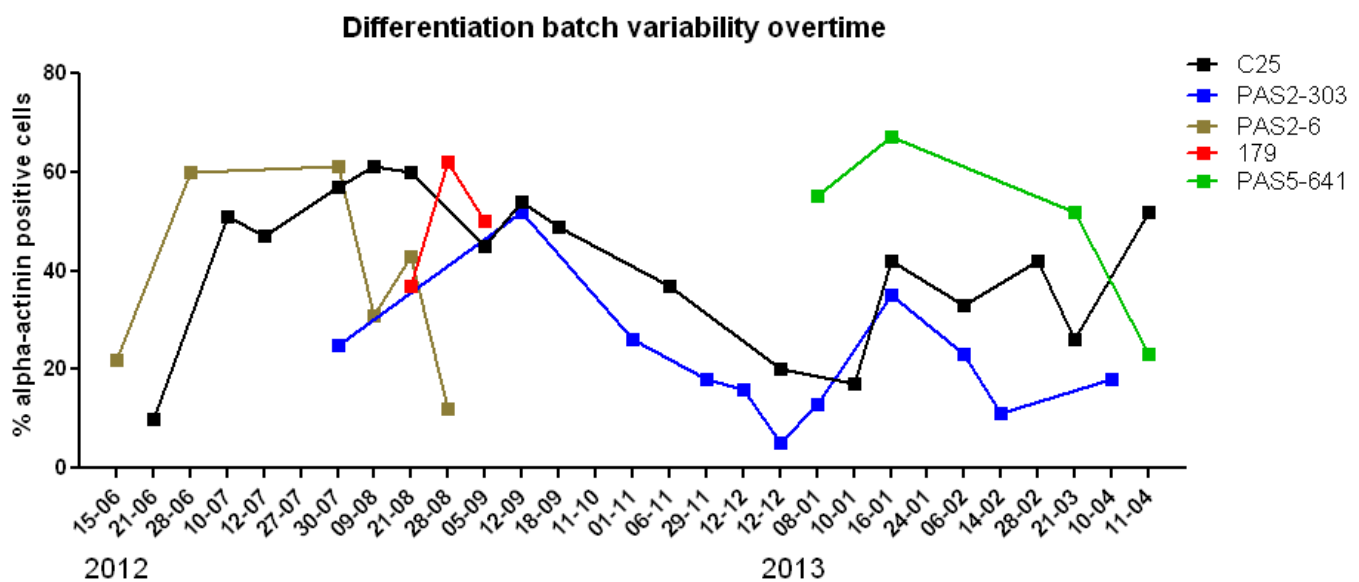
Fig. 16: Cardiomyocyte purity was measured through α-actinin staining for multiple differentiation runs and different cell lines. It could be seen that differentiation was both batch- and cell line-dependent during almost an entire year.

Multiple differentiation runs were performed by the team on several iPS cell lines over months. Despite using the same differentiation protocol, cardiomyocyte yield was very variable from run to run and from cell line to cell line. Cell line-independently, cardiomyocyte purity varied between 20% and 60% (**Fig. 16**). I therefore questioned the assumption that the iPS culture itself was stable overtime as the variation of differentiation

efficiency over long-time periods would suggest a concomitant variation in iPS cell state just before starting the differentiation run. It was thought that the quality of the culture could be affected by sub-clonal dynamics, a concept that we further explain in the third part of this dissertation (cf. **Part 3**).

Part 2: CPVT modelling in Engineered Heart Tissues

A very exciting possibility that emerged with iPS cells is to create a cell line from a patient with genetically caused disease to create cellular human models of hereditary diseases. In our case, we established a patient-specific cell line of the CPVT disease in order to evaluate if EHTs would be a suitable model. Our patients had a mutation in the RYR2 very close to the N-terminal of the protein, leading to an amino acid change at position 11 (I11S).

After the establishment of the disease-specific cell line, it first needed to be verified if the mutation was still present in the DNA of the cell line, and second, if it was expressed on mRNA levels. Contraction characteristics of the EHTs then needed to be further characterised by studying both spontaneous and paced beating contraction to see if well-established characteristics of heart physiology could be confirmed in our model. Post-rest potentiation, force-frequency relationship, β-adrenergic response and calcium sensitivity were then further investigated.

As outlined in the Introduction, the expected phenotype of the CPVT model would be a display of arrhythmic contractions in the presence of a β-adrenergic agonist like isoprenaline. If this would be observed, the RYR2-dependant arrhythmia should be able to °be rescued by a RYR2 stabiliser like JTV-519.

1. **Selecting patients**

1.1. Clinical observations

Before reprogramming of cells from patients with a RYR2 mutation, clinical data should be gathered from the patient to know more about its condition. Our family was selected as the patient died from cardiac arrhythmia during a swimming race. Sequencing of the RyR2 gene revealed a T>G missense variant on the 32nd nucleotide. The missense mutation led to an isoleucine to serine substitution on position 11 (I11S) and has not been described in the literature yet. Cells from this patient couldn't be gathered, because the lethal incidence occurred in the USA, but his mother and his brother agreed to participate in the study and donated some dermal fibroblasts, later reprogrammed into iPS cells.

Relationship to the deceased	Cell line code	Sex	Age	Maximum exercise capacity compared to norm (100%)	Heart rate (min^{-1}) exercise	Heart rate (min^{-1}) long-term
Patient	Deceased	M				
Brother	PAS5-641	M	22	64%	145	137/45
Mother	PAS7-763	F	52	97%	128	128/46

	RYR2 mutation	Blood pressure (mmHg)	VES (during exercise)	VES (long-term recording)	Treatment	Death
Patient	RYR2 c.32T>G					swimming 2010
Brother	RYR2 c.32T>G	159/84	3	2/24h	Nadolol, 120 mg/day, ICD	no
Mother	RYR2 c.32T>G	188/94	14	2/24h	Nebivolol, 120 mg/day	no

Fig. 17: Clinical data of the two relatives of the deceased patient used for iPS cell reprogramming. The same mutation is carried by the three family members. Clinical data were gathered during long-term measurements and short exercise periods. Both of the surviving family members were then further on treated with β-blockers.

Both the long-term and short term ECG records were within the normal range. Ventricular extrasystolies (VES) were observed only rarely (14 during exercise and 2 in the following 24 h recording). Thus, despite the presence of a variant/mutation in the RyR2, the clinical data did not give conclusive evidence of a penetrance of the CPVT disease in these probands. However, by analysing the ECG itself, further evidence could be provided (**Fig. 18**).
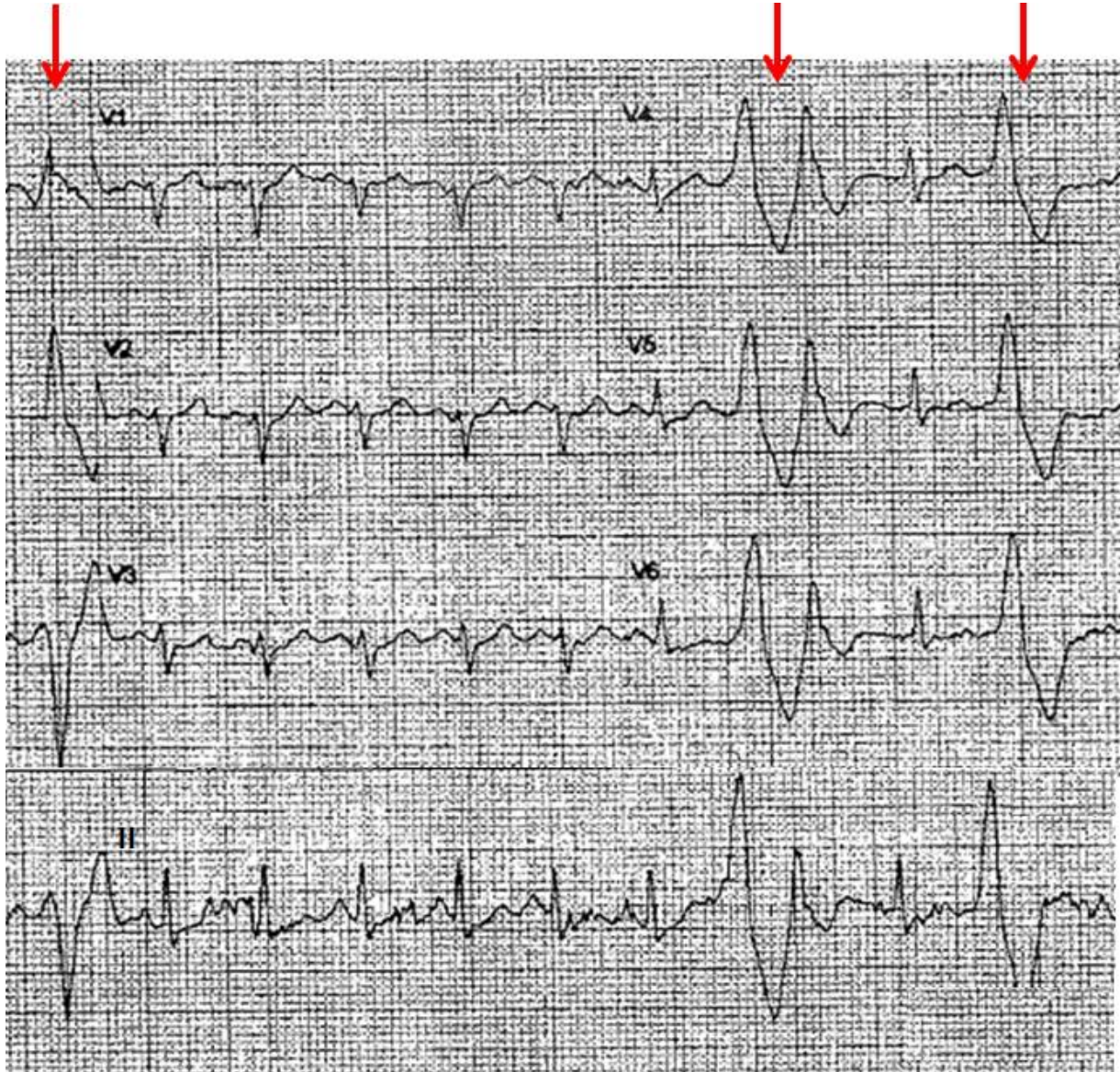
Fig. 18: *ECG of the mother of the deceased patient (cell line PAS7-763) during exercise. Leads V1 to V6 are displayed, as well as a longer recording of the lead II. Three abnormal beatings c be observed (red arrows) with a couplet on the second arrow. X axis: 25 mm/s, Y axis: 10 mm/mV. Every line corresponds to 1 mm.*

All three of the abnormal beatings were different from each other's, thereby confirming the polymorphic aspect of the arrhythmia. Furthermore, the second arrow was interpreted to be a couplet, which is typical in CPVT arrhythmias (**Fig. 18**). The CPVT diagnostic of the patient

was further confirmed by Dr. Jorge McCormack from the Congenital Heart Institute of Florida (USA).

The CPVT diagnostic of the patient's mother was clinically diagnosed and it could therefore be reasonably assumed that CPVT was the cause of the disease of the patient and that the other brother who is a carrier of the identical mutation is also suffering from CPVT.

1.2. Genotyping DNA and mRNA

Before starting to analyse disease-specific EHTs, it first had to be verified that the mutation was present in the reprogrammed iPS cell line as well as expressed in the mRNA of the derived cardiomyocytes. The mutated region was amplified by PCR and sequenced (**Fig. 19**).
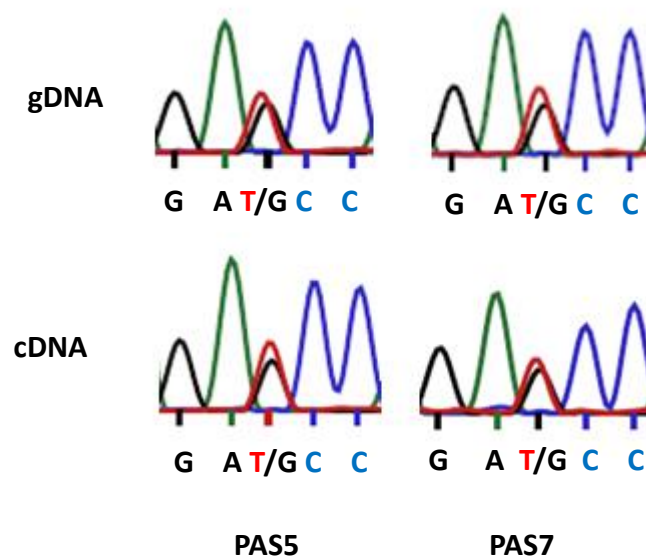
Fig. 19: DNA sequences of the patient-derived iPS cell lines. Sequencing of iPS cell-derived genomic DNA (gDNA) verified the heterozygote mutation. The relative similar expression of the two peaks in cDNA transcribed from isolated cardiomyocyte mRNA suggests that the expression of the mutated and wildtype allele is relatively similar.

All the sequencings show the presence of the mutated allele. In addition, the results of the RT-PCR on the mRNA show similar peak intensities, roughly indicating similar mRNA expression levels. The mutation of the patients leads to an isoleucine to serine change on the amino acid position 11, which is at the very beginning of the N-terminal end of the RYR2

protein. The first mutation cluster of the protein is indicated to start at amino acid 44, as no mutation was found before this point in the sequence. It is however fair to consider that the *de novo* mutation of this family is probably included in this first cluster, as it is now the closest known mutation to the N-terminal.

2. Baseline recordings

Before β-adrenergic stimulation was tested on the disease-specific EHTs, their baseline contractile activity were first recorded and compared to the control EHTs. I started by measuring force, beating frequency, contraction and relaxation time to get an impression of contraction properties. The muscles were furthermore paced to check for post-rest potentiation effects and force-frequency relationships.

2.1. Spontaneous beating

Spontaneous contractions were recorded after a minimum of 15 days of maturation following EHT casting. The EHTs were selected so that their spontaneous beating frequency was in the range of 55-65 beats per minute (BPM). EHTs beating over 100 BPM were excluded as relaxation time of contraction depends on the beating frequency (frequency dependent acceleration of relaxation) (Bowditch 1871).

Normalised averaged contractions
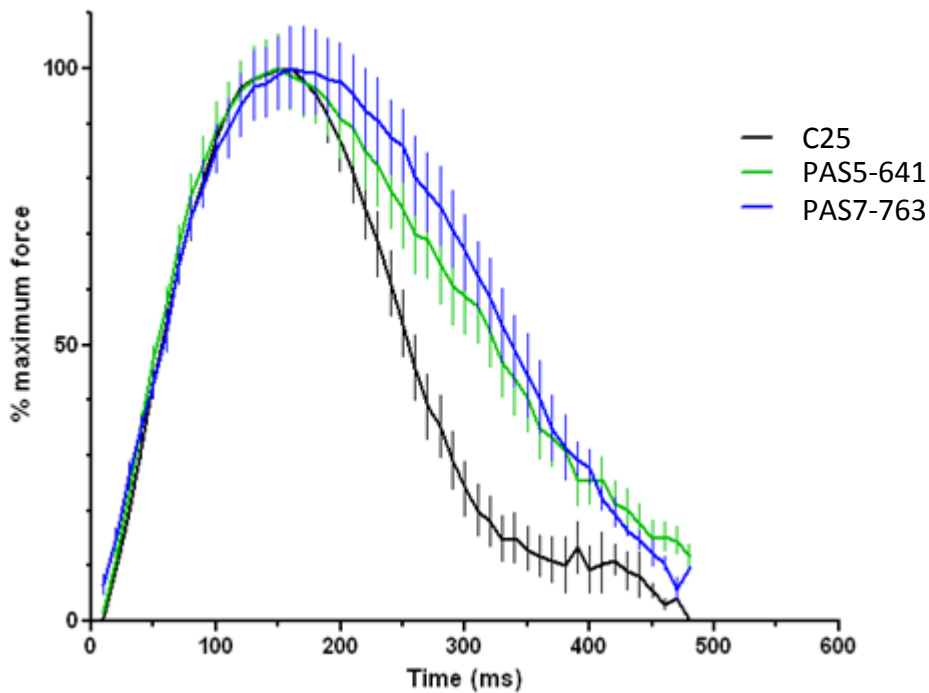
Fig. 20: *Average normalised contraction peaks of EHTs from control cell line (C25) and disease-specific cell lines from related family members (PAS5-641 and PAS7-763). For every differentiation run, 3 contractions of 3 EHTs were taken to calculate an average contraction peak. EHTs beating spontaneously at a frequency superior to 100 beats per minute were excluded due to its effect on relaxation time and the force of the contraction was normalised. It could be noticed on the average peak that disease-specific EHTs displayed a longer relaxation time than controls for both family members. The force was normalised. Runs: C25 n=9, PAS5-641 n=8, PAS7-763 n=2.*

Average normalised contraction peaks of EHTs from control (C25) and disease-specific (PAS5-641, PAS7-763) cell lines over different runs were calculated and compared. It could be observed that all cell lines had a very similar contraction curve with similar times and velocity, but a clear difference could be noticed in term of relaxation. A clearly longer relaxation time for PAS5-641 and PAS7-763 could be observed compared to C25by analysing the normalised average contraction graphs obtained for respectively eight ,two and nine different differentiation runs (**Fig. 20**).

The $T2_{80\%}$, which is the time needed for the muscle to reach 80% relaxation, was measured for all the contraction peaks in order to get a precise quantitative difference between the disease-specific EHTs and the controls. A $T2_{80\%}$ of 157 ms (SD: 27) was found for C25 EHTs while PAS5-641 and PAS7-763 had respectively 231 ms (SD: 50) and 250 ms (SD: 22). $T2_{80\%}$ of the EHTs derived from the two different patients differed significantly from control (one-way ANOVA with Tukey post-hoc test, $p < 0.001$), but not from each other (**Fig. 21**). The patient-derived EHTs had therefore a significantly longer relaxation time than those derived from healthy individuals (C25).
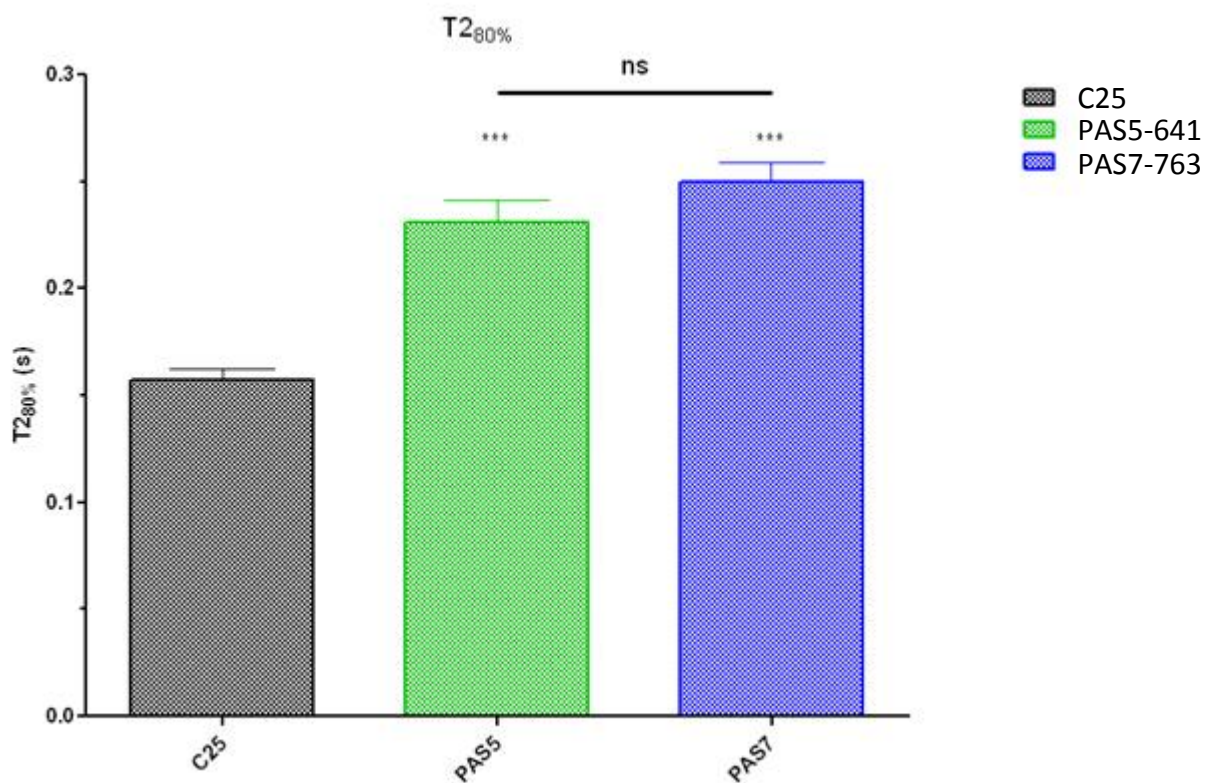
Fig. 21: *Average time required for the EHT to relax 80% of its force ($T2_{80\%}$). Patient-specific EHTs have a $T2_{80\%}$ about 50% more than control EHTs and no significant difference could be found between them. Runs: C25 n=9, PAS5-641 n=8, PAS7-763 n=2. ***, p value < 0.001 compared to control. ns, non-significant, one-way ANOVA, with a Tukey post-hoc test.*

This result was unexpected as CPVT patients are not known to display diastolic dysfunction, which made the finding of a longer relaxation time relaxation time hard to interpret. We hypothesised that this $T2_{80\%}$ increase could be due to a leak in the RYR2, which would

compete with SERCA-mediated calcium reuptake from the cytoplasm into the SR and cause slowing of relaxation. The validity of this hypothesis was tested later (cf. paragraph 3.3).

2.2. Contractile function under electrical stimulation

As previously mentioned, beating frequency influences contraction kinetics. It is therefore crucial to be able to control beating frequency through electrical pacing to perform more complex experiments and go deeper in the physiological understanding of the muscle. It was first required to verify if our EHT model displayed the same well-established characteristics of heart muscles, such as post-rest potentiation, force frequency relationship or the influence of frequency on relaxation time (Bowditch 1871; Koch-Weser and Blinks 1963). These aspects were investigated and the results are described in this section.

2.2.1. Post-rest potentiation

Post-rest potentiation is a fundamental mechanism in which a pause in the electrical pacing of the muscle results in increased calcium loading of the SR, leading to a higher contraction force in the following contraction when the muscle is paced again. A longer pause leads to a stronger contraction, as more calcium has time to be pumped back into the SR (**Fig. 22**) (Koch-Weser and Blinks 1963; Fabiato 1983) .
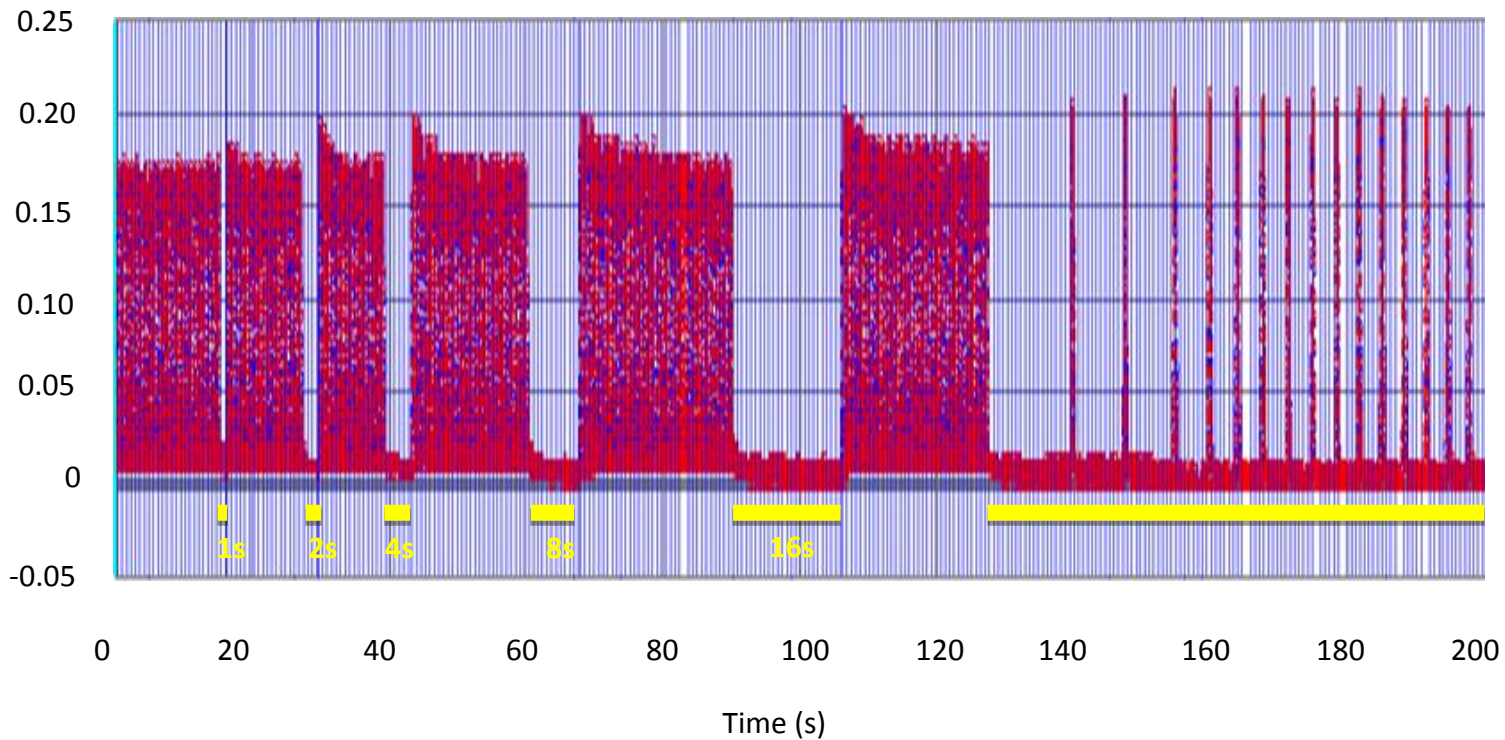
Fig. 22: Recording of a C25 EHT paced at 1.5 Hz, with unpaced intervals indicated by yellow marking. Successive unpaced intervals were respectively done for 1, 2, 4, 8 and 16 seconds and the last one till the end of the experiment. The force difference between the last contraction of a paced episode and the first contraction of the following was measured: 5 µN for the 1 second gap and of around 25 µN for the others. In the end the EHTs were left unpaced for more than a minute. This experiment showed that EHTs could display a post-rest potentiation mechanism.

The first contraction following an unpaced interval was systematically stronger than the contraction preceding it, providing evidence that the post-rest potentiation mechanism was occurring in the EHT model. The force difference started at 6 µN for a 1 s unpaced interval before increasing to 25 µN for a 2 s pause. The force increase then stayed stable around 25 µN (= ~15% compared to steady state force) with increasing unpaced time intervals, suggesting that the sarcoplasmic reticula of the EHT had reached their maximum calcium concentration after 2 seconds without contraction. The pacer was then left off at the end of the recording, displaying spontaneous beating contractions of the EHTs with around the same contraction force as the first contraction after an unpaced interval (**Fig. 22**).
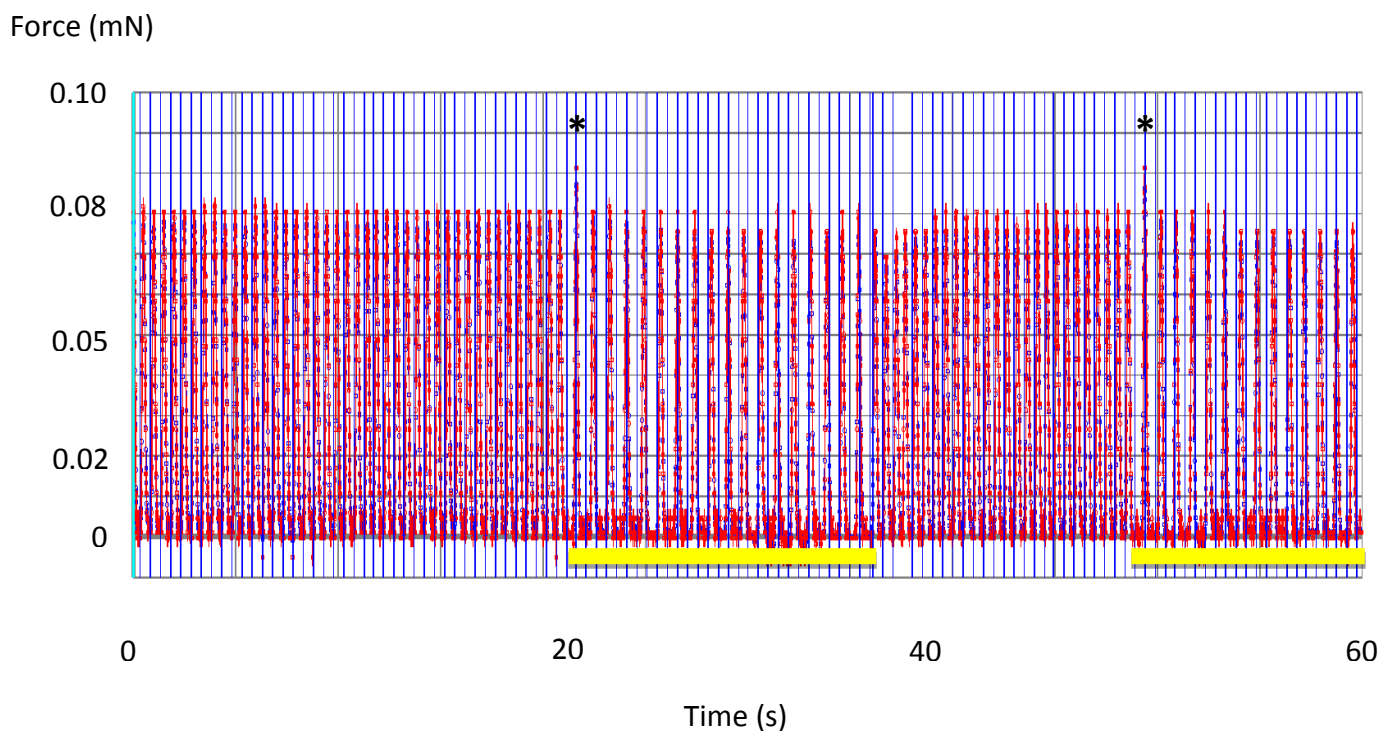
Fig. 23: *Recording of a PAS5-641 EHT paced at 1.5 Hz (blue lines), with unpaced intervals indicated by yellow marking. It could be observed that for a spontaneous beating frequency of 60 BPM, the muscle was still beating spontaneously, even during the absence of pacing. The first spontaneous contraction (asterisk) after pacing however showed a higher force, confirming the presence of post-rest potentiation in EHTs from different cell lines.*

It was often technically difficult to test the post-rest potentiation as the EHTs tend to beat spontaneously even if not paced. In a more classical model of post-rest potentiation, adult cardiomyocytes which have no spontaneous beating activity are used. In such a model, every single contraction can be precisely controlled and an increase in force for the first contraction after an unpaced interval can be observed. The increase in force is then proportional to the time of the unpaced interval, up to a certain force limit. In this experiment, the spontaneous beating prevented investigating the effect of increasing resting time intervals on force increase as the EHT kept contracting spontaneously during the unpaced intervals. However, it could still be noticed that the first contraction following the absence of pacing shows an increase in force of approximatively 10% (asterisk). Thus, this experiment confirmed the presence of post-rest contraction mechanism also in a disease

specific cell line (**Fig. 22**). The data however did not allow quantitative comparisons between the cell lines investigated.

2.2.2. <u>Force frequency relation and frequency dependant acceleration of relaxation.</u>

Another well characterised property of human cardiac muscle is a positive correlation between force and frequency, known as the force-frequency relationship or "staircase phenomenon". A higher pacing frequency should in principle lead to a higher contraction force due to an increase in calcium cycling in the cardiomyocyte.
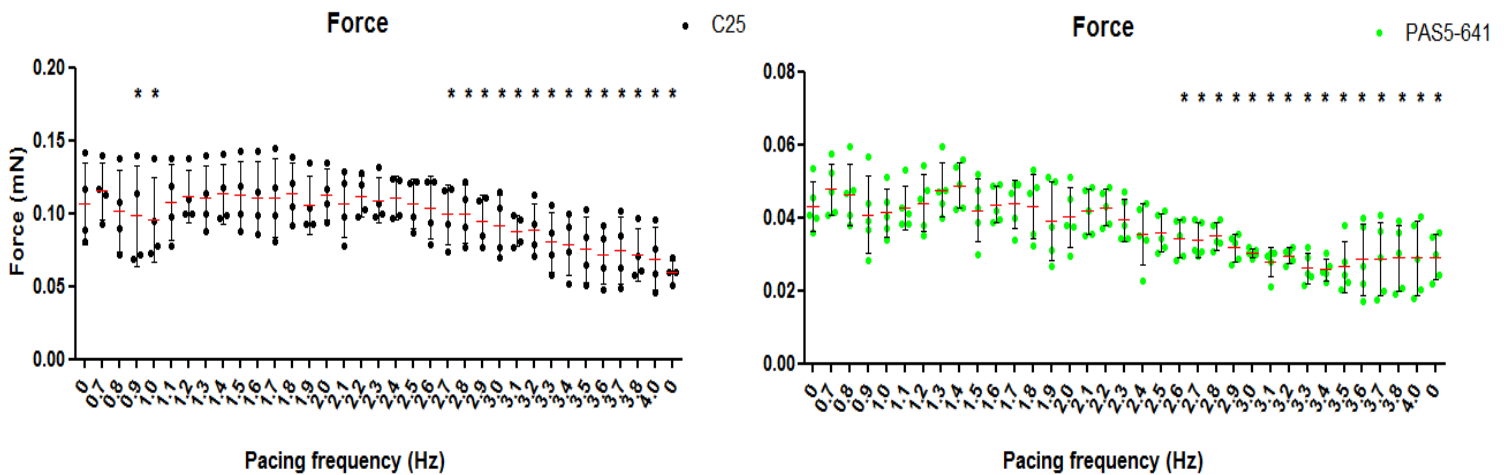
Fig. 24: *Contraction force of control (C25) and patient-specific (PAS5-641) EHT as the pacing frequency was progressively increased throughout the experiment. Measures were made at sub maximal calcium concentration: 0.6 mM so the EHTs would not already be beating at maximum force. A negative force frequency could be observed with a significant difference starting around 2.6 Hz for both models. The force decrease was similar in both models. Mean represented by a red line, * p<0.05; paired two-way ANOVA compared to pacing at 0.7 Hz, with a Bonferroni post-hoc test. C25 n=4, PAS5-641 n=5.*

The observation however was not be fulfilled by our model where a negative force-frequency relationship could be observed. In this experiment, force decreased by 42% and 38% in respectively C25 and PAS5-641 between 0.7 Hz pacing in the beginning and the 4 Hz pacing in the end. Such an effect would argue for the general presence of a negative force-

frequency in our EHT model even if additional experiments should be performed to confirm the reproducibility of the result (**Fig. 24**).
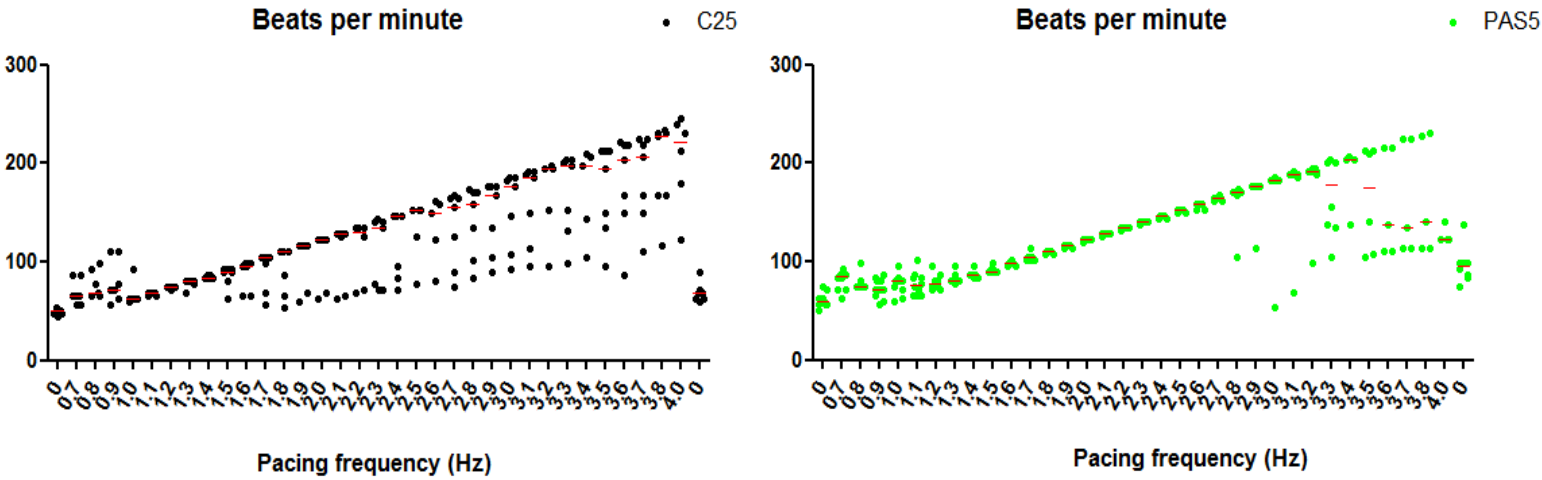
Fig. 25: *Beating frequency of control (C25) and patient-specific (PAS5-641) EHTs as the pacing frequency was progressively increased throughout the entire experiment. Measures were made at sub maximal calcium concentration: 0.6 mM. Every outlier dot represents an EHT not following the imposed pacing frequency. Mean is represented by a red line. C25 n=7, PAS5-641 n=10.*
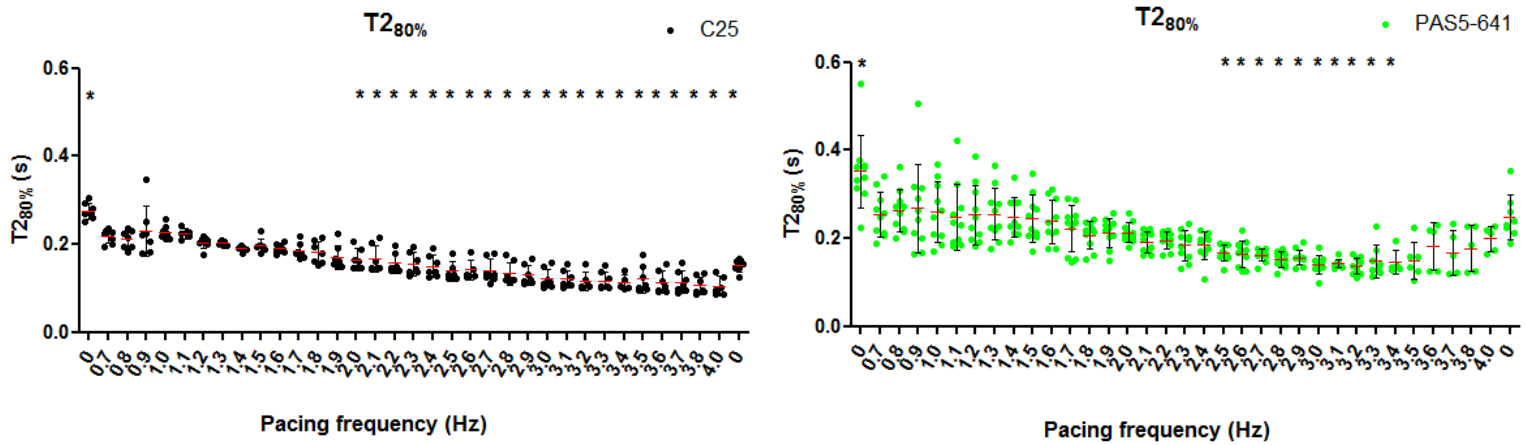
**Fig. 26:** *T2$_{80\%}$ of control (C25) and patient-specific (PAS5-641) EHTs as the pacing frequency was progressively increased throughout the entire experiment. Measures were made at sub maximal calcium concentration: 0.6 mM. A strong significant reduction of relaxation time could be observed with increasing pacing frequency. Mean represented by a red line,* p<0.05; 1 way ANOVA compared to pacing at 0.7 Hz, with a Tukey post-hoc test. C25 n=7, PAS5-641 n=10.*

A strong significant decrease in T2$_{80\%}$ was also observed, confirming that our model follows fundamental properties of cardiac muscle. In C25 a decrease from 275 ms (SD: 18) at baseline to 105 ms (SD: 22) at 4 Hz while in PAS5-641 a maximum decrease from 350 ms (SD: 82) at baseline to 145 ms (SD: 27) at 3.4 Hz could be observed (one-way ANOVA, p<0.05). The decrease was in both cases progressive and inversely correlated with the pacing frequency (**Fig. 26**). As mentioned previously for spontaneous beating, faster beating contractions leads to faster repolarisation and shortening of the T2$_{80\%}$. No clear differences were observed between control and patient-specific EHTs, suggesting that the frequency-dependent acceleration of relaxation (FDAR) is consistent throughout cell lines.

3. **Drug stimulation**

After observing basic parameters, I decided to take advantage of the EHT model that is very well adapted to experiments involving drug stimulation. It's 24-well plate format and the automatic recording make it perfectly adapted to establish a concentration-response curve. The characteristic phenotype of CPVT patients is their arrhythmic response to stress or physical activity (β-adrenergic stimulation). An isoprenaline concentration response-curve was therefore performed with the control and disease-specific EHT in order to verify if the patient phenotype could be found in our model.

A second attempt was to rescue the prolonged relaxation time found in our disease-specific model by a stabiliser of the RYR2. Indeed, if the relaxation time would be rescued to normal with such a substance, it would strongly suggest that the RYR2's mutation in our patient-specific cell line is related to the observed prolonged relaxation time.

Finally the last attempt was to see if the mutation in the patient did lead to a shift of the calcium cycling in the cardiomyocyte. A calcium leak of the RYR2 could have led to a remodelling of the cardiomyocyte's calcium cycles leading to a higher transport by the NCX antiporter of the cell membrane.

3.1. β-adrenergic stimulation

The main phenotype of CPVT patients is ventricular tachycardia during an episode of β-adrenergic stimulation, for example during physical activity or an emotional event. It was therefore decided to perform a concentration response curve for isoprenaline, a non-selective β-adrenergic agonist, for both control and disease-specific EHTs.
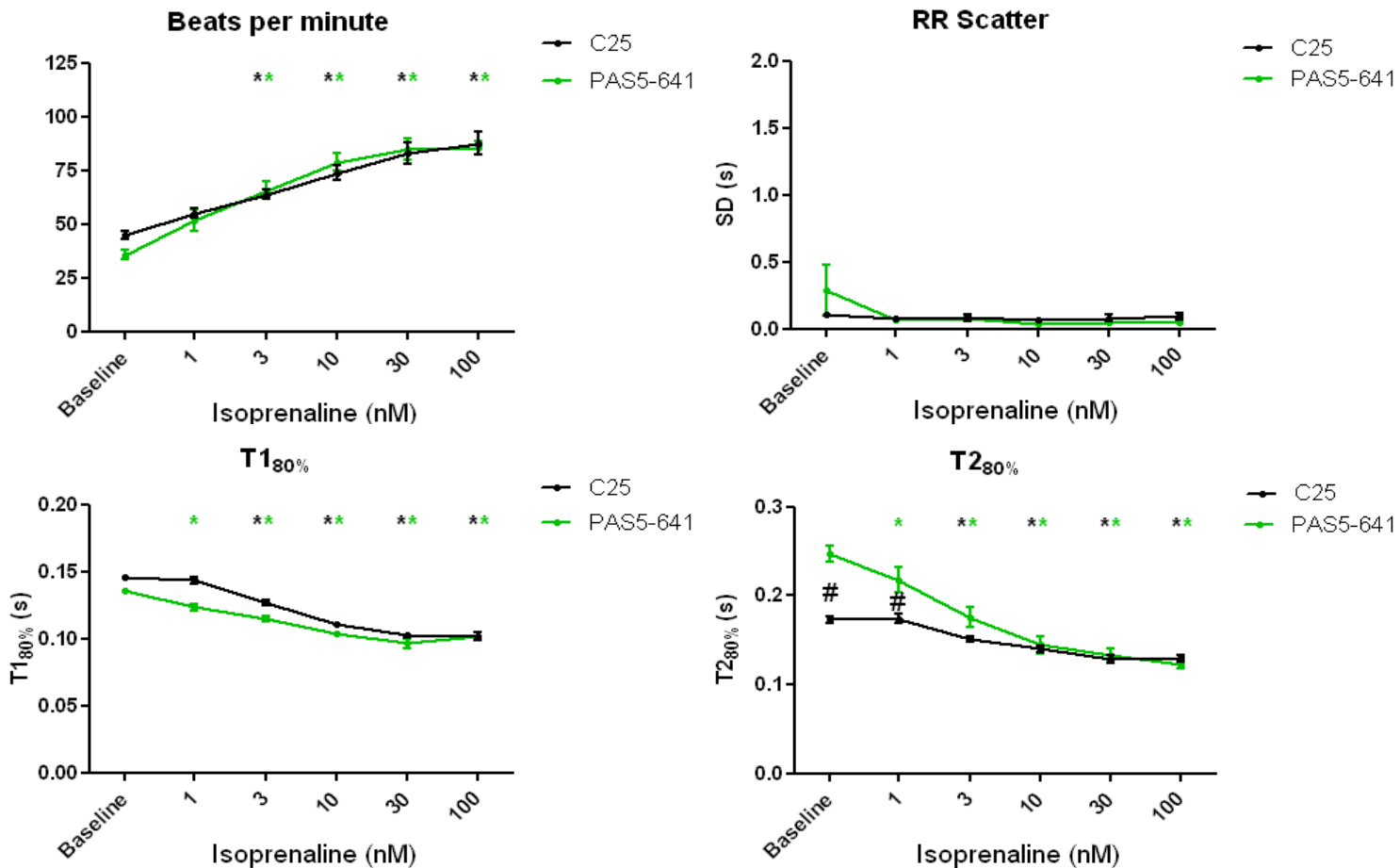
*Fig. 27: A semi-logarithmic isoprenaline concentration-response curve was performed on both control and disease-specific EHTs from 1 to 100 nM. Increasing concentrations led to an expected increase in spontaneous beating frequency and decrease in both $T1_{80\%}$ and $T2_{80\%}$. As it can be deducted from the very low RR-scatter values for all muscles, no irregular beating pattern was present even in the higher concentrations. *, $p<0.05$ compared to baseline; # , $p<0.05$ compared to the other cell line, two-way ANOVA with a Dunnett post-hoc test, C25 n=11, PAS5-641 n=3.*

As expected, a positive chronotopic reaction was observed in C25 EHTs with an increase of beating frequency from 44.7 bpm (SD: 6.3) at baseline to 87.6 bpm (SD: 17.4) at 100 nM isoprenaline and PAS5-641 with 35.7 bpm (SD: 4.2) at baseline and 85.5 bpm (SD: 17.4) at 100 nM (p<0.05, two-way ANOVA). No statistical differences were observed between the two cell lines. The results confirm a well-known consequence of β-adrenergic stimulation in heart muscles. However, a positive inotropic effect was not observed (data not shown), probably as it was counter-balanced by the positive chronotropic response. Furthermore, the concentration-response curve was performed at physiological calcium concentrations (1.8 mM) which leads to a full contraction force in the EHT, therefore probably blunting the possible force increase (**Fig. 27**).

The RR scatter parameter is an indicator of the irregularity of beating by indicating the standard deviation of the time occurring between the beats. Its low absolute value for both C25 and PAS5-641 throughout the concentration response clearly showed an absence of arrhythmia even at the highest isoprenaline concentration (**Fig. 27**). The patient-specific EHTs therefore did not display the typical β-adrenergic phenotype that can be found in patients.

As expected, isoprenaline shortened $T1_{80\%}$ and $T2_{80\%}$ of the EHT's contraction. $T1_{80\%}$ decreased from 146 ms (SD: 4) at baseline to 101 ms (SD: 9) at 100 nM for C25 and from 136 ms (SD: 0.5) at baseline to 101 ms (SD: 3.2) at 100 nM for PAS5-641, again without difference between the two cell lines (p<0.05, two-way ANOVA) (Fig. 25.). However, surprisingly, isoprenaline shortened relaxation time more in disease-specific EHTs (from 247 ms (SD: 16) at baseline to 122 ms (SD: 7) at 100 nM) than in control (from 173 ms (SD: 13) at baseline to 129 ms (SD: 13) at 100 nM; p<0.05, two-way ANOVA). $T2_{80\%}$ after full β-adrenergic stimulation did not differ between the lines. The difference between the two cell line's $T2_{80\%}$ was only significant during baseline and 1 nM isoprenaline, with higher concentrations masking the difference between the cell lines (p<0.05, two-way ANOVA) (**Fig. 27**).

3.2. Stabilising the RYR2

The significantly longer relaxation time of disease-specific EHTs compared to those of healthy individuals could be interpreted as a consequence of the mutation in the RYR2. If the mutation leads to a calcium leak from the SR through the RYR2, causing a longer $T2_{80\%}$, RYR2 stabilising drugs provide a rescuing effect on the relaxation time of the patient-specific EHTs.
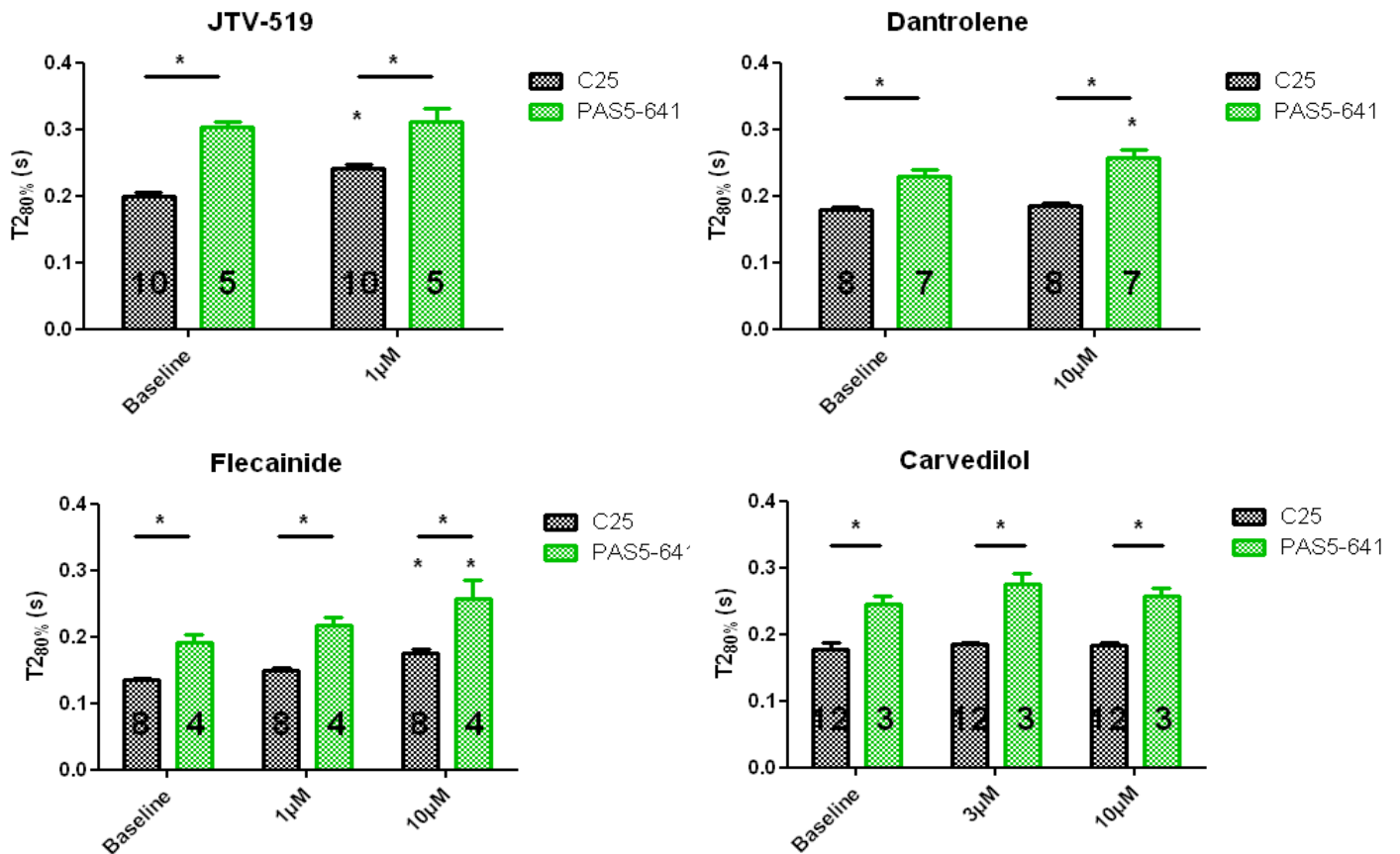
Fig. 28: *Analysis of RyR2 stabilising drugs. $T2_{80\%}$ of control and patient-specific EHTs were measured in the presence of moderate to high concentrations of RYR2 stabilising drugs. No rescuing effects on $T2_{80\%}$ could be observed. Numbers in bars represent the number of EHTs used in the experiment.* p<0.05 compared to baseline, two-way ANOVA with a Dunnett post-hoc test .*

All drugs tested in these experiments have been reported to exert stabilising effects on the RYR2 by decreasing its opening probability (P_o) (Watanabe et al. 2010; Zhou et al. 2011; Jung et al. 2012; Sacherer et al. 2012). However, none of them was able to reduce the relaxation time to levels comparable to control's baseline. Carvedilol for example, had no significant

effect on $T2_{80\%}$ in both C25 and PAS5-641. JTV-519 had no effect on PAS5-641's relaxation time, but slightly increased it in C25 (42 ms; SD: 25). Dantrolene increased $T2_{80\%}$ in PAS5-641 (from 229 ms (SD: 25) to 258 ms (SD: 29; $p<0.05$, two-way ANOVA), but had no effect in C25. Flecainide increased relaxation time in both PAS5-641 (from 192 ms (SD: 22) to 257 ms (SD: 40)) and C25 (from x to y). These results clearly demonstrate the absence of rescuing of the $T2_{80\%}$ parameter. The observed increase in $T2_{80\%}$ suggests effects of dantrolen and flecainide on repolarization. In any case, the data suggest that the prolongation of $T2_{80\%}$ observed in disease-specific EHTs is not occurring through a leakiness of the RYR2.

3.3. NCX block

An indirect consequence of the possible leakiness of the RYR2 in the disease-specific EHTs would be that more calcium is pumped out of the cardiomyocyte via the NCX antiporter as a compensatory mechanism to the RYR2 mutation. Indeed, as more calcium accumulates in the cardiomyocyte's cytoplasm, the NCX antiporter should become more active and pump the calcium out of the cell in exchange for sodium coming in. It was therefore tried to block this exchanger with a specific antagonist, which should lead to a higher $T2_{80\%}$ prolongation in the disease-specific EHT compared to the control.
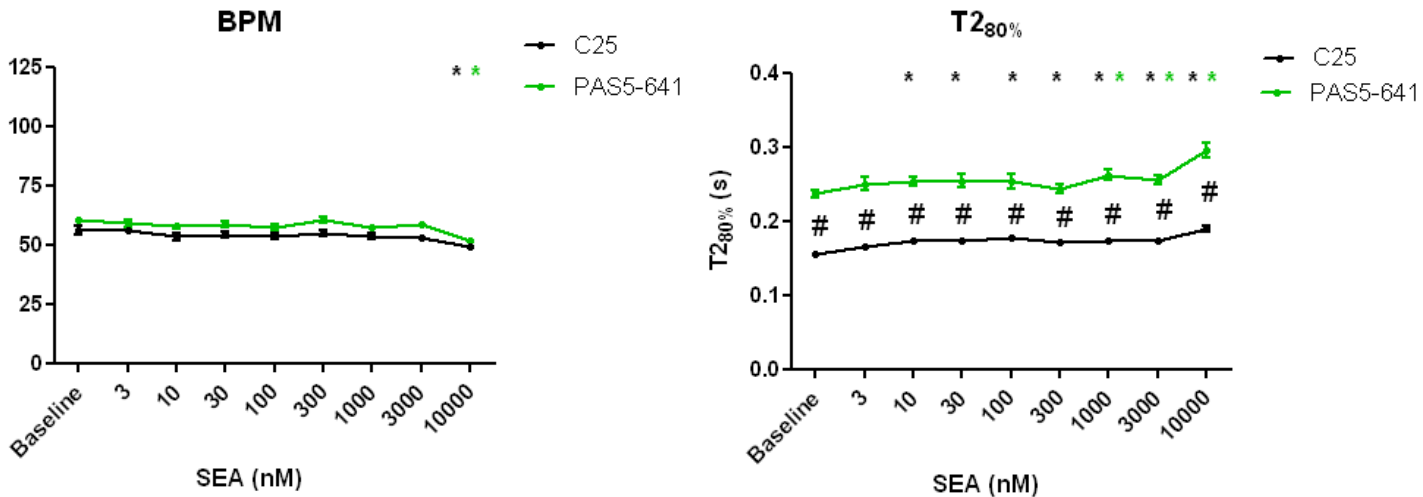
Fig. 29: *A semi-logarithmic concentration response curve with SEA-0400 was performed. Only a slight increase of relaxation time can be observed at higher concentrations. C25 n=12, PAS5-641 n=7, * p<0.05 compared to baseline, # p<0.05 compared to the other cell line, two-way ANOVA, with a Dunnett post-hoc test.*

Increasing concentrations of SEA-0400 had only little effect on the relaxation time of the disease-specific EHTs and only at higher concentrations. $T2_{80\%}$ was increased from 156 ms (SD: 10) to 189 ms (SD: 14) in C25 and from 237 ms (SD: 14) to 295 ms (SD: 26) in PAS5-641, comparing baseline to 1 µM SEA (p<0.05, two-way ANOVA). A very slight frequency reduction was observed at the highest concentration of the drug, which could be due to unspecific binding or to interference with the calcium clock (**Fig. 29**). The findings suggest that NCX is not more active in disease-specific EHTs compared to controls and therefore provide no evidence for the hypothesis of a leaky RYR2 in these cells.

3.4. Reactions to different external calcium concentrations

Calcium handling is a key parameter of heart muscle function. Hypo- or hypersensitivity of myofilaments to calcium is a disease mechanism in inherited cardiomyopathies. In this section, experiments were performed to compare calcium sensitivities of control and the disease-specific EHT as an integrated parameter of calcium handling. Furthermore, as arrhythmic beating could not be induced by β-adrenergic stimulation, we tried to induce it with high extracellular calcium concentrations. The arrhythmia was then also tried to be rescued through a RYR2 stabiliser to see if the mutation of the disease-specific EHT was one of the causes of the arrhythmic behaviour.

3.4.1. Sensitivity to external calcium

Calcium sensitivity was tested in both control and patient-specific EHT with force and relaxation time measured as output parameters. Data obtained from human ventricular muscle strips from a patient with Hypertrophic Cardiomyopathy (HCM) were included for comparison. Concentration response curves were performed in order to measure the different calcium sensitivities.
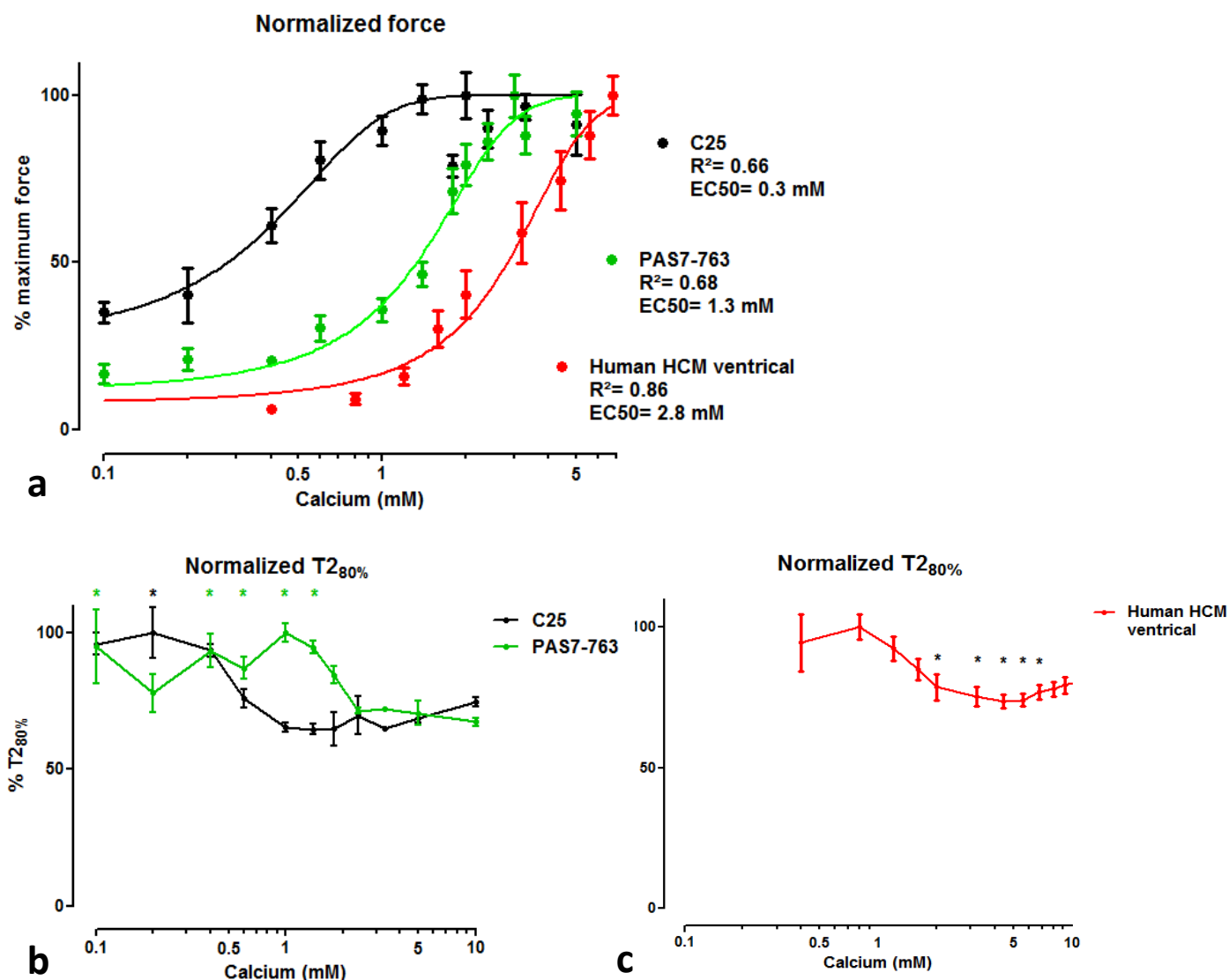
Fig. 30: a. *The calcium concentration response curve performed showed the highest calcium sensitivity for the control EHTs and the lowest for the human HCM ventricular strips. A Fischer test was performed and the EC_{50} values were significantly different. The experiments were kindly performed by Dr. Eder and PD Dr. Christ.* **b.** *Relaxation time was also measured throughout the increasing calcium concentrations and results were normalized to maximum values. Increasing concentrations of calcium overall led to a decrease in $T2_{80\%}$ independently of the cell line, or the model. * $p < 0.05$, two-way ANOVA compared to 10 mM calcium, with a Dunnett post-hoc test .***a. b.** *C25 n=12, PAS7-763 n=25* **c.** *As a model comparison purpose, relaxation times were also measured on ventricular strips of an HCM patient. The results would suggest that the HCM model had a similar calcium sensitivity to the disease-specific EHTs which is lower than control EHTs. * $p < 0.05$, n=10, one-way ANOVA compared to 0.7 mM calcium, with a Tukey post-hoc test, results kindly provided by PD Dr. Christ.*

The experiments showed that disease-specific EHTs had a lower calcium sensitivity than the controls, both in terms of force and relaxation ($T2_{80\%}$). Force EC_{50} was 1.6 mM (95%

confidence interval: 1.37-1.75) in PAS7-763 compared to 0.4 mM (95% confidence interval: 0.19-0.59) in controls (**Fig. 30a**). The analysis of the $T2_{80\%}$ lead to a similar conclusion with an EC_{50} of 1.8 mM for PAS7-763 and 0.5 mM for C25 (**Fig. 30b**). Furthermore, the EC_{50} of the calcium sensitivity of the human ventricular HCM was the lowest compared to the two other models with 2.8 mM (95% confidence interval: 2.6-3.1) for the force, but relatively similar to PAS7-763 with an EC_{50} of 1.5 mM (95% confidence interval: 1.1-1.9) for the relaxation time (**Fig. 30c**). The experiment would suggest that our disease specific model for CPVT has a closer calcium sensitivity to adult ventricular cells from an HCM patient, suggesting some similarities in the two diseases possibly in term of calcium handling. Such result would however need to be supported by extra experiments as it is not a well-known literature fact of the CPVT disease.

3.4.2. Overnight recording

It was previously shown that the longer $T2_{80\%}$ of the disease-specific EHTs could not be rescued by RYR2 stabilising drugs which suggest that this phenotype was not a consequence of the RYR2 mutation. Furthermore, β-adrenergic stimulation did not lead to the expected arrhythmic beating in the patient-specific EHTs. I therefore decided to induce arrhythmia not indirectly through the β-adrenergic receptors, but directly through an increase of the extracellular calcium concentration. Overnight recording was therefore performed in Tyrode´s medium with different calcium concentrations (physiological 1.8 mM, medium-high 3 mM and high 5 mM).

3.4.2.1. Irregular beating characteristic of disease-specific EHTs

As arrhythmic beating of the disease-specific EHT could not be provoked with β-adrenergic stimulation, the EHTs were measured overnight in different calcium concentrations.
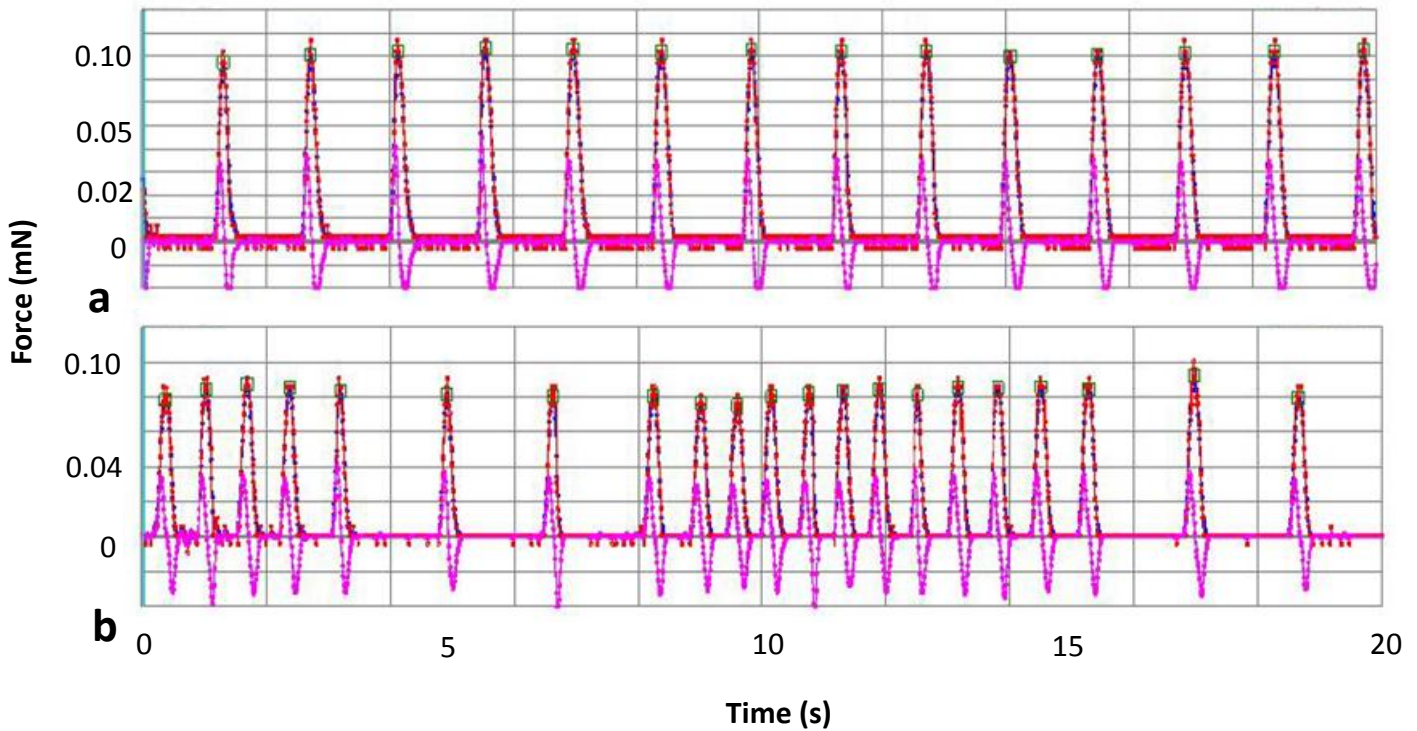
Fig. 31: *Representative recordings of C25 (**a.**) and PAS7-763 (**b.**) during overnight recording at 5 mM calcium. The recording of the disease-specific EHT showed a clear arrhythmic phenotype, in contrast to the control EHT displaying a very regular contraction pattern. The red line represents the measure of the force of the EHT calculated by the software and the pink line its derivative which corresponds to the contraction or relaxation velocity.*

In this recording, the EHTs were measured overnight at 5 mM calcium for 20 seconds, every 30 minutes during 14 hours. In a representative example of one single recording it can be appreciated that every recording could be characterised as regular (**Fig. 31a**) or irregular (**Fig. 31b**). Statistically, almost exclusively the disease-specific EHTs became arrhythmic (**Fig. 31**).
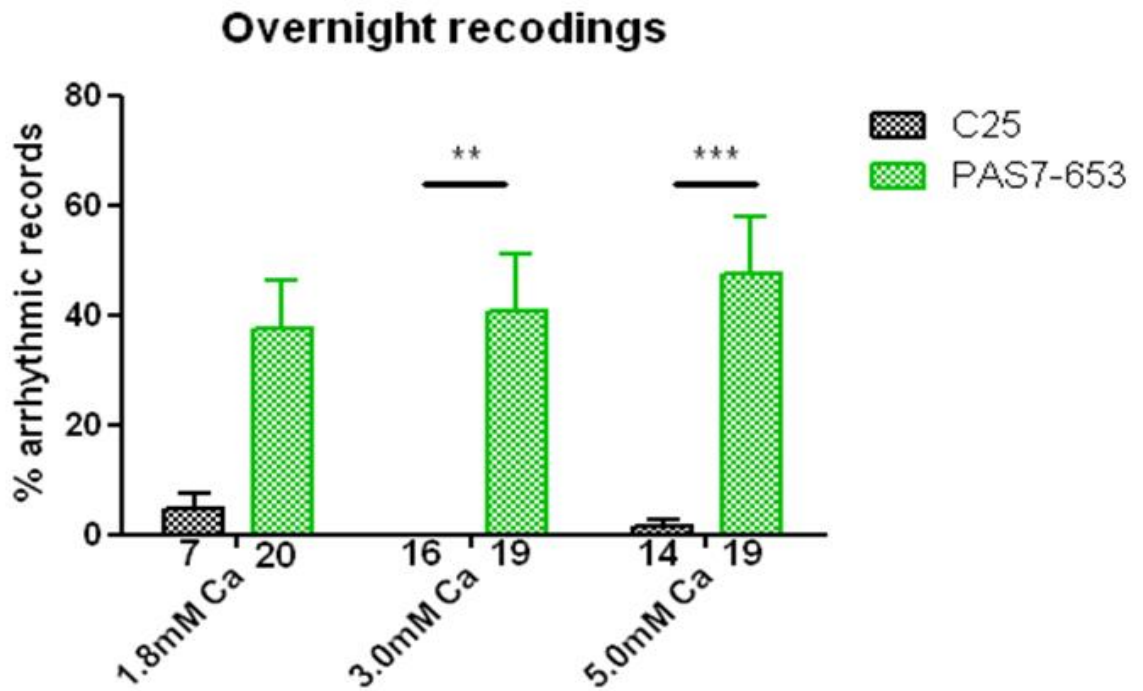
Fig. 32: *Overnight recordings of control and patient-specific EHTs for 20 seconds, every 30 minutes during 14 hours. Every recording was analysed and determined if it was or was not arrhythmic. A percentage of arrhythmic recordings for every EHTs could then be calculated. It was observed that disease specific EHTs were clearly more arrhythmic than the controls and a slight tendency of increased arrhythmia with increased calcium concentrations could also be observed. Part of the data kindly provided by Anika Benzin. ** p < 0.01 , *** p < 0.001 , two-way ANOVA with a Dunnett post-hoc test, n number noted under the bar.*

The percentage of arrhythmic events of each EHT during the 14 hours recording period was compared and analysed, showing a clear increased arrhythmia in the disease-specific EHT group. The C25 EHTs showed 4.5, 0 and 1.4% arrhythmic recordings (SEM: 3.1, 0, 1.4) for 1.8, 3.0 and 5.0 mM calcium, respectively, compared to 37.4, 40.6, 47.6% (SEM: 9.0, 10.5, 10.1) for PAS5-641 (**Fig. 32**). The arrhythmic behaviour was sometimes only observed during a longer time of recording as it tended to occur after the first 7 hours of measure. The previous experiments had overlooked the phenomenon as they were only performed during 3 to 4 hours.

3.4.2.2. Absence of JTV rescue

Since irregular beating behaviour was observed exclusively in disease-specific EHTs, we tried to reverse the phenotype by RYR2 stabilising drugs. After an overnight measure, a RYR2 stabilizing compound, JTV-519, was added to each EHT to try and stop the irregular beating pattern.
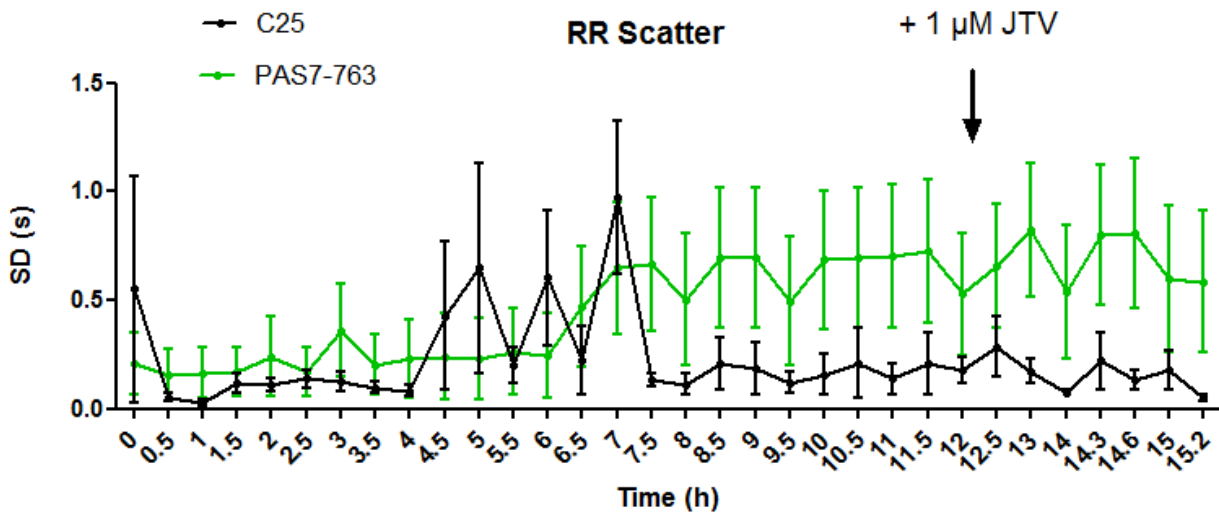
Fig. 33: *Standard deviation of the time between contractions during an overnight measurement of control and disease-specific EHTs. After 7 hours of incubation at 5 mM calcium, the disease-specific EHTs display a higher irregular beating pattern than the controls. JTV-519 was then added after 12 hours, but no significant reduction of the arrhythmia could be observed. C25 n=4, PAS7-763 n=8.*

During the first 6 hours of recording, only sporadic arrhythmic events could be observed in C25 and none in PAS7-763. Such arrhythmic events usually happened in long term recordings where only a few irregular EHTs could rapidly increase the RR-scatter average of the entire recording, explaining its sporadic nature. After 7 hours of incubation at 5 mM calcium, spontaneous beating pattern could be observed exclusively in disease-specific EHTs with a RR-scatter of C25 never exceeding 0.3 s while PAS7-763 only had values superior to 0.5 s during the same period. The arrhythmicity of the disease-specific EHTs progressively rose after 6 hours to then stay stable till the end of the recording. JTV-519, a RYR2 stabilizer, was

added after the 12th hour to all EHTs, but no difference in the number of arrhythmias could be noticed afterwards with RR-scatter peaking up to 0.8 s (SEM: 0.35) for PAS7-763. It would therefore seem that the observed arrhythmia was not linked to the RYR2 (**Fig. 33**).

It was shown in this chapter that the EHT model was successful in reproducing fundamental cardiac mechanisms such as post-rest potentiation, frequency-dependent acceleration of relaxation and response to β-adrenergic stimulation. Even if the typical CPVT phenotype was not found in our patient-specific EHTs, differences in phenotypes could still be observed between the disease-specific and the control EHTs. Those differences were a longer relaxation time, lower calcium sensitivity and an increased arrhythmic behaviour with increased calcium concentration for the disease-specific EHTs compared to controls. However, these phenotypes could not be rescued by RYR2-stabilising substances and therefore the observed phenotypes could not be linked to the RYR2 mutation present in the patient-specific EHTs.

Part 3: Sub-clonality dynamics in hiPS cell culture

iPS cells are becoming an increasingly used tool for disease modelling, drug development and regenerative medicine. However, the value of this cell culture method could legitimately be questioned as the cells used for modelling purpose often carrying a single nucleotide mutation might get affected by the relatively long cell culture process during which new mutations spread through the culture. Indeed, they are usually kept in culture for a minimum of forty to fifty passages. Selection or modification during this time period lead to changes in cellular characteristics and could have profound impact on downstream applications. It was therefore decided to study deeper cell culture dynamics by using a cell tracking method.

The cell lineage was tracked by transduction of three different lentiviruses expressing each a red, green or blue fluorescing protein which is therefore called RGB (Red Green Blue) marking. As cells are transduced by a random number of lentiviral particles which randomly insert into the genome and randomly express, thousands of colours are theoretically expressed. Each colour is then inherited by all the daughter cells, which allows a very easy and cost-effective cell tracking.

The question was then to see what will happen to the global colour expression of the culture after virus transduction. In theory, the number of colours should show an initial decrease as not all cells are taken from passage to passage, but this colour decrease should rapidly stop after a few passages. A second colour decrease should follow due to the competition between the cells. If some cells in the culture would attach better, proliferate faster or have a higher survival rate, some "sub-clones", should gradually overgrow the entire culture. This process could easily be monitored by confocal microscopy pictures or FACS analysis.

1. RGB marking as a tool for sub-clonal tracking

The RGB marking was performed on three different cell lines of different passage number: one cell line of medium passage number (~p45) and high passage number (>p100) as well as a different cell line of medium passage to compare cell line variability. It was hypothesised that as the older cultures should have had more time to adapt to cell culture conditions, the competition between the sub-clones should be slower or inexistent compared to the younger passage culture. Therefore the unique cell line with middle and high passage number was expected to display a reduced colour loss in the high passage culture compared to the medium passage one. The second cell line of middle passage number was also taken to be able to observe potential cell line variability.

First, all cell lines had to be transduced and checked if they had an even repartition of colours. The verification was done both visually by confocal pictures and more statistically with FACS analysis. The cells were then passaged further following a standard cell culture protocol for about 50 passages. The evolution of colours was then regularly measured by both confocal pictures and FACS analysis.

1.1. Uniform lentiviral transduction

Sub-clonal cellular dynamics were studied in two different cell lines: C25, reprogrammed by lentivirus and BJ, reprogrammed by a non-integrative sendai virus. The C25 was itself split into two different cultures: one of a similar passage number than the BJ cell line (~p45) named C25-middle, and an older passage number (p>100) named C25-old. The investigation's purpose was to test if the passage number of the culture would influence its sub-clonal dynamics or not.
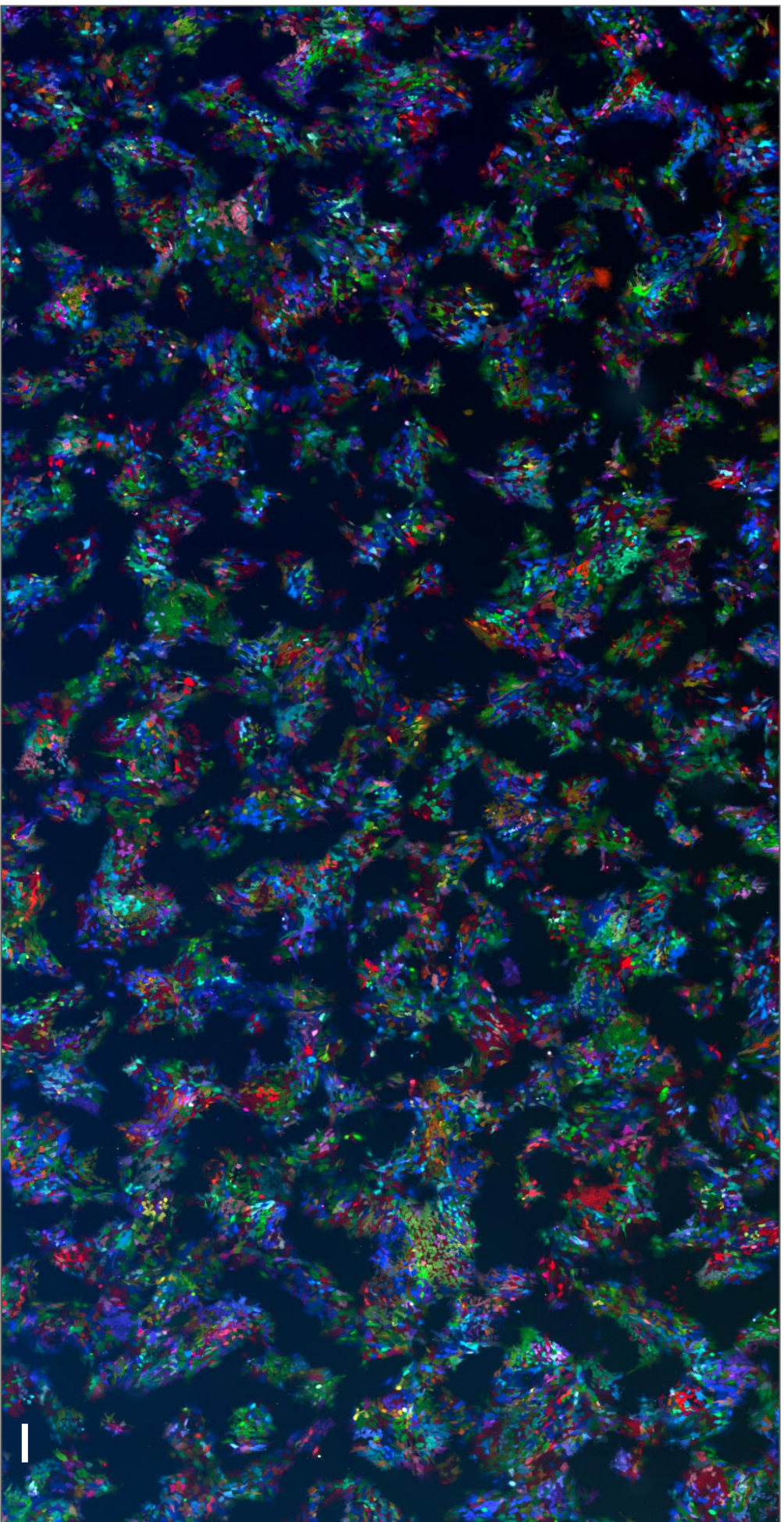
Fig. 34: BJ cell line p7 after RGB transduction. This picture is a part of a meta-picture composed of 64 stitched single pictures. The cells could be checked visually only a few passages after transduction. It can be observed that the colour patches are still relatively small and colour diversity seems to be relatively high, giving indications of a polyclonal state as it would be expected in an ideal iPS cell culture. Cell line scale bar 200 μm.

For the experiment, RGB transduction was noted passage 0, as it is the time point when all cell are considered of being of a different colour. After the transduction, the cells could be controlled visually for an even colour repartition as a control of the transduction quality. On this meta-picture of 64 stitched single pictures, patches of the same colour appeared relatively small and the total amount of colour relatively high (**Fig. 34**). However, this method was not very precise, and only big differences would have been noticeable. Therefore further cell analysis was performed by FACS method analysis.

a

Population	#Events	%Parent
■ All Events	35,179	####
■ P1	30,000	85.3
■ P2	18,442	61.5
■ P3	18,873	62.9
■ P4	18,848	62.8
■ P2 AND NOT(P3) AND NOT(P4)	3,197	10.7
■ P3 AND NOT(P2) AND NOT(P4)	4,004	13.3
■ P4 AND NOT(P2) AND NOT(P3)	3,763	12.5
■ P2 AND P4 AND NOT(P3)	3,868	12.9
■ P2 AND P3 AND NOT(P4)	3,652	12.2
■ P3 AND P4 AND NOT(P2)	3,492	11.6
■ P2 AND P3 AND P4	7,725	25.8
⊠ P2 OR P3 OR P4	29,701	99.0
⊠ NOT(P2 OR P3 OR P4)	299	1.0

b
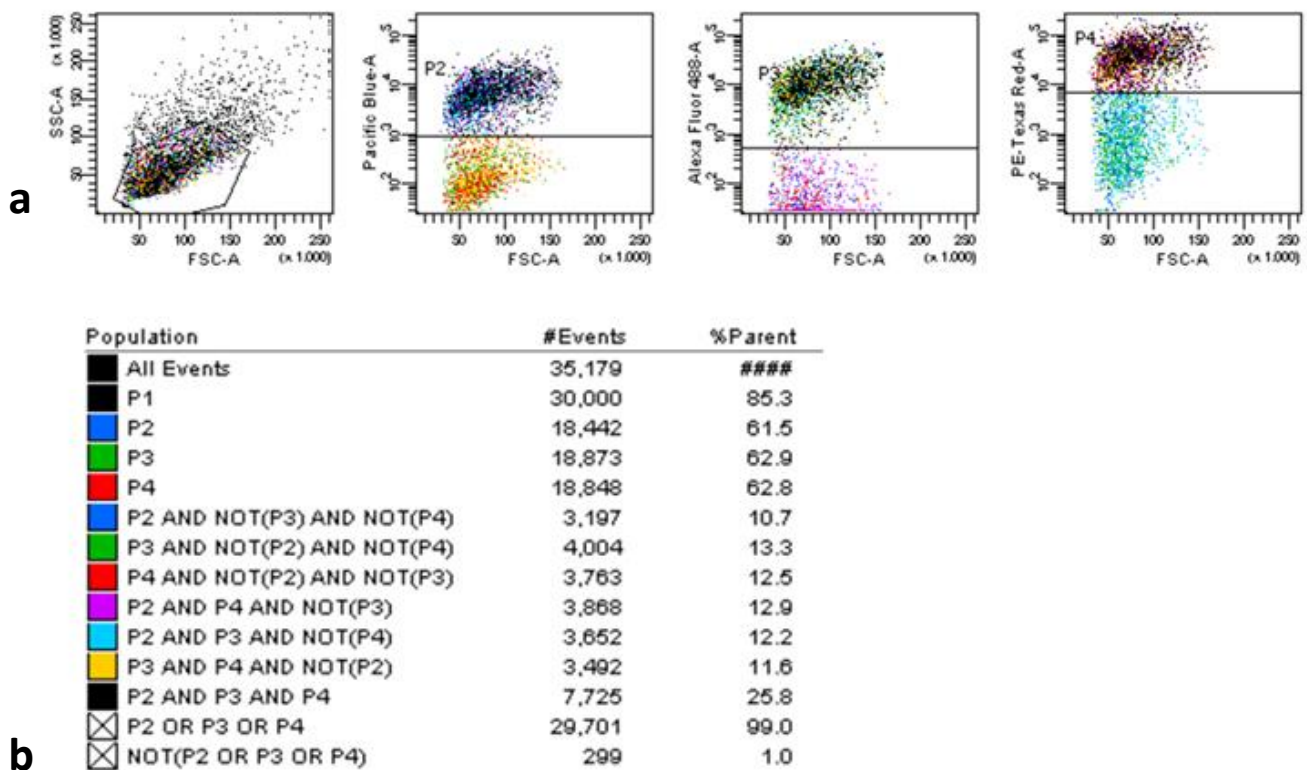
*Fig. 35: A few passages after transduction by RGB vectors, the FACS analysis showed that the expression of the three colours was evenly distributed throughout the cells. **a.** Forward scatter and sideward scatter plot of the cell culture. The data is then further plotted according to the three different colours: Pacific Blue for blue, Alexa Fluor 488 for green and PE-Texas Red for red. **b.** For each colour around 60% of the cells was expressing it (P2, P3, P4), around 13% expressing two of every colour combination (purple, cyan and yellow) and 25% triple positive cells (black). The RGB transduction was therefore adapted for sub-clonal tracking. Cell line: C25-old p6, as a representative example.*

An analysis of transduced cells after 6 passages showed an even repartition in the expression of the three basics colours and their combinations (**Fig. 35**). An effective selection of the transduced cells thanks to antibiotic resistance was also achieved, leading to only 1% of non-transduced cells (**Fig. 35b**). The quality of the transduced culture was therefore sufficient to be able to track sub-clonal dynamics over a longer time period.

1.2. Sub-clonal dynamics

The evolution of colour expression could then easily be analysed both by confocal imaging and by FACS analysis. Confocal pictures and FACS analysis of the cell culture were performed every other passage in order to have a clear view of the colour dynamics over time. It was specifically investigated to which extent colours would decline and if a colour loss speed difference between the different cell lines could be noticed. The sub-clonal dynamics were then also further used to investigate deeper into the run-to-run differentiation variability.

1.2.1. Confocal imaging

Cell colour could be visually controlled by taking confocal pictures with the simultaneous three colour channels. In our case, meta-pictures composed of 64 different pictures were taken in order to have an overview impression (**Fig. 34**). However as the observed colour loss was drastic, bigger magnifications were also sensitive enough to observe the phenomenon (**Fig. 35**).
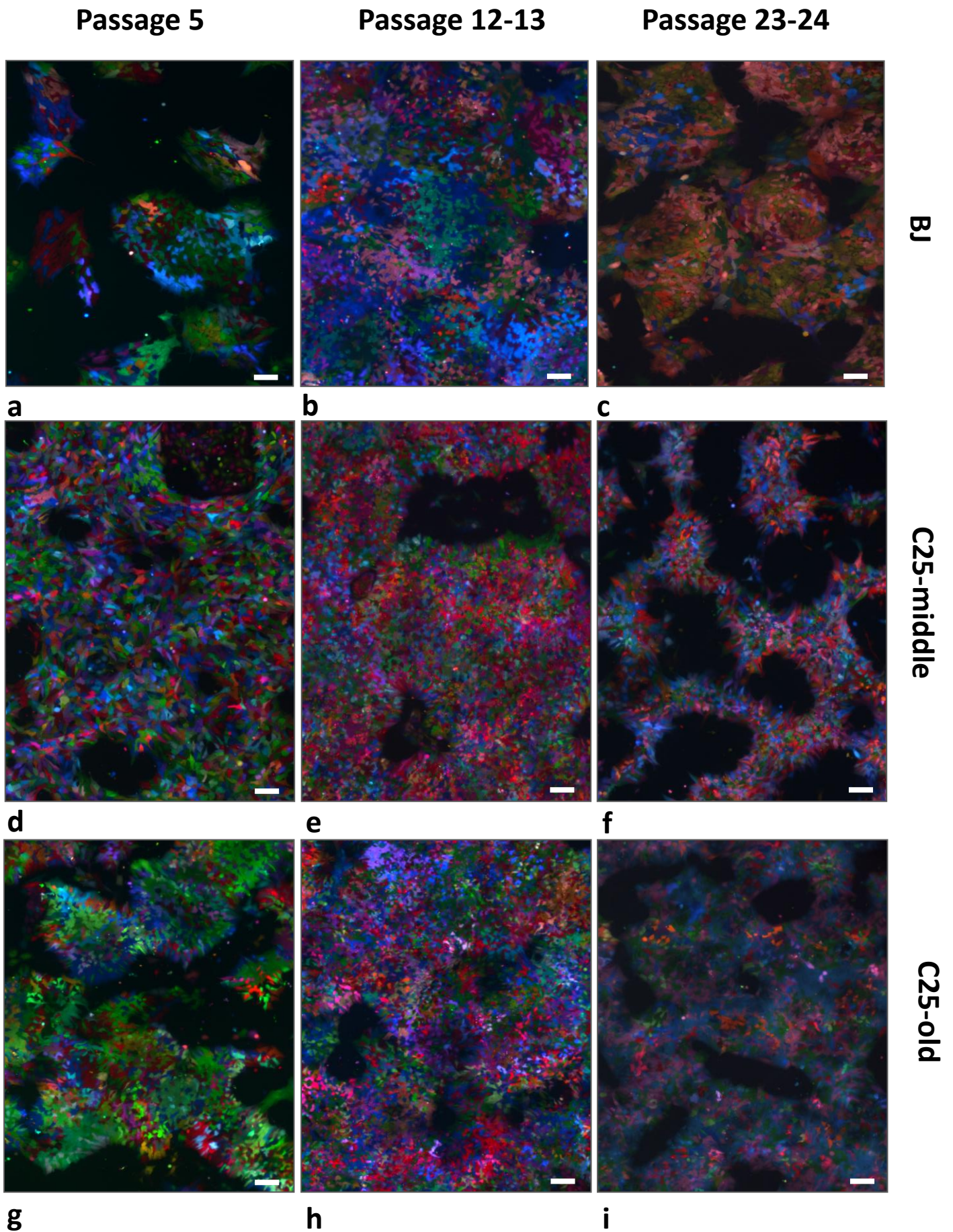
Fig. 36: *Pictures in the left column were taken at passage 5 after transduction, middle column passage 12-13 and last column 23-24. Scale bar: 100 μm.* **a.b.c.** *Pictures from the BJ cell line showing a drastic reduction of colours 20 passages only after transduction. A beige and an olive coloured sub-clone seemed to start taking over the culture.* **d.e.f.** *Pictures from C25-middle cell line did not show a striking change in colour over the different passages.* **g.h.i.** *Pictures from C25-old cell line, clearly showing an overgrowth by a grey-blue sub-clone.*

was not as clear for the cell line C25-middle which still had a polyclonal aspect. This could be due to the fact that this cell line's growth rate was slightly slower than the other two, leading to lower splitting ratios during the passages.

1.2.2. FACS analysis

FACS analysis of the RGB transduced cells showed the overgrowth of some sub-clones of the cell cultures more clearly. This figure (**Fig. 37**) represents BJ cell line at different splitting time points. Throughout the passage numbers, the polyclonal state appeared as a homogeneous cloud of plotted dots, each of the dots representing a cell. Progressively as later passages were reached oblique alignment of dots became visible, indicating the overgrowth of some sub-clones. After passage 38, a single sub-clone had almost totally overgrown the colony becoming 90% of the total cell number
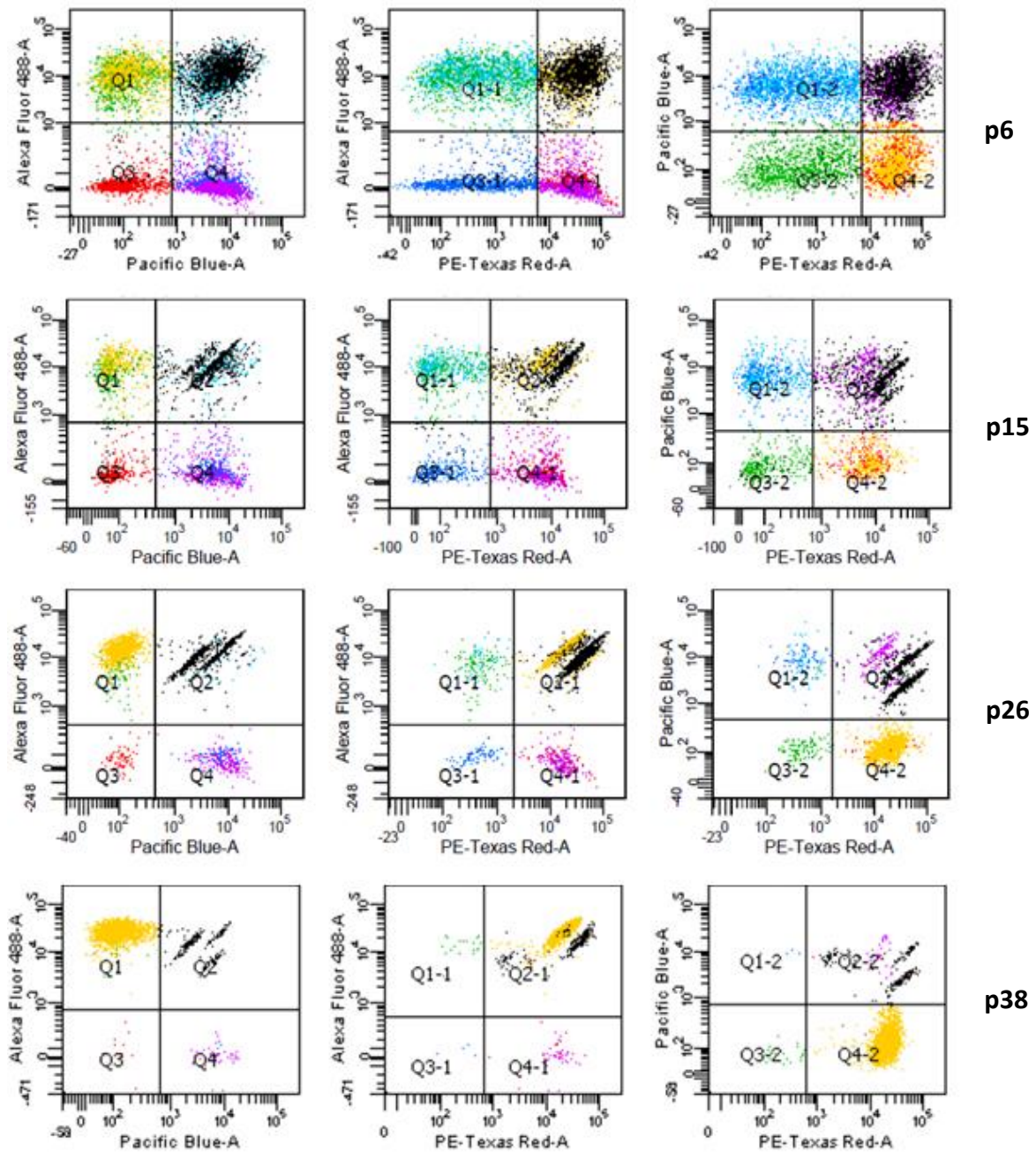
Fig. 37: *FACS analysis of the BJ cell line over cell culture passages 6, 15, 26 and 38. Each graph is composed of two axis on which is plotted one of the three basic colour's intensity on a logarithmic scale. Alexa Fluor 488 is green, Pacific Blue is blue and Texas Red is red. The three graphs represent all the combinations of colour plotting, it is a way to visualise a three-dimensional plotting on a two-dimensional support. The gradual taking over of sub-clones could be noticed by the appearance of oblique lines in the plot. The lines represent a unique colour with different intensity expressions. At passage 38, the sub-clone represented in a yellow colour represented 90% of all cells.*

When the three cell lines were analysed at later passage it was noticed that BJ and C25-old displayed only one or two sub-clones while C25-middle still displayed an oligoclonal state (**Fig. 37**). It was still clear however that the last passage of C25-middle clearly showed the taking over of some sub-clonal elements (**Fig. 37 p6; Fig 37**). The first hypothesis was therefore not confirmed as C25-middle was supposed to have a faster sub-clonal dynamic but showed a slower one. Furthermore, it did not seem in this experiment that C25-old cell line clonal overtake was slower than BJ's. It could however still be noticed that C25-middle had a slower division rate than BJ and C25-old, which could explain the slower sub-clonal overgrowth.
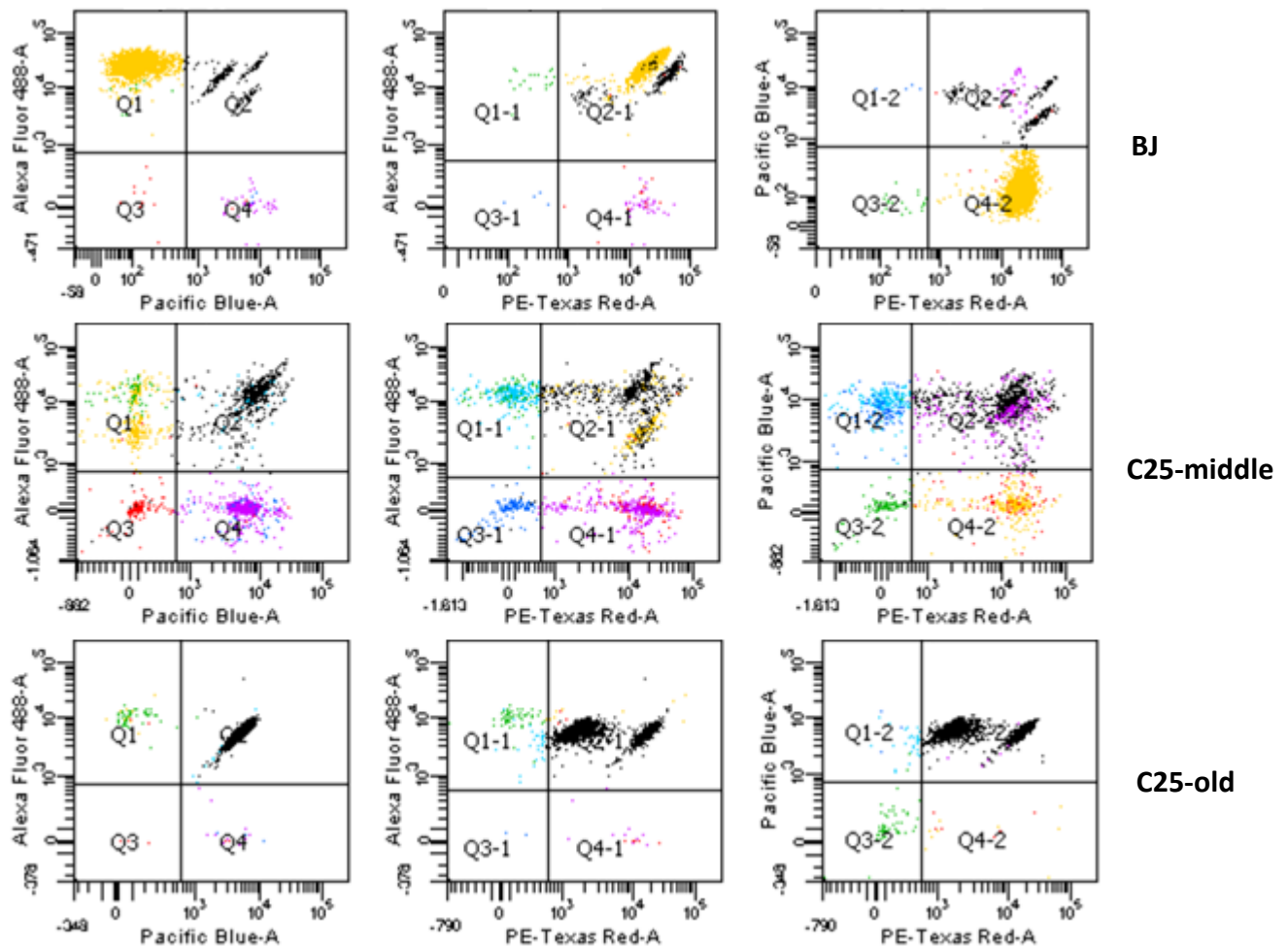
Fig. 38: The three cell lines at p37-38 showing the overgrowth of one or two sub-clone for BJ and C25-old, and an oligoclonal state for C25-middle. For the BJ cell line, the yellow clone represented 90% of the total cells, and in C25-old the two tripled coloured sub-clones represented together 95% of the culture. Each sub-clone could be FACS sorted and cultured in three different cultures with over 95% sorting purity.

After being cultured for almost 40 passages, C25-old was overgrown by two sub-clones making up 95% of the culture and BJ by one making up 90% (**Fig. 37**). The single clones were then FACS sorted, their karyotype was analysed and found to be free of aberrations.

2. RGB marking as a tool for EHT characterisation

As described in the previous section, RGB marking is a very useful tool for lineage tracking, but it could also be used in the EHT itself for a better visualisation of cell limits and a better understanding of cells interactions inside the EHT itself. The RGB staining could show clear cell-to-cell contact in the EHT as well as elongated cells organising in bundle structures. This bundle organisation is very interesting as it is a sign of a more mature cardiac structure. A live confocal video of coherently beating cardiomyocytes was also recorded as an indirect evidence of electrical coupling.

2.1. Cell-to-cell contact

Cell-to-cell contact is a fundamental aspect of EHT's properties. Before reaching maturity, the EHT was only composed of independently beating cells. The cells then progressively coupled and the EHT started beating coherently, providing a measurable force contraction, and therefore usable as a heart model.
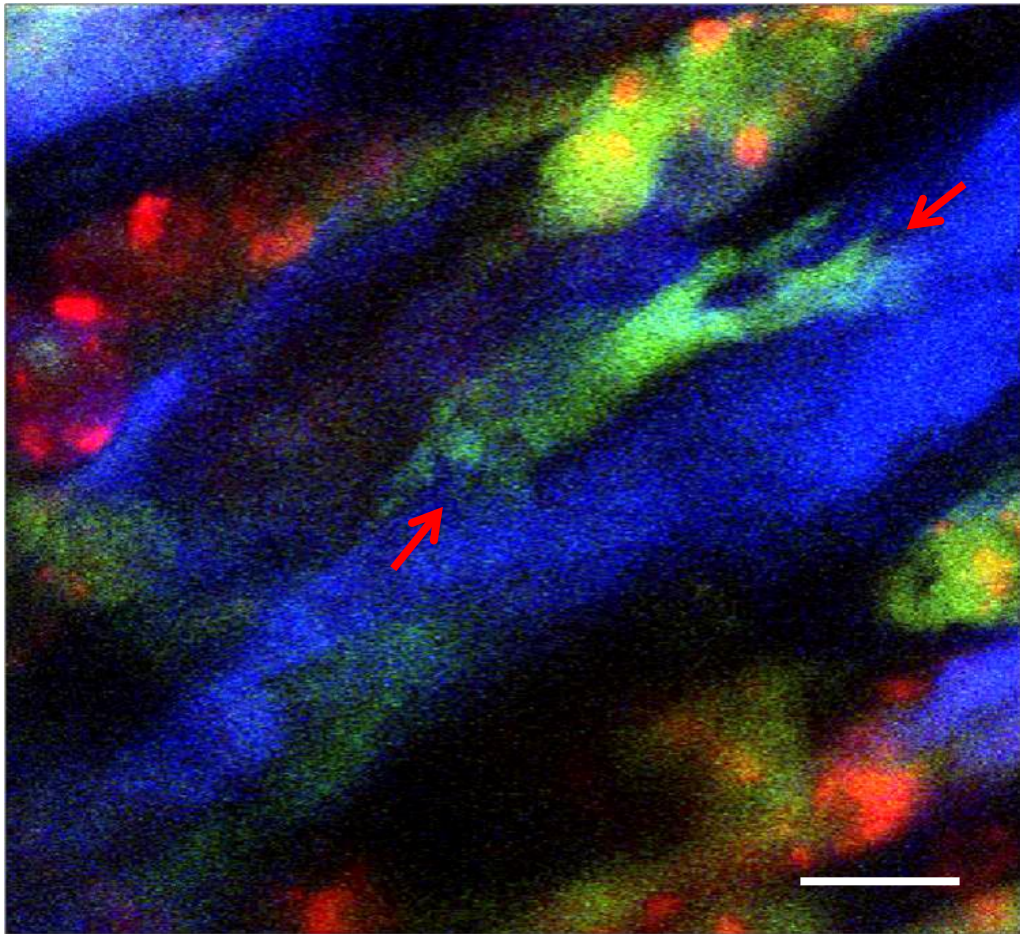
Fig. 39: Live confocal image of a RGB transduced iPS cell-derived human EHT. Two cell-cell contacts of the green elongated cardiomyocyte are marked by red arrows. Thanks to RGB staining, adjacent cells of different colours make cell-cell contact easily detectable. Scale bar 25 µm.

On this confocal live image from an EHT, elongated cardiomyocytes can be observed with cell-cell contact (red arrows) for example between the red and the blue cells (**Fig. 39**). Cell-cell contacts of elongated cardiomyocyte are a good evidence of the beginning of cell maturation in human iPS cell-derived EHTs. The contact will then allow electrical coupling and the coherent beating of the entire EHT.
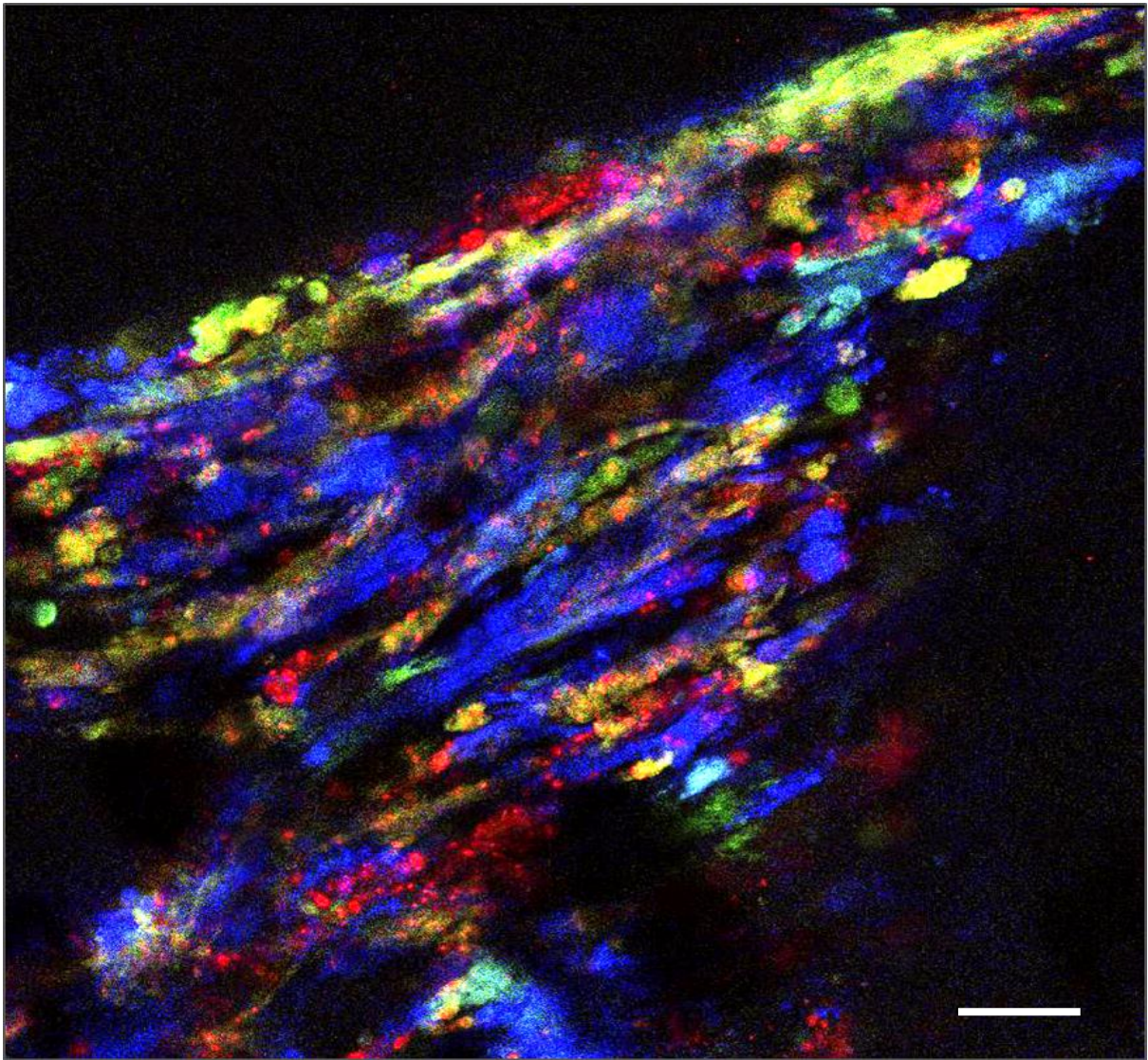
Fig. 40: Live confocal image of a RGB transduced iPS cell-derived human EHT at a lower magnification. Large bundles of elongated cardiomyocyte are visible with numerous cell-cell contacts visible with adjacent cells of different colours, indicating a relatively mature state of the heart tissue. Scale bar 100 µm.

At a lower magnification, the elongated morphology of some cardiomyocytes was even clearer and numerous cell-to-cell contacts could be noticed for adjacent cells of different colours. The edge of the EHT (top left corner) was also found to be more densely populated with cells, which could be explained by the tension forces developed inside the EHT due to its spontaneous contractions (**Fig. 40**).

Overall the elongated shape of the cardiomyocytes and their numerous cell-to-cell contacts argues for a good maturity of the human EHT.

2.2. Electrical coupling

Live confocal imaging could also capture beating cardiomyocytes at the cellular level. Two adjacent cells of different colours beating coherently were found to give an indirect evidence of electrical coupling.
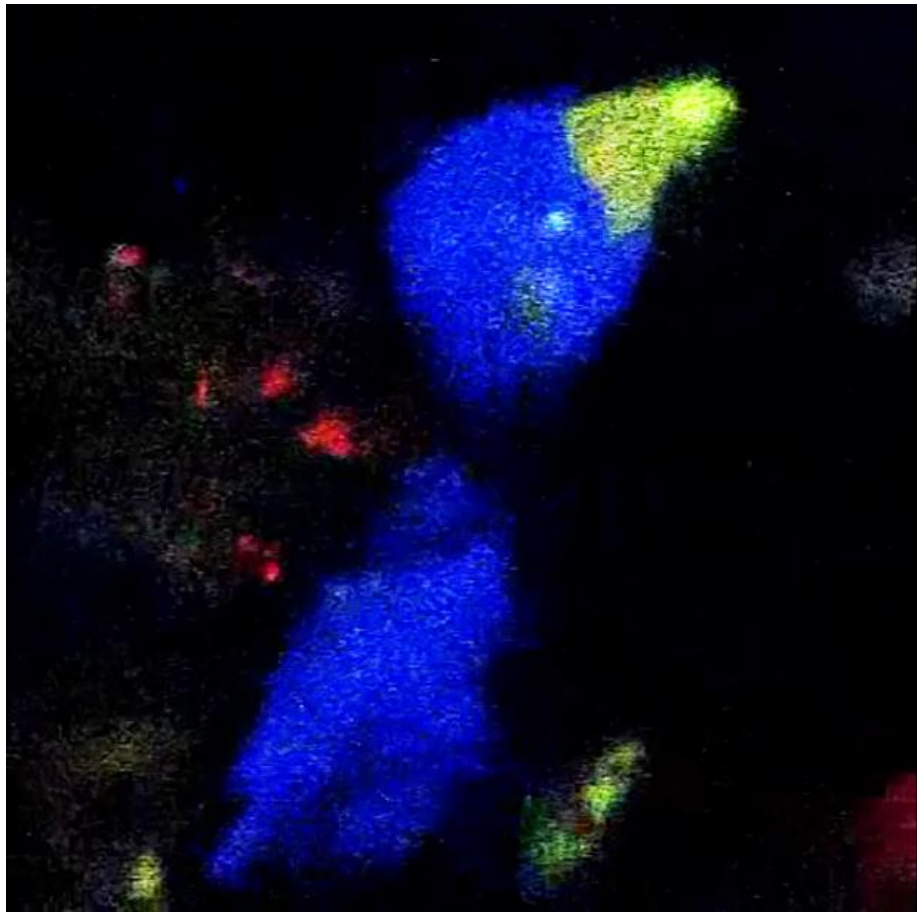
Video 4: *Live confocal video of RGB human iPS cell-derived EHTs showing a coherent contraction between two adjacent single cardiomyocytes of different colours: a large blue cell and a small green one. The coherent contraction of the two cells is an indirect proof of electrical coupling.*

In this live video two beating cardiomyocyte of two different colours, blue and green can be seen contracting coherently, which is an indirect proof of electrical coupling. After building cell-to-cell contact, the cardiomyocyte would then couple electrically, leading to the coherent contraction of the EHT. Evidence of electrical coupling was more arguments for a

relatively mature state of the EHT model. The RGB staining allowed here again to easily distinguish between two different cells and to make functional interpretations.

Discussion

1. **Differentiation**

Differentiation of pluripotent stem cells into cardiomyocytes has been largely improved over the past 5 years without being solved entirely. During this project we developed a new differentiation technique capable of producing a large number of beating cardiomyocytes suitable for tissue engineering approaches. Indeed tissue engineering is a field which usually requires more cell quantity than other traditional research areas like electrophysiology or multi electrode array which only require a moderate amount of cells.

1.1. Hallmarks of the differentiation protocol

As the total amount of cardiomyocyte required is more important in cardiac tissue engineering, there was a need to upscale iPS cell-derived cardiac differentiation production by optimising three major criteria: the cost, the purity and the productivity. Those three aspects have been a major focus in the elaboration of our differentiation protocol, as a working differentiation protocol would require all those three different points to be perfectly optimised. This paragraph will only discuss some major hallmarks of our cardiomyocyte differentiation protocol, keeping in mind that much more smaller optimisation steps were fine-tuned and also necessary for an efficient optimised protocol.

One of the major hallmarks was the introduction of spinner flasks for EB formations. Indeed, the original method described and still mostly used nowadays uses V-shaped 96 well plates where EBs would individually be formed by centrifugation (Burridge et al. 2007). This method is not applicable for large production numbers, as a large amount of consumable and manual labour would be required thereby enormously increasing the costs of the protocol. The two alternatives we tested in the laboratory, spontaneous EB formation and forced aggregation, were also not entirely satisfying.

The first one: spontaneous EB formation lead to a high variability in shape and size of EBs and was not suitable for all cell lines. Some cell lines did not spontaneously form EB with this technique making it hard to use as a cell line-independent protocol.

The second one, the forced aggregation technique, was a big improvement compared to V-shaped 96 well plate aggregation, but still very labour-intensive (Ng et al. 2005). Indeed the pyramidal-shaped silicone microcavities had to be cleaned and autoclaved, the system had to be used in a 6-well plate format, making it hard to upscale and the EBs were also relatively hard to be taken out of their microcavities.

EB differentiation in spinner flasks can be performed in large quantities thanks to their total volume reaching up to one liter and work efficiently independently of the cell line. The protocol is extremely straight forward with only dissociation, cell counting and resuspension with an optimised cell concentration. The technique is however not very adapted to small EB productions as the minimum cell amount required could still be too high for low-scale differentiations.

The other major hallmark of the differentiation protocol was the replacement of the protein-based inhibitor DKK1 by a small inhibitory molecule (DSI-7) to block the Wnt pathway. This small molecule was kindly provided free of costs by Dr. Schade, but its commercially available equivalent IWR-1 has a comparable mode of action. First, the potency of the small molecule was much higher, and therefore could be used at very low concentrations and second, the price of the molecule itself is much lower as proteins are always more expensive to produce than small molecules. This drop in price made it possible to culture large quantities of cells in the presence of Wnt inhibitor for a whole week with a daily medium change.

In the end, our protocol is very well adapted to large-scale production of cardiomyocytes, however, the purity of cardiomyocytes and the cell output is however still very variable over time. Despite using constantly the same protocol, large differences of efficiency were obtained with the same cell line from one run to another. The cause of this differentiation variability is not clear. Two different explanations are possible. First, the variance could be caused by technical problems during the differentiation. The differentiation protocol consists of numerous steps, uses about 30 compounds and human mistakes or variability of the

quality of commercially available substances could result in sub-optimal differentiation conditions. Standardising protocols, storage conditions and incorporating quality controls might be ways to avoid these issues. Second, the variability in differentiation efficiency could be due to variability of the initial differentiation potential of the hiPS cells at the beginning of the differentiation protocol. As pluripotency of hiPS cells is dependent on the culture conditions, different stem cell media could be tested to reduce the variability. Another idea would be to establish a method to select the different clones obtained after iPS cell reprogramming. Indeed, large clone-to-clone differences where observed despite similar expression of the traditional markers like Oct4 and Sox1, suggesting that a more careful selection could lead to lower variability in the future cell lines.

1.2. Comparison to published protocols

Several differentiation protocols have been published in 2012 claiming to reach over 90% of cardiomyocyte purity from an iPS cell culture (Lian et al. 2012; Zhang et al. 2012; Minami et al. 2012). All these protocols are actually relatively similar to one another except for a few details. They have, however, two relatively important differences compared to our protocol: they are all performed on adherent cells, not EBs, and the mesodermal differentiation is triggered by direct activation of the Wnt pathway and not through Activin and BMP signalling.

Wnt activation is performed through a small molecule: CHIR-99021. Being able to use a small molecule to induce mesoderm instead of BMP and Activin would indeed be a good improvement to reduce the costs of this step. As previously described for the replacement of DKK1 by DSI-7, small molecules are usually much cheaper and more potent than their protein-based counterparts. The activation time is also much shorter: one day against three in our protocol with a very high concentration of CHIR-99021. This step resembles the firsts protocols of Laflamme et al., using a high Activin concentration during one day to induce mesodermal induction (Laflamme et al. 2007; Zhu et al. 2011). However, in this previous protocol only 30-60% of the differentiated cells were cardiomyocytes.

The proceeding of the entire protocol as a monolayer would be a significant spare of manual labour. Indeed, dissociating the cells, counting them, and transferring them to a new recipient is more time consuming than just changing the medium of the same recipient.

As the new protocols present some significant improvements to our current in-house protocol, it could be very interesting in term of efficiency to try and implement one or both of the different steps previously described which would hopefully reduce costs and labour time. However, despite performing these protocols, we were not able to reproduce the results, suggesting that the published protocols are still subject to lab-to-lab variations. One of the major differences between laboratories is the medium used for iPS cell culture, as numerous media are available and all have a unique composition.

Another difference could also be found in the reprogramming method, especially differences in marker selection or even the initial type of cells used for reprogramming such as hairs or blood cells which are also commonly used as reprogramming material. In the end, so many steps are present between the selection of the somatic cells and the beating cardiomyocytes that laboratories never have the exact same procedures. The protocols should therefore be optimised and established for our own laboratory.

2. <u>Sub-clonality</u>

In parallel to cardiac differentiation, we were also interested in the undifferentiated cell culture itself as its status before starting a differentiation run seemed to have major impact on the efficiency. In addition, we could get access to a very easy and elegant cell tracking tool thanks to collaborators, using multicolour fluorescent protein expression (Weber et al. 2011).

2.1. <u>Adaptation to cell culture conditions</u>

The initial idea at the start of this project was that cells cultured *in vitro* might be subjected to environmental selection that is probably mainly due to three main factors: proliferation rate, attachment capacity to the matrix used (in this case Matrigel®) and survival rate. Those factors should lead to a selection of sub-clones more adapted to the cell culture environment than the others.

As the cells are marked with the RGB method, every transduced cell in the culture has theoretically a unique colour. After a few passages, as only a fraction of cells are transferred from one passage to the next, the number of colours should decrease rapidly. This diminution of colour will be called a statistical decrease. When the number of different colours present in the dish is considerably lower than the total amount of cells, this statistical loss should become negligible, as the probability of losing a colour by chance approaches zero. The other possibility of losing colours would be, as explained previously, by a competitive loss, as the sub-clones which are the more adapted to the cell culture should progressively take over the culture (for more extensive understanding, see review: Raj & van Oudenaarden, 2008).

We therefore decided to compare the same cell line with a young and an old passage number, respectively C25-middle and C25-old. The older cell line should have a sub-clonal population which is more adapted to cell culture conditions and therefore have a lower competitive colour loss than C25-middle and also BJ, another cells line with a similar passage number to C25 middle

However, the expected effect was not observed, both C25-old and BJ displayed a similar competitive loss of colours. C25-middle on the other hand had a slower loss of colour. However, C25-middle also had a slower cell division rate. As during cell culture the passages of the cell lines are always synchronised to decrease labour time and the splitting ratio is consequently adapted, the numbers of passages do not fully correlate with cell proliferation. Slower dividing cells will *a priori* take more time to outgrow each other by cell division and thus the slower colour loss of C25-middle compared to BJ and C25 old probably only reflects the slower rate of cell division.

The experiment showed that 40 passages after transduction the sub-clonality was reduced to one or two clones in all cell lines. This meant that the sub-clonal population present at passage 40 stems from one common ancestor cell 40 passages ago. Reasons why no difference in competitivity was found between the old and the new passages could be as follows. The cells only adapt very slowly to the cell culture and numerous more passages would be needed to see a stabilizing effect. On the contrary, the cells could be already adapted to the cell culture conditions at the beginning of the experiment and even the younger cell lines were not young enough to see an effect. A last interpretation could be that the even if the cell culture conditions seem to be stable overtime, some subtle changes keep occurring with the cells continuously adapting to the new culture conditions, leaving no sub-clonal differences between young and old cell lines. Either way, the main finding remains more practical: a cell culture seems to be much more dynamic and evolving than previously thought. The generation of new sub-clones is probably a constant phenomenon that can occur during every cell division in the cell culture, but the experiment can tell us that after 40 passages all cells have one unique common ancestor different from the initial reprogrammed clone. Keeping the cells for only around 20 passages in culture for example could be a good solution to avoid variability.

However, an artefact due to lentiviral transduction cannot be excluded, even if the probability is extremely low. The random lentiviral transduction in the genome could indeed induce an abnormal behaviour in our cell line. Other papers however proved genetic and epigenetic modifications during cell culture (Garitaonandia et al. 2015), making it more likely that lentiviral transduction was not the cause of the sub-clonal dynamics observed in our experiment. In conclusion, more investigation on the characterisation of the sub-clonal state

should be performed in the future to try and increase our understanding of cell culture dynamics.

2.2. Impact on differentiation

The results with the RGB system could actually be a very interesting explanation of the variability found in our differentiation efficiency over time, as the variability between sub-clones could translate to better or lower differentiation efficiency. The slow replacements of the cell cultures would explain the observed "periods" of low or high differentiation rates which were experienced throughout the different differentiations, rather than a random scatter of either low or high differentiation efficiency for every single run.

The three different clones obtained from C25-old and BJ were FACS sorted and cultivated independently. Their karyotype was checked and they did not show anomaly. The results suggest that karyotype check is not a sufficient to detect sub-clonal abnormalities.

A recent publication also tried to investigate the genomic effects of long term culture of iPS cells. Their results find accumulation of deletions, duplications and cell number variants (CNVs) with increasing passage number (Garitaonandia et al. 2015). Those genomic aberrations would explain the sub-clonal differences observed. It would however not really explain why so efficient differentiation "periods" can follow less efficient ones if the genetic mutations only accumulate.

3. iPSC-derived EHTs as a heart- and disease-specific model

Modelling of human heart has always been a challenge for several reasons. Tissue availability has always been extremely limited, especially for ventricular cells, adult cardiomyocyte have a very short life span in culture and classically used small rodent animal models like mice or rats depict a very different heart physiology than bigger animals like dogs, pigs or humans. For all those reasons, EHT from human iPSC-derived cardiomyocytes offers a unique opportunity to an easily available and relatively inexpensive 3D human based heart model.

3.1. hiPSC-derived EHTs as a heart model

The multiple experiments performed with the C25 iPS cell line, derived from fibroblasts from healthy individuals, showed that EHTs depict overall, similar responses as animal models, adult cardiomyocytes or heart tissue. As iPS cells were freshly differentiated in cardiomyocyte, their phenotype has a lot of common characteristics with immature cardiomyocytes. The most obvious one is the spontaneous beating, as adult cardiomyocytes require pacing to beat. Despite this fact, our observations show also common characteristics to more traditionally used models. Their spontaneous beating is occurring at a frequency of 60 bpm, which is very similar to a healthy human heart. They react to β-adrenergic stimulation by increasing their beating frequency and reducing both their contraction and relaxation time (compare for example Borea, 1992; Monte et al., 1993). They display a post-rest potentiation mechanism with an increased contraction force in the contraction after the resting period. Their relaxation time decreases with increasing pacing frequency, which is commonly called the frequency-dependent acceleration of relaxation (Bowditch 1871; Koch-Weser and Blinks 1963). A notable difference between EHTs and adult cardiomyocyte models was the neutral force-frequency-relationship compared to a positive one in the classical model. The very slight decrease of force observed is probably misleading as it is probably due to a prolonged recording in Tyrode´s medium which tends to decrease EHT force over longer time periods. In summary, the experiments in hiPSC-EHTs reproduced the basic physiological properties of the human heart and argue for EHTs to be an accomplished human heart model.

3.2. <u>Baseline phenotype of spontaneous contractions</u>

After having shown that hiPSC-EHT was a promising heart model, I decided to measure baseline contractions of EHTs derived from healthy individual (C25) and patients (PAS5-641 and PAS7-763) to see if any difference could be detected in the contraction properties.

3.2.1. <u>Calcium leak through RyR2</u>

The baseline recordings reproducibly showed a longer relaxation time in the patient-derived EHTs PAS5 and PAS7 compared to the control C25. For PAS7-763 cell line however, most of the runs displayed a beating frequency over 100 bpm, obscuring direct comparison with the rest of the recordings with standard beating frequencies around 60 bpm due to the frequency-dependent acceleration of relaxation effect. They were therefore excluded from the calculation.

In order to explain this longer relaxation time in the disease-specific models, we formulated a hypothesis. The hypothesis was that the mutation in the RyR2 created a calcium leak from the SR to the cytoplasm, thereby increasing the calcium amount that the SERCA protein needed to actively transport back into the SR to finish the relaxation. This extra calcium would therefore increase the relaxation time as more calcium would need to be transported back to the SR after a contraction (**Fig. 1**).
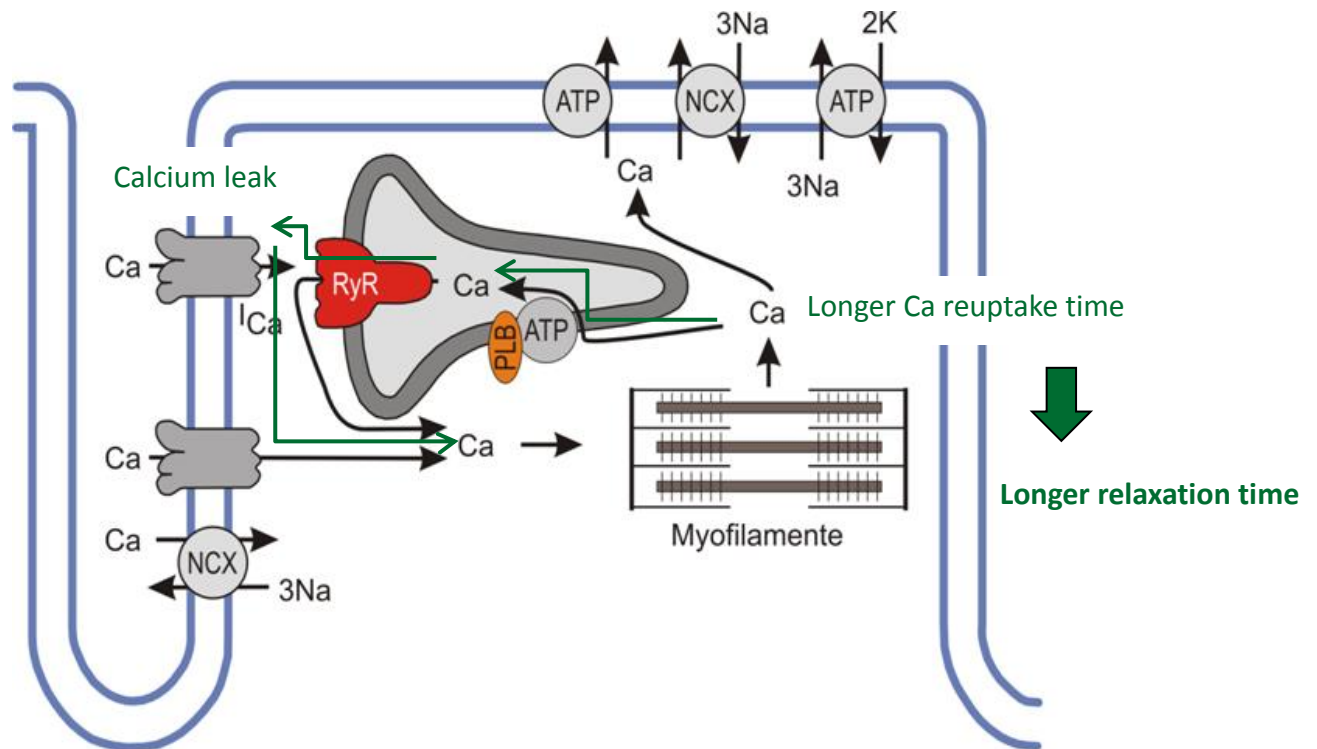
Fig. 1: *Hypothesis of a leaky RyR2 receptor. The mutation in the RyR2 creates a calcium leak from the SR to the cytoplasm (green arrows). The calcium of this leak accumulates on top of the normal calcium cycle (black arrows) and increases the cytoplasmic calcium concentration before it is transported back in the SR. However, if SERCA is already saturated, any extra calcium would stay longer in the cytoplasm, leading to a longer relaxation time.*

3.2.2. Testing the hypothesis

To test the hypothesis, I decided to try and reduce the leak in the RyR2 with stabilising drugs of proven efficiency: JTV-519, dantrolene, flecainide and carvedilol (Watanabe et al. 2010; Zhou et al. 2011; Jung et al. 2012; Sacherer et al. 2012). However, the RyR2-stabilising drugs did not decrease the relaxation time of the patient-specific EHTs, suggesting that the $T2_{80\%}$ prolongation observed in those EHTs was not a consequence of the RyR2 mutation. In addition, a longer relaxation time was never a diagnostic feature for CPVT patients, nor a property found in other heart models (Priori et al. 2013). The prolongation of relaxation is therefore hard to interpret in our model and could be for example simply due to the fact that our control cell line is derived from a unique clone and could therefore present unexpected phenotype variability due to a randomly acquired mutation during the reprogramming process.

3.3. β-adrenergic stimulation

The main phenotype characteristic of CPVT patients is a ventricular arrhythmia caused by a β-adrenergic stimulation. In our model, the effect of isoprenaline on the EHTs led to a classical positive chronotopic and lusitropic response as well as a diminution of the contraction time. However, it did not lead to an arrhythmia in the disease-specific EHTs. This result was rather unexpected, as β-adrenergic induced arrhythmia is the only clear symptom of the CPVT disease (Novak et al. 2012). I therefore tried to induce arrhythmias in our EHT model by other means to see if we could observe a difference between the control cell line and the disease-specific one.

3.4. Overnight arrhythmias

The disease-specific and control EHTs were regularly recorded overnight for 14 hours in different calcium concentrations. The experiment demonstrated that an incubation of more than 7 hours in different calcium concentrations induced arrhythmic beating in patient-specific EHTs, but not in the controls. Such an arrhythmia therefore could be a phenotype of the mutation present in the RyR2 of our EHT model.

3.4.1. High calcium hypothesis

To explain this arrhythmia, it could be supposed that the higher extracellular calcium concentration present in the medium leads to an increased amount of calcium cycling through the SR. This increase of calcium would lead to a SR calcium overload leading to SOICR and arrhythmias.

3.4.2. Absence of rescue

As previously described, we tried to stabilise the RyR2 with JTV-519, a compound reported specific and efficient drug reducing RYR2's opening probability (Sacherer et al. 2012).

However, no effect was observed on the patient-specific EHTs which remained arrhythmic for the last hour of the recording.

Once again, despite a more typical phenotype for CPVT this time, we were not able to provide experimental evidence that the observed arrhythmia is indeed caused by the RyR2 mutation.

4. Limitations of the model

The fact that no typical CPVT phenotype was observed that could be directly linked to the patient's mutation may be explained by several reasons. One of them could be that measuring contractile function in EHTs is an experiment occurring at the very end of a chain of multiple selections and manipulation of an original cell. Indeed, at first a specific patient was selected and sampled, the cells were then reprogrammed, selected and cultured over several months, frozen, re-cultured, differentiated to cardiomyocytes and then engineered into a heart tissue model. Every single of these steps is not trivial and subjected to technical variability. In this part I will discuss which steps are more likely to cause problems for disease-modelling.

4.1. Maturity and complexity of the EHT

A first reason of the absence of disease-specific phenotype found in our model could be due to its immaturity. Indeed, iPS cell-derived cardiomyocyte are only a few weeks old when they are recorded as a patient-specific model, which would be a typical age of an immature foetal phenotype (Claire Robertson, David D. Tran 2013; Yang et al. 2014). Foetal cardiomyocyte present a very different physiology compared to the adult's. An obvious one is spontaneous beating which is always observed in our freshly differentiated iPS cell-derived cardiomyocytes and never in adult ventricular cardiomyocytes. This indicates that their electrophysiology and calcium handling mechanisms differ. An example are T-type calcium channels or the inositol trisphosphate receptors (IP$_3$R) present in foetal, but not adult cardiomyocytes (Cribbs et al. 2001; Janowski et al. 2010). It is possible, for example, that the

IP$_3$R compensates the mutation of the RyR2 in the patient-derived hiPSC-CM and EHTs, therefore masking the disease phenotype.

Another reason could be that the 3D EHT model is compensating the consequences of RyR2 mutations and therefore masking the phenotype. Indeed, a multicellular 3D model is more complex than an isolated single cardiomyocyte or a 2D monolayer and that the 3D network prevents spreading of single cells automaticity. This may explain why others, using single cells, could see arrhythmias in patient-derived hiPSC-CM from patients with RyR2 mutations (Moretti et al. 2010; Fatima et al. 2011).

4.2. Penetrance of the mutation

Another interpretation would be that the genetic variant detected in our cell-donors is in fact not disease-causing. If we look at the clinical data of the mother we can see that the arrhythmia observed during exercise is not very severe. While it is compatible with a CPVT phenotype, it is certainly not proving it. The patient lived her life without suffering any clinical problems, which would argue in favour of a difference of severity in the phenotypes. Since her son (index patient) died suddenly, no ECG could be collected. Similarly, no arrhythmias were documented for the brother who received the ICD prophylactically. Thus, it is not entirely clear whether the brother and the mother of the deceased index patient really have CPVT, and it is not entirely clear whether the variant found in RyR2 is indeed causally related to the death of the index patient. Reasons for doubts are that it has been found on the basis of a candidate gene approach, no other gene has been sequenced, this very variant has never been associated with other cases of CPVT. Furthermore, RyR2 is a very large gene, giving a high chance of variants without disease relevance. Thus, it cannot be excluded that this specific variant in RyR2 has no disease-relevance at all. Alternatively, this variant causes a mild CPVT phenotype which requires either other genetic variants to clinically unmask or very strong physical exercise as in the case of a swimming race in the index patient (van der Werf et al. 2012).

4.3. Inter and intra cell line variability

Another limitation of the model is the inter-cell line variability. Throughout the project, multiple cell lines or even different clones of the same cell line were differentiated in parallel through the same protocol. However those different clones or *a fortiori* cell lines reacted very differently to the differentiation protocol and some could never be differentiated. It is therefore possible that the inter-cell line variability is more important than the effect of the mutation itself. The differentiation protocol for example could lead to different cardiomyocyte populations within the EHT, or even non-myocytes which could also play an important role, which would change its contraction physiology (Cahan and Daley 2013).

The effect was indeed also visible within different runs of the same cell line, for example in PAS7-763 which had some runs with a very high spontaneous beating frequency which could not be compared to the previous differentiation runs.

5. **Outlook**

A number of experiments are suggested for future work to try and model the CPVT disease *in vitro.*

5.1. Characterisation of EHT's immaturity

The immature state of our EHTs could be investigated more deeply to understand how it could influence our results. For example, the presence of IP_3R on the SR could rescue abnormalities of RyR2 as this receptor is not a carrier of any mutations. IP_3R are only present in relevant density in immature cardiomyocytes and its role in cardiac physiology is not as well-known as the RyR2. IP_3R could replace part of the RyR2's function in our EHT model. A deeper investigation of the role of IP_3R could tell if this hypothesis holds to be true. Some electrophysiology could be performed on iPS cell-derived cardiomyocytes, or some inhibitor drugs like Xestospongin C could be used in order to block the IP_3R (Miyamoto et al. 2000).

T-type calcium channels could also be investigated in a similar way to determine their potential influence on the CPVT phenotype. Blockers such as ML 218 hydrochloride could for example be used to specifically block the T-type channel (Xiang et al. 2011).

5.2. Clone diversification and CrispR technique

Another limitation of the study was the low amount of cell lines that could be differentiated, especially for the control cell line. Comparisons of EHTs of at least three different healthy individuals would be necessary to confirm that the C25 cell line is indeed representative of healthy individuals. To go even further, EHTs could be made of three different clones for each cell line to investigate clonal variability.

Another promising idea would be to directly repair the mutation in the patient-derived iPS cells thanks to the novel CRIPR/Cas9 technology (Cong et al. 2013; Perez-Pinera et al. 2013). This method can directly repair the point mutation and replace it by a non-mutated sequence. This way, the CRISPR modified disease-specific iPS cell line could be directly compared to its repaired cell line, and all observed differences would be specific of the RyR2 mutation.

5.3. Reprogramming iPSCs from a different family

As mentioned previously, there is also a possibility that the RyR2 variant studied in this work was not inducing a sufficiently severe CPVT phenotype. It would therefore be useful to test the model with a patient with more severe CPVT symptoms, i.e. a drastic ventricular arrhythmia during exercise or β-adrenergic stimulation, without any β-blocker treatment. Another conclusion from this thesis is that future disease modelling projects should concentrate on mutations that have been definitely linked to disease by sufficiently conclusive genetics, i.e. linkage analysis in a sufficiently large pedigree.

5.4. Using single cell recording as a more sensitive model

Another reason of why the CPVT phenotype could not be seen would be that our complex multi-cellular 3D model compensates the mutation. As this compensation might not take place in a single-cell cardiomyocyte, it would be interesting to test our cell line in single cell models like electrophysiology or calcium spark imaging.

Conclusion

In conclusion, the cardiac differentiation protocol optimised during the course of this work was very efficient and regularly reached 90% cardiomyocyte purity. However, the cardiac differentiation efficiency still depended on the cell line, the clone and was time dependent, leading to an unpredictable variability. Part of this variability may be explained by the random clonal pick performed after the reprogramming to iPS cells, where only a single colony is picked for the first passage, thereby potentially increasing the clonal variability observed later on between the different cultures. Some published protocols claiming a similar efficiency as the one we optimised have a less labour-intensive handling, especially because of the absence of an EB formation step. It could therefore be interesting to test them with our cell lines.

The RGB staining results suggests the presence of a sub-clonal dynamic in every iPS cell culture, in which the cells from a common sub-clone overgrow all other cells during 40 passages. The results suggest to keep the cells only for 20 passages in culture before going back to a frozen sample. This sub-clonal dynamic could also be an important explanation of the differentiation variability overtime observed with our protocol.

The human iPS cell derived EHT model proved itself to display most of the fundamental mechanisms of heart models such as post-rest potentiation, increase of frequency after β-adrenergic stimulation and a positive lusitropic effect with an increased beating frequency. Even though the disease-specific EHTs did not show the expected phenotype of β-adrenergic induced arrhythmias, EHTs from both patient-derived iPS cell lines from the mother and the brother of the deceased index patient displayed longer relaxation time than the controls. They also displayed arrhythmias when kept overnight in high calcium tyrode solution, which was not the case of their control counterparts, suggesting a role of the patient's mutation. However, none of these two EHT phenotypes, the longer relaxation time and overnight arrhythmia, was rescued by a RyR2 stabiliser, casting doubts on the role of the patient's mutation in the displayed phenotype.

A few reasons might explain why no typical phenotype was found in the disease-specific EHTs, or why the found phenotypes could not be rescued by RYR2 stabilisers. The first one relates to the patient. It is possible that the RyR2 mutation of the family was only one of the

causes of the death of the patient and that another mutation, specifically harboured in the deceased patient´s genome, was overlooked. Furthermore, the disease phenotype found in the mother and the brother was not very severe, which could mean that our EHT model was not sensitive enough to detect this more subtle CPVT phenotype. Another reason could be that iPS cell-derived cardiomyocytes are too immature to successfully model the CPVT disease. The presence of ion channels only in immature cardiomyocytes could completely change the cardiomyocyte's physiology. Finally, the EHT model's three-dimensional and multicellular complexity might compensate for the RYR2 mutation and mask the phenotype.

Future experiments need to be done to decide whether iPS cells or disease-specific EHTs are indeed a valuable model for the modelling of Mendelian diseases. For this type of experiments iPS cell lines should be chosen that come from patients with a definite RyR2 mutation genetically linked to β-adrenergic induced arrhythmia. Cardiomyocytes cultured in 2D may be a simpler model with less compensating mechanisms and should be studied by patch-clamp or calcium dye experiments in parallel to EHTs. Finally, a more systematic comparison of EHTs from several healthy probands and several clones per proband is likely necessary to decide whether phenoytpes such as the calcium-induced arrhythmias and longer relaxation times are indeed mutation specific or mere variability between clones.

Summary

Title: Modelling catecholaminergic polymorphic ventricular tachycardia with patient-specific iPSC-derived engineered heart tissues.

Catecholaminergic polymorphic ventricular tachycardia (CPVT) is a Mendelian disease often caused by mutations in the ryanodine receptor 2 (RyR2), in which life-threatening arrhythmias depend on β-adrenergic stimulation. The disease was already successfully modelled *in vitro* in single patient-specific induced pluripotent stem cell (iPSC)-derived cardiomyocytes, but studies in single cells ignore the complexity of cell-cell interaction. Fibrin matrix-based 3-dimensional engineered heart tissue (EHT) can provide such a multicellular complexity level. The aim of this study was the combination of the new technique of patient-specific iPSC-derived cardiomyocytes and tissue engineering to establish a multicellular disease model for CPVT phenotype. Main parts of the study were experiments to control the quality of the iPSC in long-term culture, the establishment of a cardiomyocyte differentiation protocol and functional tests of patient-specific and control EHTs.

To evaluate the behavior of iPSC over time of culture, different iPSC lines were transduced with lentiviral gene ontology (LeGO) vectors encoding either red, blue or green fluorescent protein and further selected by puromycin treatment, resulting in a unique colour in every single cell. After being cultured for almost 40 passages, FACS analysis of two of the three cell lines, C25-old and BJ, showed that two and one sub-clones made up 95% or 90% of the culture, respectively. The presence of such sub-clonal dynamic, in which the cells from a common sub-clone overgrow all other cells during 40 passages, suggests to keep iPSC only for 20 passages in culture.

To establish a multicellular disease model for CPVT phenotype, iPSC from two related patients PAS5-641 and PAS7-763 with a missense mutation in the RYR2 and a control iPSC line were differentiated into cardiomyocytes with a small molecule based, home-made protocol. Cardiomyocytes were dissociated, embedded in a fibrinogen matrix around two flexible silicone posts to make EHTs. Two to five weeks after casting, EHTs were analysed by an automated video-optical recording system capable of continuous force measurements

and paced with carbon electrodes when required. Average contraction curves were calculated on spontaneously beating patient-derived and control EHTs. A relaxation time ($T2_{80\%}$) of 157 ms (SD 27) was found for C25 (control) EHTs (n=9), while PAS5-641 and PAS7-763 (patient-specific) had 231 ms (SD 50) (n=8) and 250 ms (SD 22) (n=2), respectively. EHTs were then paced with increasing frequencies to study the frequency-dependent acceleration of relaxation. While an increase in rate from 0.7 to 4 Hz decreased $T2_{80\%}$ from 275 ms (SD 18) to 105 ms (SD 22) in C25 control (n=7), $T2_{80\%}$ decreased from 350 ms (SD 82) to 145 ms (SD 27) at 3.4 Hz in PAS5-641 (n=10). The β-adrenergic agonist isoprenaline (100 nM) increased beating frequency from 45 bpm (SD: 6.3) to 88 bpm (SD: 17.4) in C25 (n=10) and from 36 bpm (SD 4.2) to 86 bpm (SD 17.4) in PAS5-641 (n=3). While isoprenaline did not induce arrhythmias in either patient-derived EHT lines, overnight incubation in 5 mM calcium-containing Tyrode´s solution induced beating irregularities in PAS7-763 EHTs, but not in C25 control. The irregularity could not be rescued by a RyR2 stabilising drug.

Taken together, the human iPSC-derived EHT model displayed most of the fundamental mechanisms of heart models such as frequency-dependant acceleration of relaxation or increase of frequency after β-adrenergic stimulation. Even though the disease-specific EHTs did not show the expected phenotype of β-adrenergic induced arrhythmias, EHTs from both the mother (PAS7-763) and the brother (PAS5-641) of a deceased index patient displayed longer relaxation time than the control and arrhythmias when kept overnight in high calcium Tyrode´s solution. However, none of these two EHT phenotypes, the longer relaxation time or overnight arrhythmia, was rescued by a RYR2 stabiliser, casting doubts on the role of the RyR2 mutation in the displayed phenotype.

Future experiments need to be done to decide whether phenotypes such as the calcium-induced arrhythmias and longer relaxation times are indeed mutation-specific or mere variability between clones. Such experiments should include the systematic comparison of EHTs from several healthy probands and patients with a RYR2 mutation that is definitely genetically linked to a clinical CPVT phenotype.

Zusammenfassung

Titel: Entwicklung eines Krankheitsmodells für katecholaminerge polymorphe ventrikuläre Tachykardie basierend auf Patienten-spezifischem künstlichen Herzgewebe

Katecholaminerge polymorphe ventrikuläre Tachykardie (CPVT; englisch für *catecholaminergic polymorphic ventricular tachycardia*) ist eine nach den Mendel'schen Regeln autosomal-dominant vererbte Krankheit, die unter anderem durch Mutationen im Ryanodinrezeptor (RyR2) verursacht wird und durch unter β-adrenerger Stimulation auftretende lebensbedrohliche Arrhythmien gekennzeichnet ist. Ein bereits erfolgreich etabliertes *in vitro* Modell für diese Krankheit verwendete einzelne Patienten-spezifische Kardiomyozyten, die aus induzierten pluripotenten Stammzellen (iPS-Zellen) abgeleitet wurden. Allerdings können Untersuchungen an Einzelzellen die Komplexität von Zell-Zell-Interaktionen nicht erfassen. Im Gegensatz dazu kann diese Komplexitätsebene mit dem hier verwendeten, auf einer Fibrin-Matrix basierenden künstlichen Herzgewebe (EHT; englisch für *engineered heart tissue*) sehr gut dargestellt werden. Das Ziel dieser Studie war daher die Kombination von Tissue Engineering mit Patienten-spezifischen Kardiomyozyten, die aus iPS-Zellen hergestellt wurden, um ein multizelluläres Krankheitsmodell für den CPVT-Phänotyp zu etablieren. Hauptbestandteile der Studie waren Experimente zur Qualitätskontrolle von iPS-Zellen in Langzeitkultur, die Etablierung eines Differenzierungsprotokolls für Kardiomyozyten sowie die funktionelle Analyse von Patienten-spezifischen EHTs und Kontroll-EHTs.

Um das Verhalten von iPS-Zellen über längere Kulturperioden zu studieren, wurden verschiedene iPS-Zelllinien mit lentiviralen Vektoren transduziert, die für rot-, blau- oder grün-fluoreszierendes Protein kodieren, so dass jede einzelne Zelle eine eindeutige Farbe aufwies. Anschließend wurden die transduzierten Zellen mit Hilfe einer ebenfalls auf dem Vektor kodierten Puromycin-Resistenz selektiert. Nach einer Kulturzeit von fast 40 Passagen zeigten die Ergebnisse der FACS-Analyse, dass sich bei zwei der drei Zelllinien Sub-Klone, das heißt Zellpopulationen, die auf eine Mutterzelle zurückgehen, in den Kulturen durchgesetzt hatten. Bei C25-alt (hohe Passagenummer) bestanden 95% der Zellen aus zwei Sub-Klonen, und bei BJ ließen sich 90% der Zellen auf eine einzige Mutterzelle zurückführen. Das Vorhandensein dieser Dynamik, bei der die Zellen eines einzelnen Sub-Klons alle anderen

Zellen innerhalb von 40 Passagen überwachsen, legt nahe, iPS-Zellen nur für etwa 20 Passagen in Kultur zu halten.

Für die Etablierung eines multizellulären Krankheitsmodells für den CPVT-Phänotyp wurden Proben von zwei verwandten Patienten verwendet. IPS-Zellen von PAS5-641 und PAS7-763, die beide eine Mutation im Gen für den Ryanodinrezeptor tragen, sowie einer Kontroll-Zelllinie wurden mit einem eigenen, auf kleinmolekularen Substanzen basierenden Protokoll zu Kardiomyozyten differenziert. Diese wurden dann zwischen zwei flexiblen Silikonhalterungen in eine Fibrin-Matrix eingebettet. Die so hergestellten EHTs wurden mit einem intern entwickelten und automatisierten System analysiert, mit dem kontinuierliche video-optische Messungen der Kontraktionskraft möglich sind. Diese können gegebenenfalls auch unter elektrischer Stimulation durchgeführt werden. Es erfolgte die Berechnung von gemittelten Kontraktionskurven für spontan kontrahierende Patienten-spezifische EHTs und Kontroll-EHTs. Die Relaxationszeit ($T2_{80\%}$) betrug 157 ms (Standardabweichung [SD] 27) für C25-EHTs (Kontrolle), aber 231 ms (SD 50) und 250 ms (SD 22) für PAS5-641 bzw. PAS7-763 (Patienten-spezifisch). EHTs wurden mit ansteigenden Frequenzen elektrisch stimuliert, um die Frequenz-abhängige Beschleunigung der Relaxation zu untersuchen. C25-EHTs (n=7) zeigten eine hoch signifikante Abnahme der Relaxationszeit von 275 ms (SD 18) bei 0,7 Hz auf 105 ms (SD 22) bei 4 Hz. Bei PAS5-641-EHTs (n=10) betrugen die Werte 350 ms (SD 82) bei 0,7 Hz und 145 ms (SD 27) bei 3,4 Hz. Der β-adrenerge Agonist Isoprenalin erhöhte die Schlagfrequenz von 0,75 Hz (SD 0,11) auf 1,5 Hz (SD 0,3) bei C25 (n=10) und von 0,6 Hz (SD 0,07) auf 1,4 Hz (SA: 0,3) bei PAS5-641 (n=3). Allerdings konnten keine Arrhythmien bei den krankeitsspezifischen EHTs beobachtet werden. Dagegen löste Übernacht-Inkubation in 5 mM Ca^{2+}-haltiger Tyrodelösung bei PAS7-763-EHTs, nicht aber bei C25, Arrhythmien aus, die aber nicht durch Zugabe einer RYR2-stabilisierenden Substanz aufgehoben werden konnten.

Zusammengefasst eignen sich humane iPS-EHTs also dazu, grundlegende Mechanismen der Herzfunktion wie zum Beispiel *post-rest potentiation*, die Erhöhung der Schlagfrequenz nach β-adrenerger Stimulation und den positiv-lusitropen Effekt der Steigerung der Schlagfrequenz darzustellen (siehe oben). Obwohl die krankheitsspezifischen EHTs nicht den erwarteten Phänotyp der durch β-adrenerge Stimulation induzierten Arrhythmien zeigten, hatten EHTs beider Patienten, das heißt von der Mutter (PAS7-763) und des Bruders (PAS5-

641) des verstorbenen Patienten eine längere Relaxationszeit als die Kontrollen und zeigten Arrhythmien bei Übernacht-Inkubation in Tyrode mit hoher Ca^{2+}-Konzentration. Jedoch konnten diese phänotypischen Merkmale nicht durch eine RYR2-stabilisierende Substanz verbessert werden, was die Rolle dieser Mutation für den Krankheitsphänotyp in Frage stellt.

Deshalb sind zukünftige Experimente nötig, um zu entscheiden, ob phänotypische Merkmale wie die lange Relaxationszeit oder die Ca^{2+}-induzierten Arrhythmien tatsächlich mutationsspezifisch sind oder ob es sich schlichtweg um Variabilität verschiedener iPS-Zelllinien handelt. Besonders wichtig hierfür ist der systematische Vergleich von EHTs, die von verschiedenen gesunden Probanden stammen, mit EHTs von Patienten, deren RYR2-Mutation durch genetische Untersuchungen definitiv mit einem klinischen CPVT-Phänotyp assoziiert sind.

Bibliography

Abecasis GR, Altshuler D, Auton A, et al (2010) A map of human genome variation from population-scale sequencing. Nature 467:1061–73. doi: 10.1038/nature09534

Ackerman MJ, Priori SG, Willems S, et al (2011) HRS/EHRA expert consensus statement on the state of genetic testing for the channelopathies and cardiomyopathies: this document was developed as a partnership between the Heart Rhythm Society (HRS) and the European Heart Rhythm Association (EHRA). Europace 13:1077–109. doi: 10.1093/europace/eur245

Bar-Nur O, Russ H a, Efrat S, Benvenisty N (2011) Epigenetic memory and preferential lineage-specific differentiation in induced pluripotent stem cells derived from human pancreatic islet beta cells. Cell Stem Cell 9:17–23. doi: 10.1016/j.stem.2011.06.007

Ben-David U, Mayshar Y, Benvenisty N (2011) Large-scale analysis reveals acquisition of lineage-specific chromosomal aberrations in human adult stem cells. Cell Stem Cell 9:97–102. doi: 10.1016/j.stem.2011.06.013

Birks EJ, Latif N, Enesa K, et al (2008) Elevated p53 expression is associated with dysregulation of the ubiquitin-proteasome system in dilated cardiomyopathy. Cardiovasc Res 79:472–80. doi: 10.1093/cvr/cvn083

Bock C, Kiskinis E, Verstappen G, et al (2011) Reference Maps of human ES and iPS cell variation enable high-throughput characterization of pluripotent cell lines. Cell 144:439–52. doi: 10.1016/j.cell.2010.12.032

Borea P (1992) β1- and β2-adrenoceptors in sheep cardiac ventricular muscle. J Mol Cell Cardiol 24:753–763. doi: 10.1016/0022-2828(92)93389-2

Bowditch H. (1871) Über die Eigenthumlichkeiten der Reizbarkeit, welche die Muskelfasern des Herzens zeigen. Ber Sachs Akad Wiss 23:652–689.

Breckwoldt K (2015) Kardiale Gewebeersatztherapie mittels künstlichem Herzgewebe aus humanen induzierten pluripotenten Stammzellen. Universitätsklinikum Hamburg Eppendorf

Burridge PW, Anderson D, Priddle H, et al (2007) Improved human embryonic stem cell embryoid body homogeneity and cardiomyocyte differentiation from a novel V-96 plate aggregation system highlights interline variability. Stem Cells 25:929–38. doi: 10.1634/stemcells.2006-0598

Burridge PW, Matsa E, Shukla P, et al (2014) Chemically defined generation of human cardiomyocytes. Nat Methods. doi: 10.1038/nmeth.2999

Burridge PW, Thompson S, Millrod M a, et al (2011) A universal system for highly efficient cardiac differentiation of human induced pluripotent stem cells that eliminates interline variability. PLoS One 6:e18293. doi: 10.1371/journal.pone.0018293

Cahan P, Daley GQ (2013) Origins and implications of pluripotent stem cell variability andheterogeneity. Nat Rev Mol Cell Biol 14:357–368. doi: 10.1038/nrm3584.Origins

Chen G, Gulbranson DR, Hou Z, et al (2011) Chemically defined conditions for human iPSC derivation and culture. Nat Methods 8:424–9. doi: 10.1038/nmeth.1593

Claire Robertson, David D. Tran SCG (2013) Concise Review: Maturation Phases of Human Pluripotent Stem Cell-Derived Cardiomyocytes. Stem Cells 31:1–17. doi: 10.1002/stem.1331.Concise

Cohen ED, Tian Y, Morrisey EE (2008) Wnt signaling: an essential regulator of cardiovascular differentiation, morphogenesis and progenitor self-renewal. Development 135:789–98. doi: 10.1242/dev.016865

Cong L, Ran FA, Cox D, et al (2013) Multiplex Genome Engineering Using CRISPR/Cas Systems. Science (80-) 339:819–823. doi: 10.1126/science.1231143.Multiplex

Conradi L, Pahrmann C, Schmidt S, et al (2011) Bioluminescence imaging for assessment of immune responses following implantation of engineered heart tissue (EHT). J Vis Exp 1–4. doi: 10.3791/2605

Coumel P, Fidelle J, Lucet V, et al (1978) Catecholamine-induced severe ventricular arrhythmias with Adams-Stokes syndrome in children: report of four cases. Br Hear J 40(suppl):28–37.

Cribbs LL, Martin BL, Schroder EA, et al (2001) Identification of the T-Type Calcium Channel (CaV 3.1d) in Developing Mouse Heart.

Dahlmann J, Kensah G, Kempf H, et al (2013) The use of agarose microwells for scalable embryoid body formation and cardiac differentiation of human and murine pluripotent stem cells. Biomaterials 34:2463–71. doi: 10.1016/j.biomaterials.2012.12.024

Eisner D a, Trafford a W, Díaz ME, et al (1998) The control of Ca release from the cardiac sarcoplasmic reticulum: regulation versus autoregulation. Cardiovasc Res 38:589–604.

Eschenhagen T, Fink C, Remmers U, et al (1997) Three-dimensional reconstitution of embryonic cardiomyocytes in a collagen matrix: a new heart muscle model system. FASEB J 11:683–94.

Eschenhagen T, Mummery C, Knollmann BC (2015) Modelling sarcomeric cardiomyopathies in the dish: from human heart samples to iPSC cardiomyocytes. Cardiovasc Res 105:424–38. doi: 10.1093/cvr/cvv017

Eschenhagen T, Zimmermann WH (2005) Engineering myocardial tissue. Circ Res 97:1220–31. doi: 10.1161/01.RES.0000196562.73231.7d

Evans MJ, Kaufman MH (1981) Establishment in culture of pluripotential cells from mouse embryos. Nature 292:154–156. doi: 10.1038/292154a0

Fabiato a (1983) Calcium-induced release of calcium from the cardiac sarcoplasmic reticulum. Am J Physiol 245:C1–14.

Fatima A, Xu G, Shao K, et al (2011) In vitro Modeling of Ryanodine Receptor 2 Dysfunction Using Human Induced Pluripotent Stem Cells. 579–592.

Feng Q, Lu S-J, Klimanskaya I, et al (2010) Hemangioblastic derivatives from human induced pluripotent stem cells exhibit limited expansion and early senescence. Stem Cells 28:704–12. doi: 10.1002/stem.321

Fernández-Velasco M, Rueda A, Rizzi N, et al (2009) Increased Ca2+ sensitivity of the ryanodine receptor mutant RyR2R4496C underlies catecholaminergic polymorphic ventricular tachycardia. Circ Res 104:201–9, 12p following 209. doi: 10.1161/CIRCRESAHA.108.177493

Frank S, Zhang M, Schöler HR, Greber B (2012) Small molecule-assisted, line-independent maintenance of human pluripotent stem cells in defined conditions. PLoS One 7:e41958. doi: 10.1371/journal.pone.0041958

Fredersdorf S, Thumann C, Zimmermann WH, et al (2012) Increased myocardial SERCA expression in early type 2 diabetes mellitus is insulin dependent: In vivo and in vitro data. Cardiovasc Diabetol 11:57. doi: 10.1186/1475-2840-11-57

Freire AG, Resende TP, Pinto-do-Ó P (2014) Building and repairing the heart: what can we learn from embryonic development? Biomed Res Int 2014:679168. doi: 10.1155/2014/679168

Friedrich FW, Wilding BR, Reischmann S, et al (2012) Evidence for FHL1 as a novel disease gene for isolated hypertrophic cardiomyopathy. Hum Mol Genet 21:3237–54. doi: 10.1093/hmg/dds157

Garitaonandia I, Amir H, Boscolo FS, et al (2015) Increased risk of genetic and epigenetic instability in human embryonic stem cells associated with specific culture conditions. PLoS One 10:e0118307. doi: 10.1371/journal.pone.0118307

Gaziano T, Reddy KS, Paccaud F, Horton S (2001) Disease Control Priorities in Developing Countries. 2nd edition. Chapter 33.

Guo T, Cornea RL, Huke S, et al (2010) Kinetics of FKBP12.6 binding to ryanodine receptors in permeabilized cardiac myocytes and effects on Ca sparks. Circ Res 106:1743–52. doi: 10.1161/CIRCRESAHA.110.219816

Gurdon JB (1962) The developmental capacity of nuclei taken from intestinal epithelium cells of feeding tadpoles. J Embryol Exp Morphol 10:622–40.

Hansen A, Eder A, Bönstrup M, et al (2010) Development of a drug screening platform based on engineered heart tissue. Circ Res 107:35–44. doi: 10.1161/CIRCRESAHA.109.211458

He W, Ye L, Li S, et al (2012) Stirred Suspension Culture Improves Embryoid Body Formation and Cardiogenic Differentiation of Genetically Modi fi ed Embryonic Stem Cells. 35:308–316.

Hennekens CH (1998) Increasing Burden of Cardiovascular Disease : Current Knowledge and Future Directions for Research on Risk Factors. Circulation 97:1095–1102. doi: 10.1161/01.CIR.97.11.1095

Hirt MN, Hansen A, Eschenhagen T (2014) Cardiac tissue engineering: state of the art. Circ Res 114:354–67. doi: 10.1161/CIRCRESAHA.114.300522

Hirt MN, Sörensen N a, Bartholdt LM, et al (2012) Increased afterload induces pathological cardiac hypertrophy: a new in vitro model. Basic Res Cardiol 107:307. doi: 10.1007/s00395-012-0307-z

Hu B-Y, Weick JP, Yu J, et al (2010) Neural differentiation of human induced pluripotent stem cells follows developmental principles but with variable potency. Proc Natl Acad Sci U S A 107:4335–40. doi: 10.1073/pnas.0910012107

Hussein SM, Batada NN, Vuoristo S, et al (2011) Copy number variation and selection during reprogramming to pluripotency. Nature 471:58–62. doi: 10.1038/nature09871

Itzhaki I, Maizels L, Huber I, et al (2012) Modeling of catecholaminergic polymorphic ventricular tachycardia with patient-specific human-induced pluripotent stem cells. J Am Coll Cardiol 60:990–1000. doi: 10.1016/j.jacc.2012.02.066

Itzhaki I, Maizels L, Huber I, et al (2011) Modelling the long QT syndrome with induced pluripotent stem cells. Nature 471:225–9. doi: 10.1038/nature09747

Janowski E, Berríos M, Cleemann L, Morad M (2010) Developmental aspects of cardiac Ca(2+) signaling: interplay between RyR- and IP(3)R-gated Ca(2+) stores. Am J Physiol Heart Circ Physiol 298:H1939–50. doi: 10.1152/ajpheart.00607.2009

John L. Spudich & D. E. Koshland J (1976) Non-genetic individuality: chance in the single cell.

Jones PP, Jiang D, Bolstad J, et al (2008) Endoplasmic reticulum Ca2+ measurements reveal that the cardiac ryanodine receptor mutations linked to cardiac arrhythmia and sudden death alter the threshold for store-overload-induced Ca2+ release. Biochem J 412:171–8. doi: 10.1042/BJ20071287

Jung CB, Moretti A, Mederos y Schnitzler M, et al (2012) Dantrolene rescues arrhythmogenic RYR2 defect in a patient-specific stem cell model of catecholaminergic polymorphic ventricular tachycardia. EMBO Mol Med 4:180–91. doi: 10.1002/emmm.201100194

Kannankeril PJ, Mitchell BM, Goonasekera S a, et al (2006) Mice with the R176Q cardiac ryanodine receptor mutation exhibit catecholamine-induced ventricular tachycardia and cardiomyopathy. Proc Natl Acad Sci U S A 103:12179–84. doi: 10.1073/pnas.0600268103

Kattman SJ, Witty AD, Gagliardi M, et al (2011) Stage-specific optimization of activin/nodal and BMP signaling promotes cardiac differentiation of mouse and human pluripotent stem cell lines. Cell Stem Cell 8:228–40. doi: 10.1016/j.stem.2010.12.008

Kensah G, Roa Lara A, Dahlmann J, et al (2013) Murine and human pluripotent stem cell-derived cardiac bodies form contractile myocardial tissue in vitro. Eur Heart J 34:1134–46. doi: 10.1093/eurheartj/ehs349

Kim K, Doi a, Wen B, et al (2010) Epigenetic memory in induced pluripotent stem cells. Nature 467:285–90. doi: 10.1038/nature09342

Koch-Weser J, Blinks JR (1963) The influence of the interval between beats on myocardial contractility.

Laflamme M a, Chen KY, Naumova A V, et al (2007) Cardiomyocytes derived from human embryonic stem cells in pro-survival factors enhance function of infarcted rat hearts. Nat Biotechnol 25:1015–24. doi: 10.1038/nbt1327

Lan F, Lee AS, Liang P, et al (2013) Abnormal calcium handling properties underlie familial hypertrophic cardiomyopathy pathology in patient-specific induced pluripotent stem cells. Cell Stem Cell 12:101–13. doi: 10.1016/j.stem.2012.10.010

Lanier M, Schade D, Willems E, et al (2013) Wnt inhibition correlates with human embryonic stem cell cardiomyogenesis: A Structure Activity Relationship study based on inhibitors for the Wnt response. 55:697–708. doi: 10.1021/jm2010223.Wnt

Lee G, Papapetrou EP, Kim H, et al (2009) Modelling pathogenesis and treatment of familial dysautonomia using patient-specific iPSCs. Nature 461:402–6. doi: 10.1038/nature08320

Levenstein ME, Ludwig TE, Xu R-H, et al (2006) Basic fibroblast growth factor support of human embryonic stem cell self-renewal. Stem Cells 24:568–74. doi: 10.1634/stemcells.2005-0247

Levy S, Sutton G, Ng PC, et al (2007) The diploid genome sequence of an individual human. PLoS Biol 5:e254. doi: 10.1371/journal.pbio.0050254

Lian X, Hsiao C, Wilson G, et al (2012) PNAS Plus: Robust cardiomyocyte differentiation from human pluripotent stem cells via temporal modulation of canonical Wnt signaling. Proc Natl Acad Sci. doi: 10.1073/pnas.1200250109

Lister R, Pelizzola M, Kida YS, et al (2011) Hotspots of aberrant epigenomic reprogramming in human induced pluripotent stem cells. Nature 471:68–73. doi: 10.1038/nature09798

Lobo PA, Van Petegem F (2009) Crystal structures of the N-terminal domains of cardiac and skeletal muscle ryanodine receptors: insights into disease mutations. Structure 17:1505–14. doi: 10.1016/j.str.2009.08.016

MacLennan DH, Chen SRW (2009) Store overload-induced Ca2+ release as a triggering mechanism for CPVT and MH episodes caused by mutations in RYR and CASQ genes. J Physiol 587:3113–5. doi: 10.1113/jphysiol.2009.172155

Maherali N, Sridharan R, Xie W, et al (2007) Directly reprogrammed fibroblasts show global epigenetic remodeling and widespread tissue contribution. Cell Stem Cell 1:55–70. doi: 10.1016/j.stem.2007.05.014

Mammucari C, Milan G, Romanello V, et al (2007) FoxO3 controls autophagy in skeletal muscle in vivo. Cell Metab 6:458–71. doi: 10.1016/j.cmet.2007.11.001

Marian a J, Belmont J (2011) Strategic approaches to unraveling genetic causes of cardiovascular diseases. Circ Res 108:1252–69. doi: 10.1161/CIRCRESAHA.110.236067

Martin GR (1981) Isolation of a pluripotent cell line from early mouse embryos cultured in medium conditioned by teratocarcinoma stem cells Developmental Biology : 78:7634–7638.

Marx SO, Reiken S, Hisamatsu Y, et al (2000) PKA phosphorylation dissociates FKBP12.6 from the calcium release channel (ryanodine receptor): defective regulation in failing hearts. Cell 101:365–76.

Mathers CD, Lopez A, Stein C, et al (2005) Disease Control Priorities Project.

McDonald T, Sachs H, DeHaan R (1972) Development of Sensitivity to Tetrodotoxin in Beating Chick Embryo Hearts, Single Cells, and Aggregates. Science (80-) 176:1248–1250.

Minami I, Yamada K, Otsuji TG, et al (2012) A Small Molecule that Promotes Cardiac Differentiation of Human Pluripotent Stem Cells under Defined, Cytokine- and Xeno-free Conditions. Cell Rep 1–13. doi: 10.1016/j.celrep.2012.09.015

Miyamoto S, Izumi M, Hori M, et al (2000) Xestospongin C , a selective and membrane-permeable inhibitor of IP 3 receptor , attenuates the positive inotropic e €ect of a -adrenergic stimulation in guinea-pig papillary muscle. 650–654.

Monte F, Kaumann AJ, Poole-wilson PA, et al (1993) Coexistence of Functioning 32-Adrenoceptors in Single Myocytes From Human Ventricle.

Moretti A, Bellin M, Welling A, et al (2010) Patient-specific induced pluripotent stem-cell models for long-QT syndrome. N Engl J Med 363:1397–409. doi: 10.1056/NEJMoa0908679

Moscona A a (1959) Tissues from dissociated cells. Sci Am 200:132–4.

Mummery C, Ward-van Oostwaard D, Doevendans P, et al (2003) Differentiation of human embryonic stem cells to cardiomyocytes: role of coculture with visceral endoderm-like cells. Circulation 107:2733–40. doi: 10.1161/01.CIR.0000068356.38592.68

Mummery CL, Zhang J, Ng ES, et al (2012) Differentiation of human embryonic stem cells and induced pluripotent stem cells to cardiomyocytes: a methods overview. Circ Res 111:344–58. doi: 10.1161/CIRCRESAHA.110.227512

Nakatsuji N, Marcus E, Sweet D, Mobed R (2013) Stem Cell Research, Trend and Perspective on the Evolving International Landscape.

Napolitano C, Bloise R, Memmi M, Priori SG (2014) Clinical utility gene card for: Catecholaminergic polymorphic ventricular tachycardia (CPVT). Eur J Hum Genet 22:1–3. doi: 10.1038/ejhg.2013.55

Neuber C, Müller OJ, Hansen FC, et al (2014) Paradoxical effects on force generation after efficient β1-adrenoceptor knockdown in reconstituted heart tissue. J Pharmacol Exp Ther 349:39–46. doi: 10.1124/jpet.113.210898

Ng ES, Davis RP, Azzola L, et al (2005) Forced aggregation of defined numbers of human embryonic stem cells into embryoid bodies fosters robust , reproducible hematopoietic differentiation. 106:1601–1604. doi: 10.1182/blood-2005-03-0987.Supported

Novak A, Lorber A, Itskovitz-Eldor J, Binah O (2012) Modeling Catecholaminergic Polymorphic Ventricular Tachycardia using Induced Pluripotent Stem Cell-derived Cardiomyocytes. Rambam Maimonides Med J 3:e0015. doi: 10.5041/RMMJ.10086

Novick A, Weiner M (1957) ENZYME INDUCTION AS AN ALL-OR-NONE PHENOMENON. Proc Natl Acad Sci 553–566.

Nyegaard M, Overgaard MT, Søndergaard MT, et al (2012) Mutations in calmodulin cause ventricular tachycardia and sudden cardiac death. Am J Hum Genet 91:703–12. doi: 10.1016/j.ajhg.2012.08.015

Olson EN, Schneider MD (2003) Sizing up the heart: development redux in disease. Genes Dev 17:1937–56. doi: 10.1101/gad.1110103

Perez-Pinera P, Kocak DD, Vockley CM, et al (2013) RNA-guided gene activation by CRISPR-Cas9-based transcription factors. Nat Methods 10:973–6. doi: 10.1038/nmeth.2600

Postma a V, Denjoy I, Kamblock J, et al (2005) Catecholaminergic polymorphic ventricular tachycardia: RYR2 mutations, bradycardia, and follow up of the patients. J Med Genet 42:863–70. doi: 10.1136/jmg.2004.028993

Postma a. V. (2002) Absence of Calsequestrin 2 Causes Severe Forms of Catecholaminergic Polymorphic Ventricular Tachycardia. Circ Res 91:21e–26. doi: 10.1161/01.RES.0000038886.18992.6B

Priori SG (2002) Clinical and Molecular Characterization of Patients With Catecholaminergic Polymorphic Ventricular Tachycardia. Circulation 106:69–74. doi: 10.1161/01.CIR.0000020013.73106.D8

Priori SG, Chen SRW (2011) Inherited dysfunction of sarcoplasmic reticulum Ca2+ handling and arrhythmogenesis. Circ Res 108:871–83. doi: 10.1161/CIRCRESAHA.110.226845

Priori SG, Wilde AA, Horie M, et al (2013) HRS/EHRA/APHRS expert consensus statement on the diagnosis and management of patients with inherited primary arrhythmia syndromes: document endorsed by HRS, EHRA, and APHRS in May 2013 and by ACCF, AHA, PACES, and AEPC in June 2013. Heart Rhythm 10:1932–63. doi: 10.1016/j.hrthm.2013.05.014

Radisic M, Marsano A, Maidhof R, et al (2008) Cardiac tissue engineering using perfusion bioreactor systems. Nat Protoc 3:719–38. doi: 10.1038/nprot.2008.40

Radisic M, Park H, Shing H, et al (2004) Functional assembly of engineered myocardium by electrical stimulation of cardiac myocytes cultured on scaffolds. Proc Natl Acad Sci U S A 101:18129–34. doi: 10.1073/pnas.0407817101

Raj A, van Oudenaarden A (2008) Nature, nurture, or chance: stochastic gene expression and its consequences. Cell 135:216–26. doi: 10.1016/j.cell.2008.09.050

Robinton D a, Daley GQ (2012) The promise of induced pluripotent stem cells in research and therapy. Nature 481:295–305. doi: 10.1038/nature10761

Sacherer M, Sedej S, Wakuła P, et al (2012) JTV519 (K201) reduces sarcoplasmic reticulum Ca^{2+} leak and improves diastolic function in vitro in murine and human non-failing myocardium. Br J Pharmacol 167:493–504. doi: 10.1111/j.1476-5381.2012.01995.x

Schaaf S (2011) Künstliches Herzgewebe aus humanen embryonalen Stammzellen als Testsystem für Arzneistoffe. Universitätsklinikum Hamburg Eppendorf

Schaaf S, Shibamiya A, Mewe M, et al (2011) Human engineered heart tissue as a versatile tool in basic research and preclinical toxicology. PLoS One 6:e26397. doi: 10.1371/journal.pone.0026397

Stöhr A, Friedrich FW, Flenner F, et al (2013) Contractile abnormalities and altered drug response in engineered heart tissue from Mybpc3-targeted knock-in mice. J Mol Cell Cardiol 63:189–98. doi: 10.1016/j.yjmcc.2013.07.011

Sun N, Yazawa M, Liu J, et al (2012) Patient-specific induced pluripotent stem cells as a model for familial dilated cardiomyopathy. Sci Transl Med 4:130ra47. doi: 10.1126/scitranslmed.3003552

Takahashi K, Tanabe K, Ohnuki M, et al (2007) Induction of pluripotent stem cells from adult human fibroblasts by defined factors. Cell 131:861–72. doi: 10.1016/j.cell.2007.11.019

Takahashi K, Yamanaka S (2006) Induction of pluripotent stem cells from mouse embryonic and adult fibroblast cultures by defined factors. Cell 126:663–76. doi: 10.1016/j.cell.2006.07.024

Tateishi H, Yano M, Mochizuki M, et al (2009) Defective domain-domain interactions within the ryanodine receptor as a critical cause of diastolic Ca2+ leak in failing hearts. Cardiovasc Res 81:536–45. doi: 10.1093/cvr/cvn303

Tchieu J, Kuoy E, Chin MH, et al (2010) Female human iPSCs retain an inactive X chromosome. Cell Stem Cell 7:329–42. doi: 10.1016/j.stem.2010.06.024

Tharmalingam T, Ghebeh H, Wuerz T, Butler M (2008) Pluronic Enhances the Robustness and Reduces the Cell Attachment of Mammalian Cells. Mol Biotechnol 167–177. doi: 10.1007/s12033-008-9045-8

Thomson J a. (1998) Embryonic Stem Cell Lines Derived from Human Blastocysts. Science (80-) 282:1145–1147. doi: 10.1126/science.282.5391.1145

Tiburcy M, Didié M, Boy O, et al (2011) Terminal differentiation, advanced organotypic maturation, and modeling of hypertrophic growth in engineered heart tissue. Circ Res 109:1105–14. doi: 10.1161/CIRCRESAHA.111.251843

Tiso N, Salamon M, Bagattin A, et al (2002) The binding of the RyR2 calcium channel to its gating protein FKBP12.6 is oppositely affected by ARVD2 and VTSIP mutations. Biochem Biophys Res Commun 299:594–598. doi: 10.1016/S0006-291X(02)02689-X

Trafford a W, Sibbring GC, Díaz ME, Eisner DA (2000) The effects of low concentrations of caffeine on spontaneous Ca release in isolated rat ventricular myocytes. Cell Calcium 28:269–76. doi: 10.1054/ceca.2000.0156

Uchinoumi H, Yano M, Suetomi T, et al (2010) Catecholaminergic polymorphic ventricular tachycardia is caused by mutation-linked defective conformational regulation of the ryanodine receptor. Circ Res 106:1413–24. doi: 10.1161/CIRCRESAHA.109.209312

Van der Werf C, Nederend I, Hofman N, et al (2012) Familial evaluation in catecholaminergic polymorphic ventricular tachycardia: disease penetrance and expression in cardiac ryanodine receptor mutation-carrying relatives. Circ Arrhythm Electrophysiol 5:748–56. doi: 10.1161/CIRCEP.112.970517

Watanabe H, Chopra N, Laver D, et al (2010) Flecainide prevents catecholaminergic polymorphic ventricular tachycardia in mice and humans. Nat Med 15:380–383. doi: 10.1038/nm.1942.Flecainide

Weber K, Thomaschewski M, Warlich M, et al (2011) RGB marking facilitates multicolor clonal cell tracking. Nat Med 17:504–9. doi: 10.1038/nm.2338

Weber, K., Bartsch, U., Stocking, C., & Fehse, B. (2008). A multicolor panel of novel lentiviral "gene ontology" (LeGO) vectors for functional gene analysis. *Molecular Therapy : The Journal of the American Society of Gene Therapy*, *16*(4), 698–706. doi:10.1038/mt.2008.6

Wehrens XHT, Lehnart SE, Huang F, et al (2003) FKBP12.6 deficiency and defective calcium release channel (ryanodine receptor) function linked to exercise-induced sudden cardiac death. Cell 113:829–40.

Willems E, Spiering S, Davidovics H, et al (2011) Small-molecule inhibitors of the Wnt pathway potently promote cardiomyocytes from human embryonic stem cell-derived mesoderm. Circ Res 109:360–4. doi: 10.1161/CIRCRESAHA.111.249540

Wilmut I, Schnieke AE, McWhir J, et al (1997) Viable offspring derived from fetal and adult mammalian cells. Nature 385:810–3. doi: 10.1038/385810a0

Xiang Z, Thompson AD, Brogan JT, et al (2011) The Discovery and Characterization of ML218: A Novel, Centrally Active T-Type Calcium Channel Inhibitor with Robust Effects in STN Neurons and in a Rodent Model of Parkinson's Disease. ACS Chem Neurosci 2:730–742. doi: 10.1021/cn200090z

Yang L, Soonpaa MH, Adler ED, et al (2008) Human cardiovascular progenitor cells develop from a KDR+ embryonic-stem-cell-derived population. Nature 453:524–8. doi: 10.1038/nature06894

Yang X, Pabon L, Murry CE (2014) Engineering adolescence: maturation of human pluripotent stem cell-derived cardiomyocytes. Circ Res 114:511–23. doi: 10.1161/CIRCRESAHA.114.300558

Zhang J, Klos M, Wilson GF, et al (2012) Extracellular Matrix Promotes Highly Efficient Cardiac Differentiation of Human Pluripotent Stem Cells: The Matrix Sandwich Method. Circ Res. doi: 10.1161/CIRCRESAHA.112.273144

Zhang M, Schulte JS, Heinick A, et al (2015) Universal Cardiac Induction of Human Pluripotent Stem Cells in 2D and 3D formats - Implications for In-Vitro Maturation. Stem Cells. doi: 10.1002/stem.1964

Zhou Q, Xiao J, Jiang D, et al (2011) Carvedilol and its new analogs suppress arrhythmogenic store overload–induced Ca2+ release. Nat Med 17:1003–1009. doi: 10.1038/nm.2406

Zhu W-Z, Benjamin Van Biber, Laflamme MA (2011) Methods for the Derivation and Use of Cardiomyocytes from Human Pluripotent Stem Cells. 767:419–431. doi: 10.1007/978-1-61779-201-4

Zimmermann W-H, Melnychenko I, Wasmeier G, et al (2006) Engineered heart tissue grafts improve systolic and diastolic function in infarcted rat hearts. Nat Med 12:452–8. doi: 10.1038/nm1394

Zimmermann W-H, Schneiderbanger K, Schubert P, et al (2002) Tissue Engineering of a Differentiated Cardiac Muscle Construct. Circ Res 90:223–230. doi: 10.1161/hh0202.103644

Acknowledgements

Curriculum Vitae

Since 2011   PhD at the Institute for Experimental Pharmacology and Toxicology at the Universitätsklinikum Hamburg-Eppendorf (Germany) on "Modelling catecholaminergic polymorphic ventricular tachycardia with patient-specific iPSC-derived engineered heart tissues" under the supervision of Prof. Dr. Thomas Eschenhagen and Prof. Dr. Arne Hansen.

2009-2010   Master of Molecular Neurosciences at the University of Bristol (UK), under the supervision of Prof. Hans Reul.

2007-2010   Agronomical engineer cursus in the "Grande École" of SupAgro in Montpellier (France).

2007-2008   Bachelor in Biology, Geology, Earth and Universe Science (L3BGSTU) at the University of Aix-Marseille.

2005-2007   "Classe Préparatoire aux Grandes Écoles" in Biology, Chemistry, Physics and Earth Sciences at the Lycée Henri IV in Paris (France).

2005   International Option of the Baccalauérat obtained at the Lycée Georges Duby in Luynes (France).

Eidesstattliche Versicherung

Ich versichere ausdrücklich, dass ich die Arbeit selbständig und ohne fremde Hilfe verfasst, andere als die von mir angegebenen Quellen und Hilfsmittel nicht benutzt und die aus den benutzten Werken wörtlich oder inhaltlich entnommenen Stellen einzeln nach Ausgabe (Auflage und Jahr des Erscheinens), Band und Seite des benutzten Werkes kenntlich gemacht habe.

Ferner versichere ich, dass ich die Dissertation bisher nicht einem Fachvertreter an einer anderen Hochschule zur Überprüfung vorgelegt oder mich anderweitig um Zulassung zur Promotion beworben habe.

Ich erkläre mich einverstanden, dass meine Dissertation vom Dekanat der Medizinischen Fakultät mit einer gängigen Software zur Erkennung von Plagiaten überprüft werden kann.

Unterschrift: ....